Experimental and Theoretical Investigations of the Effect of Gravity and Temperature Gradients on Fluid Composition in Petroleum Reservoirs

By

Abdul Karim M. Al-Jaziri

A thesis submitted to the Faculty and Board of Trustees of the Colorado School of Mines in partial fulfillment of the requirements for the degree of Doctor of Philosophy (Petroleum Engineering).

Golden, Colorado

Date *15 January 2001*

Signed : _____

Abdul Karim M. Al-Jaziri

Approved: _____

Dr. Richard L. Christiansen

Thesis Advisor

Golden, Colorado

Date *January 15, 2001*

_____

Dr. Craig W. Van Kirk

Professor and Head,

Department of Petroleum Engineering

ABSTRACT

Compositional grading in hydrocarbon reservoirs was a big concern for many investigators in the past and continues to be so at the present time. This grading in composition has been observed in many reservoirs around the world. But, from 1938 until 2000, the petroleum lite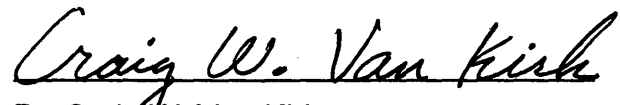rature is devoid of publications on laboratory work for the combined effect of gravity and temperature gradients on compositional grading in petroleum reservoirs. Rather, investigators approached the problem of compositional grading using numerical methods and field data. Comparisons of predicted compositional grading and field data are available, with acceptable results in some cases, but not in others. Most predicted composition gradients are smaller than the gradients observed in the field data.

Therefore the objective of this thesis research was to design and develop experimental methods to investigate the effect of gravity and temperature gradients in a thick hydrocarbon zone by applying large accelerations on a short fluid loop in centrifuge tests. Extensive efforts were spent on designing and testing an experimental setup and procedures to produce an observable compositional gradient in the lab. A single-phase binary gas mixture of 58 mole percent methane and 42 mole percent propane was selected to represent qualitatively the fluids in a hydrocarbon reservoir.

Using the binary system mentioned above, significant magnitudes of compositional gradients were established under the effect of gravity, and the combined effect of gravity and temperature gradients. The observed compositional gradients were compared with gradients predicted by a numerical model developed for this research. The measured and calculated compositional gradients for isothermal and

non-isothermal conditions were compared to see the difference for the combined effects of gravity and temperature gradients and for the gravity gradient alone. The effect of temperature gradients is of the same order of magnitude as the gravity effect. In some experiments, the effect of temperature gradient was higher than the gravity effect. Therefore the measured gradients in this research parallel the larger than predicted gradients that are often observed in various oil and gas fields around the world.

A numerical program was written to calculate the composition gradient in the binary gas mixture of methane and propane. The program uses both thermodynamic and transport approaches for calculating the composition gradient with the option of using either Peng-Robinson or Redlich-Kwong equations of state to calculate partial molar volumes, densities, and fugacities for the binary system.

TABLE OF CONTENTS

LIST OF FIGURES

LIST OF TABLES

ACKNOWLEDGEMENTS

DEDICATION

This Thesis is dedicated
To my sweet heart, Eman, and my wonderful kids Ahmed, Jinan, and Gadeer --
my big source of encouragement and inspiration.

To my dear and beloved parents, my mother, Fatima and my father, Haji
Mohammed for their continual encouragement, patience, and love and who
endeavored to show their children the difference between right and wrong and
who sacrificed and devoted themselves for their children's wellbeing and
education.

CHAPTER 1

INTRODUCTION

The nature of the fluids in petroleum reservoirs differs from one reservoir to another. And, within the same reservoir the fluids may change composition in the vertical and/or in the horizontal directions. This change in composition is known as compositional grading. Compositional grading in hydrocarbon reservoirs has been investigated by many researchers in the past few decades, and still poses many new challenges for investigators at the present time. This grading in composition has been observed in many reservoirs around the world.

These compositional gradients result from a variety of causes, which are related to thermodynamic phenomena, non-thermodynamic phenomena, and mechanics of hydrocarbon accumulations. Thermodynamic factors could be local temperature and pressure, composition, elevation of the gas and the oil columns (gravitational force). Other factors associated with non-thermodynamic phenomena and hydrocarbon accumulations include geothermal temperature gradients (causing convection, molecular and thermal diffusion), bacterial action, aquifer washing, and history of migration and entrapment of reservoir fluids.

No publication in the literature has considered all the factors causing composition grading. Some of these factors are very poorly understood. Most of these factors often yield subtle effects that have been ignored in many reservoirs. Some of the factors are quite complicated, and technically challenging. Here, the effects of temperature gradients and gravity are considered.

From 1938 until 2000 the petroleum literature is devoid of publications regarding experimental work on the combined effect of gravity and temperature gradients on compositional grading in petroleum reservoirs. Investigators treated this problem using numerical approaches and field data only. Comparisons of predicted compositional grading and field data are available, with acceptable results in some cases, but not so in some others. Most predicted composition gradients are smaller than the gradients observed in the field data.

1.1 Research Objectives

The objective of this research was to design and develop experimental methods to investigate the effect of gravity and temperature gradients on the distribution of hydrocarbon fluids in petroleum reservoirs. Under isothermal and non-isothermal conditions at low and high pressure, experiments were performed using methane-propane binary gas mixture to reproduce the effect of gravity on a thick hydrocarbon zone by applying large accelerations on a short fluid loop in a centrifuge. Another objective was verifying and testing the thermodynamic and transport theories for composition gradients.

1.2 Statement of the Problem

Considerable variations in composition and PVT properties of reservoir fluids with depth have been observed in various oil and gas fields around the world. The major effects responsible for this compositional grading are thought to be gravity and temperature gradients. This compositional grading is exaggerated for the following conditions:

1. **The presence of a large amount of intermediate components (C_2 through C_4).** This composition normally puts a mixture near its critical condition when the reservoir temperature is near the critical temperature. In the North Sea area, for instance, where near critical fluid reservoirs are produced, large gradients are encountered closer to the critical state where the values of the partial molar volumes are larger. For these reservoirs the bubble-point pressure gradient in the oil zone is reported to be 3.6 to 4.0 psi/ft.

2. **The presence of the small amounts of very heavy hydrocarbons and particularly aromatic components (asphaltene micelles) in the gas or oil.** As the asphaltene micelle molecular weight could be of the order of several thousand and even over 20,000, the compositional segregation and saturation pressure variation in an oil column can be very pronounced when asphaltene materials are present.

Such compositional grading can have a significant influence on various aspects of reservoir development. In one volatile oil field of the North Sea, the oil formation volume factor varies greatly with depth. This must be taken into account in

estimating the Original Oil in Place (OIIP) of the field. Neglecting this compositional grading will result in substantial errors in reserve estimates (up to 20%) as well as in predicted oil recovery, which in turn will result in incorrect design criteria for surface facilities. An adequate knowledge of the fluid distribution is necessary for activities relating to field delineation and development planning.

1.3 Approach to the Problem

In this Ph.D research work, extensive efforts were spent on designing an experimental setup and procedures to produce an observable compositional gradient in the lab. Centrifuge experiments in the lab were conducted at different temperatures, pressures, spin rates, and time intervals. Under isothermal and non-isothermal conditions at low and high pressure, experiments were conducted using methane/propane binary gas mixture to reproduce the effect of gravity on a thick hydrocarbon zone by applying large accelerations on a short fluid loop in a centrifuge with the following organization:

Isothermal centrifuge experiments

1. Confirm thermodynamic theory and develop experimental techniques using methane/propane binary gas mixture.
2. Measure the evolution toward equilibrium (composition profile with time) for the same gas mixture and compare the results with transport theory.

Non-isothermal centrifuge experiments (with a temperature gradient)

1. Measure the temperature gradient across the test loop.
2. Test the transport theory using methane/propane binary gas mixture.

3. Assess the evolution toward equilibrium for gas phase binary system.

4. Compare predicted thermal diffusion ratios using model developed for this work with prediction results from available thermal diffusion models.

1.4 Overview of the Rest of this Thesis

Following this introductory chapter, Chapter Two gives an overview of the literature available on compositional grading problem including a background on the problem of compositional gradients, and previous work on compositional gradients which includes both effects of gravity and temperature. In addition the theoretical studies including all the equations derived for predicting compositional gradient are summarized. In Chapter Three, experimental apparatus is described including the steps in selecting and preparing the binary gas mixture, a description of procedures for the experiments, and gas composition calculations are presented. Results obtained from the centrifuge experiments under isothermal and non-isothermal conditions at low and high pressure are presented and discussed in Chapter Four. Summaries of conclusions and recommendations for future research are presented in Chapter Five. Nomenclature, References, and Appendix with a listing of the software for numerical models are available at the end of this thesis.

CHAPTER 2

LITERATURE REVIEW

In this chapter, a wide range of literature is considered in order to develop sufficient understanding of the composition gradient problem. First, some background discussion of the problem of compositional gradients is given. Next, previous work on compositional gradients considering both effects of gravity and temperature, the equations for calculating compositional gradients, and equations for estimating thermal diffusion coefficients are given. Finally, to give additional background for the experimental effort in this research, PVT behavior of the methane-propane binary system is summarized.

2.1 Background

Compositional variation in hydrocarbon reservoirs was a big concern for many investigators in the past and continues to be so at the present time. These variations in composition have been observed in many reservoirs around the world. The mole fractions of the heavier components in a hydrocarbon fluid column increase, whereas the light fractions decrease as the depth increases from the top to the bottom of the reservoir, normally associated with the action of the gravitational force and temperature variations. These variations in composition may indicate non-equilibrium or steady state rather than equilibrium in the reservoir. But, compositional grading can also be observed in systems in

equilibrium. When a multi-component system is in thermodynamic equilibrium in a gravity field, the system must be isothermal and for each component the sum of the chemical potential and the gravity potential must be constant as will be explained later in this chapter.

The magnitude of these gradients depends on the nature and composition of reservoir fluids as well as on reservoir characteristics, as suggested by Sage and Lacey[1], Schulte[2], Holt et al.[3], and Hamoodi et al.[4] Large gradients are encountered closer to the critical state where the values of the partial molar volume of individual components are large compared to the molar volume of the system. For North Sea critical fluids, Montel[5] showed that the gravitational segregation alone can largely explain the compositional grading observed in such reservoirs. Therefore compositional gradients are more significant in gas condensate and volatile oil reservoirs than in black oil or dry gas reservoirs.

Reservoirs with large closure containing a rich gas condensate or volatile oil such as those located in the Nuggets Sandstone portion of the Wyoming Overthrust Belt, Creek et al.[6], have measurable variations in the composition of hydrocarbons in the reservoir. Also large compositional grading could be expected for a reservoir containing heavier crude with some asphalt content. In this case, compositional variations are mainly the result of asphaltene segregation, as described by Hirschberg[7]. Even for light crude containing high asphalt content, the compositional grading can be high.

The larger the reservoir thickness and the larger the difference between molecular weights of components, the more the influence of gravitational force on compositional grading.

Compositional Variations with depth have a big effect on reservoir fluid properties such as gas oil ratios, saturation pressures, density, and viscosity. Such compositional variations can have a significant influence on various aspects of reservoir development such as estimating reserves, recovery processes, field development, and design of production facilities.

2.2 Previous Work Done on Compositional Gradient

The way investigators presented and solved the problem of compositional gradient differs from one to another. Some investigators discussed compositional variations through discussion of field examples only. Others did theoretical calculations supported by field examples. From 1938 until 2000 the petroleum literature is devoid of publications on laboratory work for the combined effect of gravity and temperature gradients on compositional grading in petroleum reservoirs.

2.2.1 Theoretical Calculations

As mentioned above there are several factors responsible for initiating compositional gradient in petroleum reservoirs but the majority of the investigators considered the compositional distribution in the vertical direction is governed by the gravitational force. In general the major effects responsible for this compositional grading are thought to be gravity and temperature fields.

2.2.1.1 Effect of Gravitational Field

The formulation for calculating the variations in fluid composition due to the gravitational field for an isothermal system was first given by Gibbs. Utilizing the Gibbs criteria of thermodynamic equilibria: dG must vanish at equilibrium, the equilibrium condition for a system in a gravity field can be expressed by:

$$d\mu_i = -M_i g dz \qquad i = 1,2,3,\ldots\ldots,C \qquad (2.1)$$

In 1930, Muskat[8] solved equation 2.1 using a very simplified assumption (ideal mixing) and came up with an explicit solution. Due to the simplified assumption Muskat used in his solution, numerical examples led to the misleading conclusion that gravity has negligible effect on compositional variation in reservoir system.

In 1938, Sage and Lacey[1] studied the effect of gravity on the equilibrium of a multi-component fluid column using a more realistic equation of state model to solve equation 2.1 assuming ideal solution behavior. Sage and Lacey assumed an isothermal system and they believed that the presence of the temperature gradient would enhance the compositional gradient effect estimated from the isothermal case. They reached a conclusion that gravity has a significant effect on the variation of fluid composition in hydrocarbon reservoirs. In addition, they made the key observation that near critical fluid mixture should be expected to have more significant compositional variation than systems away from the critical condition. They reported a decrease in C_1-C_4 fractions with increasing depth and an increase in C5+ with depth. In their model, the rate of change of the mole

fraction of a component with depth is directly proportional to its mole fraction and increases rapidly with an increase in the partial molar volume of the component above the molar volume of the phase as a whole. This is shown in Figure 2.3 where the upper curve is steeper than the lower one because the partial molar volume of methane in the upper curve is higher than in the lower one.
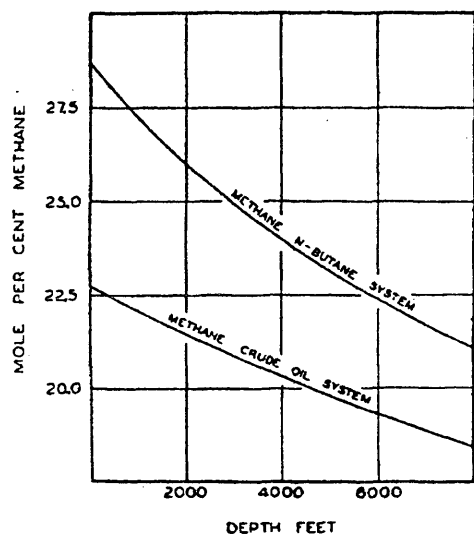
Figure 2.1 Calculated Effect of Depth upon Composition
Of Liquid Mixture of Methane-n-Butane at 220 °F
(Sage and Lacey [1])

Schulte[2] in 1980 was the first to make more realistic calculations using cubic equations of state rather than the ideal solution model used by Sage and Lacy[1] and using the assumption of isothermal system. Schulte investigated the effect of aromatic content, overall pressure, and interaction coefficients on composition gradients using the Soave and Peng-Robinson equations of states. He found that the aromatic fraction of an oil/gas column has a strong influence on the predictions of gravity segregation. The larger the aromatics fraction, the larger the compositional gradient. Also the compositional variations calculated are larger if the initial pressure is lower. Schulte found that the predicted effect of gravity on composition is sensitive to the interaction coefficients used in the equation of state, however, which equation of state to be used in the analysis will affect the result. Most modern compositional gradient calculations presented in the literature usually follow Schulte.

In 1983 Holt et al.[3] studied the effect of gravity on methane distribution in Valhall field in North Sea. He described the oil by two components methane and decane (C_1-C_{10}) and used estimated liquid data in his calculations. Holt et al. used the Soave and Peng-Robinson equation of states in his calculation procedure. Holt et al. method predicts a much smaller effect of gravity than that predicted by Schulte[2] but a larger effect than that predicted by Sage and Lacey[1] method as shown in Table 2.1. Unlike Schulte[2], Holt et al. found that the presence of aromatic components in the oil system did not have a significant effect on compositional grading. Holt et al. showed that the temperature effect could be of the same order of magnitude as the gravitational effect. The observed methane mole fraction gradient in Valhall field is 5×10^{-4} m^{-1}. From the gravitational field alone, the predicted methane mole fraction gradient in oil reservoirs is of the order 0.59×10^{-4} m^{-1} as shown in Table 2.1.

Table 2.1 Calculated Methane Gradients in Oil Reservoirs without Aromatics

Cause of Separation	Source	Mole Fraction Gradient per 100 m
Gravity	Holt[3]	0.0059
Gravity	Sage and Lacey[1]	0.0021
Gravity	Schulte[2]	0.0135
Temperature Field	Holt[3]	0.0056
Gravity and Temperature Fields	Holt[3]	0.0115

Montel and Gouel[5] in 1985 proposed an algorithm which is an iterative calculation based on fugacities of each component at different depths; knowing pressure, temperature and overall composition at a reference depth, they can predict the compositional grading, gas-oil contact location and even physical state change with depth. They discussed the effects of fluid characterization, reservoir pressure, reservoir temperature, and binary interaction coefficients on compositional grading as shown in Figures 2.2, 2.3, and 2.4.
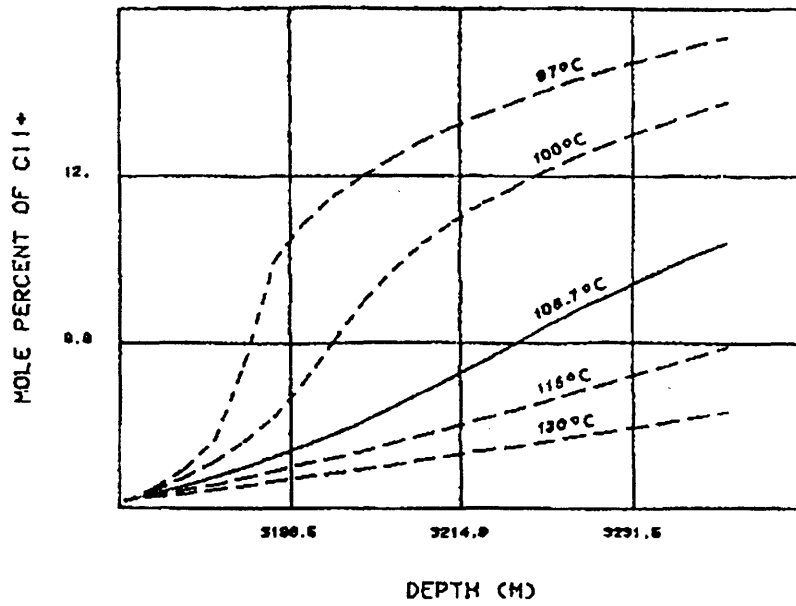
Figure 2.2 C11+ Mole Concentration vs. Depth

(Influence of Reservoir Temperature)

(Montel, *et al.* [5])
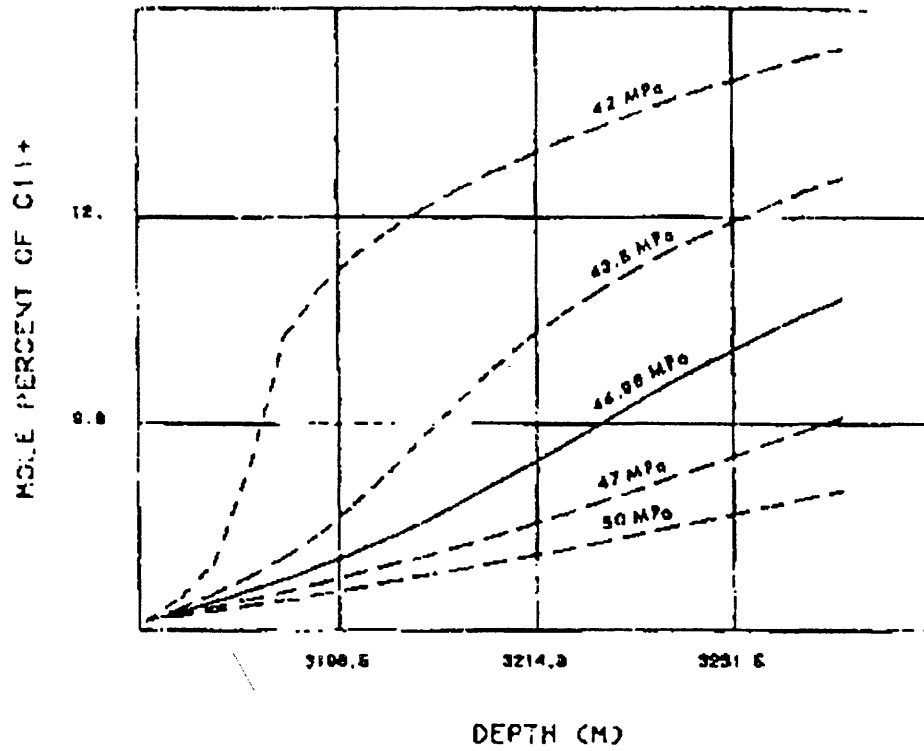
Figure 2.3 C11+ Mole Concentration vs. Depth

(Influence of Reservoir Pressure)

(Montel, et al. [5])
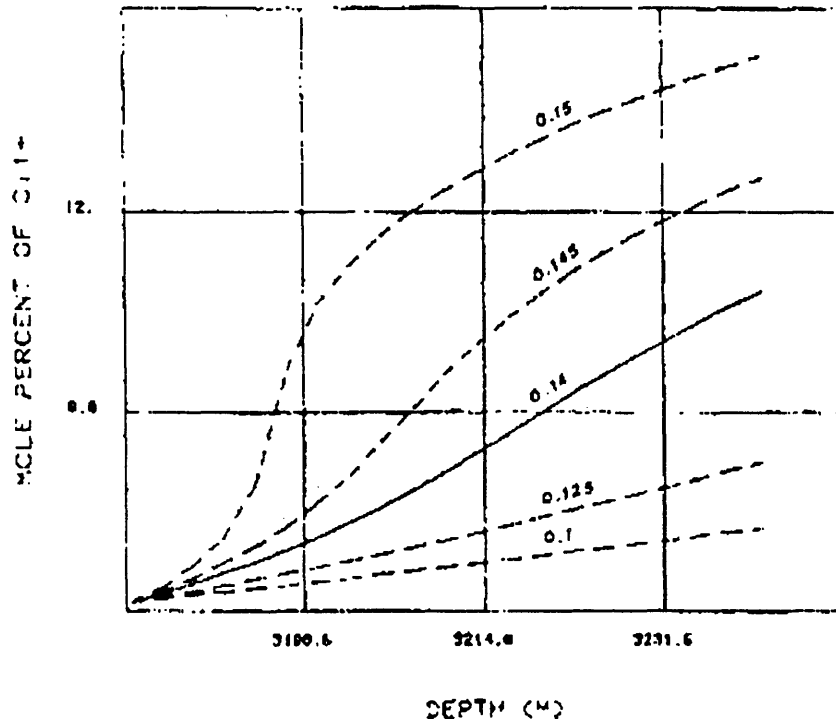
Figure 2.4 C11+ Mole Concentration vs. Depth

(Influence of C1-C11+ Interaction Coefficient)

(Montel, *et al.* [5])

Montel and Gouel[5] found that the mole fraction of C11+ decreases with increasing reservoir pressure and temperature and with decreasing interaction coefficient between C1 and C11+. For the example (North Sea real "critical" fluid) given in their paper, they clearly show that the gravitational segregation alone can largely explain the compositional grading observed in the reservoir. They used the Peng-Robinson equation of state in calculating component fugacities. Above the reference depth calculated compositional variations are much smaller than those indicated by the fluid sample. Their calculated saturation pressure variations were much smaller than measured values, which can be explained by the fact that the composition variations for C1 and C11+ are smaller than those observed.

Creek *et al.*[6] in 1984 performed calculations for the East Painter reservoir that are similar to those of Schulte[3]. Creek *et al.* presented several examples of reservoirs with large closures containing both a volatile oil and rich condensate in the Nuggets Sandstone of the Wyoming Overthrust Belt. They show that the hydrocarbons present in these sandstone reservoirs have physical properties that can be correlated with depth. They further show that for one reservoir, East Painter reservoir, the variation in fluid composition with depth may be predicted with some accuracy by including the gravitational correction term ($m_i gdh$) to the equations governing equilibrium for each component.

In 1984 Hirschberg[7] investigated the influence of asphaltene content in light and heavy oils on compositional grading. He concluded that significant compositional grading with depth could occur in a reservoir due to gravity. In lighter crudes (tank oil gravity $\geq$ 35° API), the strong gravity segregation is expected near the critical condition and depends on asphaltene content. In heavier crudes (tank oil gravity $\leq$

35° API) compositional variations are mainly the result of asphaltene segregation. The lighter the oil and the higher the asphaltene content the stronger the compositional grading is expected to be. Hirschberg[7] agrees with Schulte's[2] observation that the incorporation of heavy aromatics in the C_{7+} representation of a reservoir fluid is essential to obtain a correct description of gravity segregation.

Based on the classical theory of thermodynamic equilibrium, Lee[9] in 1989 developed a general thermodynamic formulation that expresses the component chemical as a function of pressure, temperature, composition, and gravity. The formulation is then coupled to the Peng-Robinson equation of state (PR EOS) to permit reasonably accurate predictions of the in-situ compositional and saturation variations along the capillary zone above the gas-oil contact. The theoretical derivations are made for hydrocarbon fluid systems in the gas cap and above the gas-oil contact (GOC). Lee did show that the amounts of methane in both gas and liquid phases increase gradually as the height above the GOC increases. The reverse is true for the C_{7+} variations in gas and liquid phases.

Jacqmin[10] presented a very simplified system of flow equations. The equations solved hold for a reservoir fluid with an arbitrary number of chemical components in a stratified, anisotropic, tilted reservoir. Jacqmin show how the solutions of the flow equations can be generalized to apply to time-dependent flows and to reservoirs with horizontally gradually varying properties. Lee[9] also concluded that natural convection and diffusional gravity segregation interact to produce a reservoir composition that can vary significantly in both horizontal and vertical directions.

In 1990 Belery and da Silva[11] present a formulation describing the effects of gravity, temperature, and the combined effect of gravity and temperature for a system of zero net mass flux. It has been shown that molecular separation under the geothermal temperature gradient may destroy gravitational segregation. Illustration of their gravity/thermal model is given by presenting a field example using EOS characterization and measured data from Ekofisk field, North Sea.

Wheaton[12] included the influence of capillary pressure on compositional grading. Wheaton studied the effect of neglecting compositional gradients on surface oil production and on the estimate of initial oil in place. Wheaton estimated the total amounts of components in place using full equilibration with allowance for gravity segregation as shown in Table 2.2. Also displayed are the amounts calculated if gravity segregation of components within the gas phase is neglected. Comparing the amounts of components with and without gravity segregation, it is clear that the amount of methane present was underestimated by 1.9 %, while the amounts of butane and octane were overestimated by 8.8% and 18.8%, respectively. With this large extra amount of heavy-end components assumed to be present initially, it is clear that during simulation, calculated surface oil production will be greatly overestimated. If the composition found at the top of the reservoir is assumed to exist throughout the field, the opposite error occurs. In this case, calculated surface oil production will be greatly underestimated.

To show these effects, Wheaton simulated a simple depletion of the gas-condensate reservoir, first with a full equilibration and then assuming the composition found toward the top of the reservoir to hold throughout. Results showed that neglecting compositional gradients in a gas condensate reservoir

might result in an error up to 20% in the estimation of the initial hydrocarbon in place.

Table 2.2 Estimated Hydrocarbon Content of Reservoir
$lb\ mol\ x\ 10^{-8}$ (Wheaton[12])

Component	For the equilibrated reservoir	From composition at top of reservoir	From composition at bottom of reservoir
C_1	1.600	1.635 (2.18% error)	1.579 (1.87% error)
C_4	0.263	0.229 (12.6% error)	0.283 (8.83% error)
C_8	0.138	0.102 (26.4% error)	0.162 (18.8% error)

In 1992 Chaback[13] concluded that the non-isothermal effects could be of the same order of magnitude as gravity effects. He presented a specific example of the consequences of geothermal gradients for a binary system (C_1-nC_4) and he observed that the gravitational effect was nearly twice that caused by thermal diffusion effect.

In 1994 Faissat et al.[14] presented a theoretical review of the influence of gravity and thermal diffusion on compositional grading for multi-component system. Whitson and Belery[15] presented a method for calculating the one-dimension, vertical compositional variations with depth caused by gravity and thermal diffusion. Examples for systems ranging from black oils to near critical oils are

given. They provide guidelines for when to use gradient calculations for reservoirs exhibiting compositional variations.

Recently Firoozabadi[16] in his currently published thermodynamic book gave a full theoretical explanation of the effect of gravity and temperature gradients on the compositional grading in petroleum reservoirs. Conditions for pronounced compositional variations, thermal diffusion and gravity segregation in one dimension, natural convection and diffusion in porous media with field examples were presented.

2.2.1.2   Combined Effects of Gravity and Temperature

The direct effect of temperature gradient is to create a heat flow and hence a convection phenomena. So with higher temperatures at the bottom of the reservoir the lighter components will tend to move upward and the cooler fluid at the top of the reservoir will tend to move downward. Even in the absence of convection phenomena, components of a mixture may separate under the influence of a temperature gradient causing thermal diffusion process. The magnitude and direction of this thermal diffusion process depend upon temperature, pressure, and fluid composition. The tendency of thermal diffusion may be to enhance, reduce, or completely reverse the compositional gradient.

In an attempt to quantitatively explain the observed compositional gradients, few authors have included the effect of thermal diffusion in their calculations. These are Holt et al.[3], Montel and Gouel[5], Belery and da Silva[11], Firoozabadi[16], Firoozabadi et al.[17], Arbabi and Firoozabadi[18], Riley and Firoozabadi[19], Firoozabadi

and Shukla[20], Lira-Galeana *et al.*[21], and Ghorayeb and Firoozabadi[22]. Seven of these references will be discussed below.

Holt *et al.*[3] studied the effect of gravity and temperature on methane distribution in Valhall field in North Sea using irreversible thermodynamics. Holt studied the effect of temperature field using an estimated thermal diffusion factor. Holt showed that the temperature effect could be of the same order of magnitude as the gravitational effect. The predicted methane mole-fraction gradient in oil reservoirs is of the order 5.6×10^{-4} m^{-1}.

Montel and Gouel[5] in 1985 suggested that thermal diffusion may improve the reliability of calculating compositional gradients but deliberately they neglected it since thermal diffusion coefficients (value and sign) are not known. Unfortunately, unlike the calculation of the gravitational segregation force, determining the thermal force does pose a serious problem especially under the severe temperature and pressure conditions of reservoirs. As far as the geothermal temperature gradients are concerned, the two forces are generally opposite. For methane, for instance, the thermal force is downward while the gravitational segregation force is upward; with usual gradient values, thermal force is probably the lower. However they think thermal force plays an important role in the generation process of the concentration gradient (molecular diffusion) corresponding to the stationary state.

In 1990 Belery and da Silva[11] were the first to report calculations showing qualitatively the effect of thermal diffusion for multi-component system. They proposed diffusive flux expressions that may be used to calculate the compositional equilibrium of hydrocarbon reservoir including the effect of thermal

diffusion. Illustration of their gravity/thermal model is given by presenting a field example using EOS characterization and measured data from Ekofisk field, North Sea. Order of magnitude calculations were presented to check the importance of thermal diffusion compared to gravitational diffusion. It is seen that thermal diffusion could significantly contribute to mass transport in hydrocarbon reservoir. In addition thermal diffusion has been shown to significantly affect the gravitational equilibrium.

Firoozabad[16] predicted compositional gradient under isothermal and non-isothermal conditions considering the effect of gravity and temperature gradients. He discussed the compositional gradient in one and two dimensions considering all mechanisms responsible in initiating the composition grading such as pressure diffusion, thermal diffusion, and thermal convection. Riley and Firoozabadi[19] investigate the compositional variation of a single-phase, two-component system due to the combined effects of natural convection and diffusion. The reason convection has been considered was that the horizontal compositional variation was the main issue.

Firoozabadi *et al.*[20] presented a new model for the prediction of thermal diffusion ratio in binary mixtures of reservoir fluid using the thermodynamic of irreversible process. Firoozabadi *et al.*[20] model showed better performance in different non-ideal conditions but away from the critical region. Ghorayeb, *et al.*[22] use the model to study the fluid distribution and gas oil ratio behavior in the Yufutsu fractured gas-condensate field in Japan. The major conclusion drawn in their research was that thermal diffusion significantly affects the variations of fluids in the field to the extent that such variation causes heavier reservoir fluids to float on top of the lighter reservoir fluid.

2.2.2 Field Observations

Variations of hydrocarbon fluid properties have been observed and discussed for many reservoirs around the world. Hamoodi et al.[4], Temeng et al.[23], Machel et al.[24], Worden et al. [25-27], Lira-Galeana et al.[21], Riemens[28], and Grant[29] discussed gradients for reservoirs in the Middle East; Metcalf et al.[30], Hearn and Whitson[31], Espach et al.[32], Welge[33], Rzasa[34], McCord[35] and Cupps[36] discussed gradients for reservoirs in North America; El-Mandouh et al.[37] and Alonso et al.[38] discussed reservoirs in Africa; Schulte[2], Holt et al.[3], Bachman et al.[39], Kingston et al.[40] and et al.[41] discussed reservoirs in the North Sea; Broekers et al.[42], Neveux et al.[43], Maan et al.[44], Ortega et al.[45] and Rosales et al.[46] discussed reservoirs in Venezuela; and Ghorayeb et al.[27] for the Yufutsu reservoir in Japan. Six of these references which represent the several regions will be highlighted below.

Hamoodi et al.[4] presented a compositional modeling of one of the giant reservoirs in the Middle east (Abu Dhabi) that exhibits significant areal and vertical variation in composition. The areal variation in composition is mainly due to the H_2S content, which varies from more than 10 mole percent in the North to less than 1 mole percent in the South, while the vertical variation is attributed to gravity and temperature gradient effects. They reported an established gradient of methane of 0.64 to 4.07 mole % per 100 ft compared to 1.5 mole percent per 100 ft for methane reported by Holt et al.[3]. The resulting model was validated against observed pressure and saturation data, therefore they concluded that their attempt to model compositional variation was successful.

Another study done by Riemens et al.[28] on Birba field (initial reservoir pressure is 7720 psi) located in Oman, indicated that the PVT properties of the reservoir

were strongly depth-dependent, explaining the presence of significantly undersaturated oil only 655 ft below a gas cap.

In the Ghawar field located in Saudi Arabia, Temeng et al.[23] observed compositional grading that is opposite to chemical-gravity equilibria principles. They observed that heavy and light hydrocarbon mole fractions decrease with depth while the composition of acid gases (H_2S, CO_2) increase with depth. They believed that the increase of the composition of hydrogen sulfide was in the expense of the decrease in hydrocarbon mole fractions especially the heavy end components.

Temeng et al.[23] concluded that there is an evidence of a threshold temperature (270 °F) above which hydrogen sulfide is formed. They found out that, according to a theory (the source of H_2S in the Khuff reservoirs is thermo-chemical sulfate reduction) mentioned in their study, sulfate (anhydrite) reacts with hydrocarbon (such as methane) to produce H_2S and carbonate as shown in the following reaction. For more details about these reduction reactions see Machel et al.[11]

$$CaSO_4 + CH_4 \rightarrow CaCO_3 + H_2S + H_2O$$

Warden et al.[8,9,10] made similar observations in the Khuff reservoirs of Abu Dhabi and suggested a threshold temperature of about 284 °F. Therefore H_2S is generated at the expense of methane and probably hydrocarbons of higher carbon numbers. Because of these sulfate-reduction reactions, Temeng et al. observed in the Khuff carbonate reservoir of the Ghawar field in Saudi Arabia that all hydrocarbon components including heavy ends decrease in composition with

depth while the non-hydrocarbon gases, H_2S and CO_2, increase in composition with depth.

Another indirect support for the thermo-sulfate reduction theory is the observation that in the Khuff reservoir, the deeper clastic reservoirs (which have no anhydrite) are consistently free of hydrogen sulfide.

Metcalf et al.[29] in 1985 correlated compositional variations graphically based on measured data (Anschutz Ranch East Field, USA) rather than using gravity/chemical equilibrium and the developed equation of state characterization. They developed linear correlations of compositional gradient with depth that can be used by engineers to estimate compositions at any bottom-hole location and then proceed using other methods such as equation of state to estimate fluid properties. The correlations were tested against experimental data and calculated phase equilibria and concluded that the correlations yield satisfactory results in the field studied.

Espach et al.[32] published materials which show significant change in physical characteristics of crude oil with depth in the Tensleep Reservoir located in the Rocky Mountain region (Elk Basin Field, Wyoming and Montana). The saturation pressure and gas-oil ratio at the crest of the structure are 1250 psia and 490 scf/bbl respectively and 530 psia and 134 scf/bbl on the flanks of the structure. Study of the magnitude of change in fluid properties of the sub-surface oil samples from Elk Basin definitely indicates that the fluids in a reservoir are not necessarily in equilibrium. It is concluded that either extremely long periods of time are necessary to effect equilibrium or that accumulation can be quite young, or still taking place in some petroleum reservoirs.

Two authors discussed the paper of Espach et al.[32]: Welge[33] and Rzasa[34]. Agreeing with Espach et al.., Welge concluded that reservoir fluid systems are not at equilibrium. He supported this conclusion by giving examples from Sage and Lacey[1,47] that calculate for a similar reservoir the variation expected because of gravitational segregation and segregation due to temperature difference. The calculated variations for methane were only about 1/20 of the average amount of methane in solution. This explanation obviously would not account for the differences observed at Elk Basin. In his conclusion, Welge said, "Apparently considerations other than the assumption of incomplete attainment of equilibrium lead to the conclusion that comparatively little variation in petroleum composition should be observed in reservoir at equilibrium, even though its closure extends over one thousand feet. This conclusion is demonstrated by the existence of a number of oil reservoirs having a large closure, but whose petroleum is of substantially uniform composition. Therefore, when a considerable variation in composition is encountered, as at Elk Basin, a satisfactory explanation may be incomplete diffusional approach toward equilibrium".

Rzasa[34] did not agree with the conclusion of Espach et al.[32] Rzasa said "Thermodynamic equilibrium demands that this change in properties occur with change in elevation". He gave an example about Dominguez Field crude oil which show that for a change in elevation of approximately 2000 ft, the bubble point of the oil at 160 °F changes approximately 885 psi. Rzasa also said " the isothermal effects indicating change in composition with elevation would be expected to be enhanced by a gradual increase in temperature as depth is increased".

In a reply to Rzasa, Espach *et al.* [32] said "M. J. Rzasa's comment that change in composition of reservoir oil with elevation is to be expected at conditions of thermodynamic equilibrium is correct. This does not, however, make incorrect the conclusions reached by the authors". Espach *et al.* conclusion is substantiated further by a study of the properties versus structure of the original reservoir oil in the Weber Sandstone Reservoir, Rangely Oil Field, Colorado[36] which is geologically an equivalent formation to Elk Basin. The calculated changes in composition (using equations defining thermodynamic equilibrium) still show small changes compared to the measured data. This change will account for only one fourteenth of the actual change found by sampling as shown in Tables 2.2 and 2.3. Espach *et al.* believed that the change of 885 psi in bubble point with 2000 ft change in elevation at thermodynamic equilibrium calculated by Rzasa for Domingues Field crude oil data is in error and that these data indicate a change of about 70 psi.

Table 2.3 Composition as a Function of Depth
Field Data (Espach, *et al.*[32])

Depth, ft	Butanes & lighter, mole % liquid	Pentanes & heavier, mole % liquid
0	44.29	55.71
840	30.57	69.43
%Change	-13.72	13.72

Table 2.4 Composition as a Function of Depth
Calculated (Espach, *et al.*[32])

Depth, ft	Butanes & lighter, mole % liquid	Pentanes & heavier, mole % liquid
0	44.29	55.71
840	43.35	56.65
%Change	-0.94	0.94

Ghorayeb et al.[27] reported unusual fluid distribution and production profiles for Yufutsu Field in Japan. This field is a recently discovered naturally fractured reservoir with negligible matrix porosity and permeability. It is a large reservoir containing near-critical gas condensate fluids. The initial reservoir pressure is about 8000 psi and the temperature is 302 °F at 14,800 ft vertical depth. No distinct gas-water contact or gas-oil contact has been observed.

One of the unusual and unique feature that was observed and reported by Ghorayeb et al.[27] is that gas oil ratio decreases gradually from 1350 m^3/m^3 to about 1000 m^3/m^3 which is opposite to the usual trend seen in all petroleum reservoirs. Another interesting feature of this reservoir is that gas production has a decreasing trend while the condensate rate stays constant. Measured data from some wells in the formation show that the mole fraction of the heavy components (C_{7+}) decreases while that of the lighter fractions (methane) increases with depth. Steady-state data for some wells at shut-in conditions show liquid contained in the middle, and gas in the top and the bottom.

In the conclusion, Ghorayeb et al.[27] attributed the strange features of the field to the effect of thermal diffusion, which can cause the heavier reservoir fluids to float on top of lighter reservoir fluids.

2.2.3 Experimental Studies

As mentioned earlier, the petroleum literature lacks any publications on laboratory work considering the combined effect of gravity and temperature gradients on compositional gradients in hydrocarbon reservoir. The only

experimental work on compositional gradient available in the literature was about the isothermal effect that is the effect, of gravity on the composition in petroleum reservoir, which will be given below.

Maan[48] has done experimental work using centrifuge to investigate the effect of gravity on compositional gradients. Maan did isothermal experiments using C_1-C_3 binary gas mixture and did not come up with clear compositional grading in his results.

Ratulowski, et al.[49] conducted isothermal experiments using a centrifuge system. They used simple ternary system as an initial test to fit the data to the available equation of state models. Once they build some confidence on the performance of the system, they started to use live oil samples collected from a reservoir with significant variation in fluid properties. They reported that the results obtained from the centrifuge were in agreement with the field data. Accordingly Ratulowski concluded that significant compositional variation of reservoir fluids not near their vapor-liquid critical points can be caused by gravity alone.

2.3 Equations for Calculating Compositional Gradient [50-59]

Equations for calculating compositional gradient under isothermal and non-isothermal conditions are included in this section. First, for isothermal conditions, two approaches are used to derive these equations: a thermodynamic approach, and a transport phenomena approach. Ideal and non-ideal phase behaviors are considered in developing these equations. For non-isothermal conditions, a

transport approach for calculating gradients is presented next. Finally, equations for estimating thermal diffusion coefficients are given.

2.3.1 Compositional Gradient under Isothermal Condition

For isothermal conditions, a thermodynamic approach and a transport phenomena approach are used to obtain the same equation for calculating the composition gradient. Each of these approaches is described below.

2.3.1.1 Thermodynamic Approach

In this section, a thermodynamic derivation of the basic equation for composition gradients in isothermal systems is presented. This derivation begins at the first law of thermodynamics:[50-53]

$$dU = dQ - dW \qquad (2.1)$$

In general, the effect of gravity is neglected in phase equilibria calculations for hydrocarbon fluids. The work term dW in equation 2.1 represents only the moving boundary work, $dW_b = PdV$ of expansion or compression done by the system on the surrounding

$$dW = dW_b = PdV \qquad (2.2)$$

The heat absorbed by the system dQ is given by

$$dQ = TdS \qquad\qquad (2.3)$$

Substituting equations 2.2 and 2.3 into equation 2.1 gives

$$dU = TdS - PdV \qquad\qquad (2.4)$$

Now if the fluid of mass m is experiencing both compression/expansion and a vertical change in position the work term dW will have different form from the one expressed by equation 2.2. In this case an amount of work, dW_g is required to raise the fluid certain height dz. Therefore equation 2.2 becomes

$$dW = dW_b + dW_g$$
$$dW = PdV - mgdz \qquad\qquad (2.5)$$

Substituting equations 2.3 and 2.5 into equation 2.2 gives

$$dU = TdS - PdV + mgdz \qquad\qquad (2.6)$$

Since Gibbs free energy can be expressed in the form

$$dG = dU - d(TS) - d(PV) \qquad\qquad (2.7)$$

Substituting equation 2.6 in equation 2.7 and expanding gives

$$dG = -SdT + VdP + mgdz \qquad (2.8)$$

At thermodynamic equilibrium ($dG = 0, dT = 0$), equation 2.8 becomes

$$VdP + mgdz = 0 \qquad (2.9)$$

Since $\rho = \left(\dfrac{m}{V}\right)$ then, equation 2.9 can be written as

$$dP = -\rho g dz \qquad (2.10a)$$

In terms of centrifuge parameters, equation 2.10a can be written as

$$dP = \rho \omega^2 r dr \qquad (2.10b)$$

where r is the distance from the center of spin and ω is the centrifuge spinning rate. Equation 2.10 is the hydrostatic head.

Equation 2.10 is the hydrostatic head.

For an open system (neglecting the effect of gravity), another type of work encountered due to the transfer of various components across the system (a change in composition). This type of work is called the chemical work, which is given by $dW_c = \sum_i^c \mu_i dn_i$.

Therefore the expression for dU becomes

$$dU = TdS - PdV + \sum_{1}^{c} \mu_i dn_i \qquad , \ i = 1,2,\ldots\ldots,c \qquad (2.11)$$

In the presence of gravity, for an open system, the gravitational work term will have the following form[16]

$$dW_g = d(mgz)$$

where

$$m = \sum_{i}^{c} n_i M_i$$

So

$$dW_g = d\left[\left(\sum_{i}^{c} n_i M_i\right) gz\right]$$

Including the gravitational term in equation 2.11 and rearranging gives

$$dU = TdS - PdV + \sum_{1}^{c} \mu_i dn_i + d\left[\left(\sum_{i}^{c} n_i M_i\right) gz\right], \quad i = 1,2,\ldots\ldots,c$$

$$dU = TdS - PdV + \sum_{1}^{c} \left(\mu_i + M_i gz\right) dn_i + mgdz, \quad i = 1,2,\ldots,c \qquad (2.12)$$

The expansion of the change in Gibbs free energy gives

$$dG = -SdT + VdP + \sum_{1}^{c} \left(\mu_i + M_i gz\right) dn_i + mgdz, i = 1,2,....,c \qquad (2.13)$$

At equilibrium, $dG = 0$, and $dT = 0$, therefore equation 2.13 becomes

$$VdP + \sum_{1}^{c} \left(\mu_i + M_i gz\right) dn_i + mgdz = 0, \quad i = 1,2,....,c \qquad (2.14)$$

Since z and P are dependent variables, then

$$\mu_i + M_i gz = const., i = 1,2,.........,c \qquad (2.15)$$

$$VdP + mgdz = 0, i = 1,2,.....,c \qquad (2.16)$$

Equation 2.16 is the same expression obtained previously which is the equation for the hydrostatic head, equation 2.10.

Differentiating equation 2.15 gives,

$$\left(d\mu_i = -M_i gdz\right)_T, i = 1,2,.....,c \qquad (2.17)$$

According to equation 2.17 it can be concluded that in a multi-component system under isothermal equilibrium and in the presence of gravitational field, the chemical potential of ith component, μ_i, is a function of depth or position. This functionality represents a compositional gradient.

Let us write $d\mu_i$ from equation 2.17 in terms of the independent variables, $P, x(x_1, x_2, \ldots, x_{c-1})$:

$$\left[d\mu_i = \left(\frac{\partial \mu_i}{\partial P} \right)_{x_i} dP + \sum_{j=1}^{c-1} \left(\frac{\partial \mu_i}{\partial x_j} \right)_{P, x_j} dx_j \right]_T , i = 1, 2, \ldots, c-1 \qquad (2.18)$$

Combining $\left(d\mu_i = \overline{V}_i dP \right)_{T,x}$, equations 2.17, 2.18, and 2.10 gives,

$$\sum_{j=1}^{c-1} \left(\frac{\partial \mu_i}{\partial x_j} \right)_{P,T,y_j} \left(\frac{dx_j}{dz} \right) = \left(\rho \overline{V}_i - M_i \right) g, i = 1, 2, \ldots, c-1 \qquad (2.19)$$

In this research, two-component or binary systems are considered. For a binary mixture, equation 2.19 can be written as

$$\left(\frac{d\mu_1}{dx_1} \right)_{P,T} \left(\frac{dx_1}{dz} \right) = \left(\rho \overline{V}_1 - M_1 \right) g \qquad (2.20)$$

Equation 2.20 can be expressed in terms of fugacity $\left(d\mu_1 = RTd \ln f_1 \right)_T$ as

$$\left(\frac{d \ln f_1}{dx_1} \right)_{P,T} \left(\frac{dx_1}{dz} \right) = \frac{g}{RT} \left(\rho \overline{V}_1 - M_1 \right) \qquad (2.21)$$

$$\left(\frac{dx_1}{dz} \right) = \left(\frac{d \ln x_1}{d \ln f_1} \right)_{P,T} \frac{g x_1}{RT} \left(\rho \overline{V}_1 - M_1 \right) \qquad (2.22)$$

In terms of centrifuge parameters, equation 2.22 can be written as

$$\left(\frac{dx_1}{dr}\right) = \left(\frac{d\ln x_1}{d\ln f_1}\right)_{P,T} \frac{x_1\omega^2 r}{RT}\left(M_1 - \rho\overline{V}_1\right)$$

(2.23)

The form of equation 2.23 can be altered using

$$\rho = \frac{\left[\sum\limits_{i=1}^{2} x_i M_i\right]}{\left[\sum\limits_{i=1}^{2} x_i \overline{V}_i\right]} = \frac{x_1 M_1 + x_2 M_2}{x_1 \overline{V}_1 + x_2 \overline{V}_2}$$

(2.24)

Then, equation 2.23 becomes

$$\left(\frac{dx_1}{dr}\right) = \left(\frac{d\ln x_1}{d\ln f_1}\right)_{P,T} \frac{x_1\omega^2 r}{RT}\left(M_1 - \left(\frac{x_1 M_1 + x_2 M_2}{x_1 \overline{V}_1 + x_2 \overline{V}_2}\right)\overline{V}_1\right)$$

(2.25)

Equation 2.25 provides a means for calculating composition for a given temperature and pressure. The pressure at each elevation is obtained by integrating the static pressure gradient:

$$\frac{dP}{dr} = \rho\omega^2 r$$

(2.26)

Equations 2.25 and 2.26 are two first order differential equations and their solution provides P and x_1. Pressure and composition at a reference depth should be given. A numerical method such as Euler or Runge-Kutta[60] can be used.

For an ideal system one can start with equation 2.23 setting the derivative on the right hand side equal to one:

$$\left(\frac{dx_1}{dr}\right) = \frac{x_1\omega^2 r}{RT}\left(M_1 - \rho\overline{V}_1\right)$$

(2.27)

Equation 2.27 has the same form Sage and Lacey[1] used in their model to calculate compositional gradient in petroleum reservoirs.

For an ideal gas

$$\overline{V}_1 = \overline{V}_2 = \overline{V}_m = \frac{V}{n} = \frac{RT}{P}$$

(2.28)

and the mixture density is

$$\rho = \frac{PM}{RT}$$

(2.29)

Equation 2.27 can be further simplified by substituting equations 2.28 and 2.29

$$\left(\frac{dx_1}{dr}\right) = \frac{x_1\omega^2 r}{RT}(M_1 - M)$$ (2.30)

M is the mixture molecular weight, defined as

$$M = x_1 M_1 + x_2 M_2$$
$$= x_1 M_1 + (1 - x_1)M_2$$ (2.31)

Substituting equation 2.31 in equation 2.30 gives

$$\frac{dx_1}{dr} = \frac{\omega^2 r x_1}{RT}[(M_1 - M_2)(1 - x_1)]$$ (2.32)

By substituting equation 2.29 in equation 2.26, the hydrostatic head equation for an ideal gas becomes

$$\frac{dP}{dr} = \frac{PM}{RT}\omega^2 r$$ (2.33)

Equations 2.32 and 2.33 are two first order differential equations for an ideal, binary gas, and their solution provides P and x_1. Pressure and composition at a reference depth should be given. Numerical methods such as Euler or Runge-Kutta can be used.

2.3.1.2 Transport Phenomena Approach

Equations 2.25 and 2.32 also can be derived using a transport phenomena approach as shown below.

The expression for the total diffusion mass flux in a binary system for component 1 is given by Bird et al.[53]:

$$j_1 = -j_2 = -\left(\frac{c^2}{\rho}\right)M_1 M_2 D_{12} x_1 \left[\begin{array}{l}\left(\frac{\partial \ln f_1}{\partial \ln x_1}\right)_{T,p} \nabla x_1 - \frac{M_1 x_1 \rho_2}{\rho RT}(g_1 - g_2) + \\ \frac{M_1 x_1}{RT}\left(\frac{\overline{V}_1}{M_1} - \frac{1}{\rho}\right)\nabla p + k_T \nabla \ln T \end{array}\right]$$

(2.34)

Four different diffusion processes are included in equation 2.34. These are the molecular or ordinary diffusion, the forced diffusion, the pressure diffusion, and thermal diffusion. The ordinary diffusion depends on the concentration gradients of all substances present. The forced diffusion term is of primary importance in ionic systems. In such systems, each ionic species is exposed to different external forces. If gravity is the only external force, then g_1 and g_2 are the same and the forced diffusion term vanishes completely. The pressure diffusion, which under the effect of gravity leads to gravity segregation, depends on the pressure gradient imposed on the system. Under normal pressure gradients, the tendency for a mixture to separate is very small, but in centrifuge separation where tremendous pressure gradients may be established, the separation could be achieved. The

thermal diffusion term describes the tendency for species to diffuse under the influence of a temperature gradient.

For an isothermal system ($\nabla \ln T = 0$) with no species-selective body forces ($g_1 - g_2 = 0$), equation 2.34 reduces to the following equation

$$j_1 = -j_2 = -\left(\frac{c^2}{\rho}\right) M_1 M_2 D_{12} x_1 \left[\left(\frac{\partial \ln f_1}{\partial \ln x_1}\right)_{T,p} \nabla x_1 + \frac{M_1 x_1}{RT}\left(\frac{\overline{V}_1}{M_1} - \frac{1}{\rho}\right)\nabla p\right]$$

(2.35)

Equation 2.35 describes the molar flux that produces gravity segregation of components. If it is applied to an equilibrium distribution of components the net mass flux j_1 is zero; so, equation 2.35 becomes

$$\left[\left(\frac{\partial \ln f_1}{\partial \ln x_1}\right)_{T,p} \nabla x_1 + \frac{M_1 x_1}{RT}\left(\frac{\overline{V}_1}{M_1} - \frac{1}{\rho}\right)\nabla p\right] = 0$$

(2.36)

For a single-dimension system, the gradient of composition is as follows:

$$\nabla x_1 = \frac{\partial x_1}{\partial r}$$

(2.37)

In terms of centrifuge parameters,

$$\nabla P = \frac{\partial P}{\partial r} = \rho \omega^2 r \tag{2.38}$$

Substituting equations 2.37 and 2.38 in equation 2.36 and simplifying gives

$$\left(\frac{dx_1}{dr}\right) = \left(\frac{d \ln x_1}{d \ln f_1}\right)_{P,T} \frac{\omega^2 r x_1}{RT}\left(M_1 - \rho \overline{V}_1\right) \tag{2.39}$$

The form of equation 2.39 can be altered using equation 2.24 to give

$$\left(\frac{dx_1}{dr}\right) = \left(\frac{d \ln x_1}{d \ln f_1}\right)_{P,T} \frac{x_1 \omega^2 r}{RT}\left(M_1 - \left(\frac{x_1 M_1 + x_2 M_2}{x_1 \overline{V}_1 + x_2 \overline{V}_2}\right)\overline{V}_1\right) \tag{2.40}$$

Equation 2.40 has an identical form as equation 2.25.

Equation 2.40 provides a means for calculating composition for a given temperature and pressure. The pressure at each elevation is obtained by integrating the static pressure gradient:

$$\frac{dP}{dr} = \rho \omega^2 r \tag{2.41}$$

Equations 2.40 and 2.41 are two first order differential equations and their solution provides P and x_1. Pressure and composition at a reference depth should be given. A numerical method such as Euler or Runge-Kutta ones can be used.

For an ideal system one can start with equation 2.39 setting the derivative on the right hand side equal to one:

$$\left(\frac{dx_1}{dr}\right) = \frac{x_1\omega^2 r}{RT}\left(M_1 - \rho\bar{V}_1\right) \tag{2.42}$$

Substituting equations 2.28, 2.29, and 2.31 in equation 2.42 gives

$$\frac{dx_1}{dr} = \frac{\omega^2 r x_1}{RT}\left[(M_1 - M_2)(1 - x_1)\right] \tag{2.43}$$

Equation 2.43 has an identical form as equation 2.32.

By substituting equation 2.29 in equation 2.26, the hydrostatic head equation for an ideal gas becomes

$$\frac{dP}{dr} = \frac{PM}{RT}\omega^2 r \tag{2.44}$$

Equations 2.43 and 2.44 are two first order differential equations and their solution provides P and x_1. Pressure and composition at a reference depth should be given. Numerical methods such as Euler or Runge-Kutta can be used.

2.3.2 Compositional Gradient under Non-isothermal Condition[57]

By considering molecular, pressure, and thermal diffusion processes, equation 2.34 can be written as

$$j_1 = -j_2 = -\left(\frac{c^2}{\rho}\right)M_1 M_2 D_{12} x_1\left[\left(\frac{\partial \ln f_1}{\partial \ln x_1}\right)_{T,p} \nabla x_1 + \frac{M_1 x_1}{RT}\left(\frac{\overline{V}_1}{M_1} - \frac{1}{\rho}\right)\nabla p + k_T \nabla \ln T\right]$$

(2.45)

At steady state the net mass flux j_1 is zero so equation 2.35 becomes

$$\left[\left(\frac{\partial \ln f_1}{\partial \ln x_1}\right)_{T,p} \nabla x_1 + \frac{M_1 x_1}{RT}\left(\frac{\overline{V}_1}{M_1} - \frac{1}{\rho}\right)\nabla p + k_T \nabla \ln T\right] = 0$$

(2.46)

For a single-dimension system, the temperature gradient is as follows:

$$\nabla \ln T = \frac{1}{T}\frac{dT}{dr}$$

(2.47)

Substituting equations 2.37, 2.38, and 2.47 in equation 2.46 and simplifying gives

$$\left(\frac{dx_1}{dr}\right) = \left(\frac{d \ln x_1}{d \ln f_1}\right)_{P,T} \frac{x_1 \omega^2 r}{RT}\left(M_1 - \rho \overline{V}_1\right) - \frac{k_T}{T}\frac{dT}{dr}$$

(2.48)

The form of equation 2.48 can be altered using equation 2.24 to give

$$\left(\frac{dx_1}{dr}\right) = \left(\frac{d\ln x_1}{d\ln f_1}\right)_{P,T} \left[\frac{x_1\omega^2 r}{RT}\left(M_1 - \left(\frac{x_1 M_1 + x_2 M_2}{x_1 \overline{V}_1 + x_2 \overline{V}_2}\right)\overline{V}_1\right) - \frac{k_T}{T}\frac{dT}{dr}\right] \quad (2.49)$$

Equation 2.49 provides a means for calculating composition for a given temperature and pressure. The pressure at each elevation is obtained by integrating the static pressure gradient:

$$\frac{dP}{dr} = \rho\omega^2 r \quad (2.50)$$

Equations 2.49 and 2.50 are two first order differential equations and their solution provides P and x_1. Pressure and composition at a reference depth should be given. Numerical methods such as Euler or Runge-Kutta can be used.

For an ideal system one can start with equation 2.48 setting the derivative on the right hand side equal to one:

$$\left(\frac{dx_1}{dr}\right) = \frac{x_1\omega^2 r}{RT}\left(M_1 - \rho\overline{V}_1\right) - \frac{k_T}{T}\frac{dT}{dr} \quad (2.51)$$

Substituting equations 2.28, 2.29, and 2.31 in equation 2.51 gives

$$\frac{dx_1}{dr} = \frac{\omega^2 r x_1}{RT}\left[(M_1 - M_2)(1 - x_1)\right] - \frac{k_T}{T}\frac{dT}{dr} \quad (2.52)$$

Equation 2.52 provides a means for calculating composition for a given temperature and pressure. The pressure at each elevation is obtained by integrating the static pressure gradient:

$$\frac{dP}{dr} = \rho \omega^2 r \qquad (2.53)$$

Equations 2.52 and 2.53 are two first order differential equations and their solution provides P and x_1. Pressure and composition at a reference depth should be given. Numerical methods such as Euler or Runge-Kutta can be used.

2.4 Estimating Thermal Diffusion Ratio

With thermal diffusion, a temperature gradient in a mixture, which may be gas, liquid, or solid; gives rise to a concentration gradient of the constituents. Thermal diffusion is important for the study of fluid composition variations in petroleum reservoirs (oil and gas reservoirs) and it can either enhance or weaken the separation in mixtures. The thermal diffusion ratio k_T of equation 2.49 is a measure of thermal diffusion; the sign of k_T determines the direction of thermal diffusion. k_T is proportional to the ratio of thermal diffusion coefficient D_T to the normal diffusion D_{AB}:

$$k_T = \frac{\rho D_T}{c^2 D_{AB} M_A M_B} \qquad (2.54)$$

This ratio is very sensitive to the properties of the component mixture.[53,54,57,58]

In low-pressure gaseous mixtures and in ideal liquid mixtures, k_T has been found to be small and the molecular mass and size are the main parameters that govern the magnitude of k_T.[55] On the other hand, in non-ideal gas and liquid mixtures k_T may be large, particularly when conditions are close to the critical point.

For low pressure gaseous mixtures, a method for estimating the thermal diffusion ratio k_T is given by Hirschfelder et al[55]. I wrote a Fortran 77 program to calculate the thermal diffusion ratio using the method of Hirschfelder et al. The equations for this program are listed on page 541 of Chapter 8 of Hirschfelder et al. The Hirschfelder et al. approximation of thermal diffusion ratio gives reasonable values for binary gas mixtures at low pressure. Incidentally, in Table 18.4-1 of Bird et al.,[53] which is based on Table 8.4-14 of Hirschfelder et al., the x_A for the composition of gases should read x_B. I found this error in Bird et al. while checking the predictions of the Fortran 77 program. In email communications with Professor Bird, it was learned that this error had not been detected previously. He was surprised to find such an error after 40 years in print.

For binary mixtures at high pressures, a number of models are available (Rutherford,[61] Haase,[62] Kempers,[63] Dougherty and Drickamer[64]) which are based on phenomenological and kinetic approaches. After discussing these previous models, Firoozabadi et al.[20] proposed a new model for calculating thermal diffusion coefficient using the thermodynamics of irreversible processes. The

model needs equilibrium properties of mixtures and energy of viscous flow. Equilibrium properties are obtained from the volume translated Peng-Robinson equation of state, and the energy of viscous flow is estimated from viscosity data. The expression for the thermal diffusion coefficient of component 1 in a binary mixture as given by Firoozabadi et al.[20] is as follows:

$$\alpha_T = \left[\frac{\left(\overline{U}_1 / \tau_1 - \overline{U}_2 / \tau_2\right)}{x_1 \left(\partial \mu_1 / \partial x_1\right)_{T,P}} + \frac{\left(\overline{V}_2 - \overline{V}_1\right)\left(x_1 \overline{U}_1 / \tau_1 - x_2 \overline{U}_2 / \tau_2\right)}{\left(x_1 \overline{V}_1 - x_2 \overline{V}_2\right)x_1 \left(\partial \mu_1 / \partial x_1\right)_{T,P}} \right] \tag{2.55}$$

$$\alpha_T = \frac{k_T}{x_1 x_2} \tag{2.56}$$

The model has been applied to predict thermal diffusion ratios of several mixtures consisting of non-hydrocarbon and hydrocarbon fluids. Comparisons of theoretical results with experimental data show a good performance of the model except in the near-critical region where all existing models are deficient. Firoozabadi et al.[20] modified the Rutherford,[61] Haase,[62] and Kempers[63] models by incorporating a more accurate equation of state. Firoozabadi et al.[20] concluded that his model is superior to the modified Kempers[63] and Rutherford,[61] models in describing experimental results for the thermal diffusion coefficients in binary mixtures.

In my research, I have compared thermal diffusion ratios obtained by the best-fit to the experimental data produced in this research with those predicted by Firoozabadi et al.[20] model, equation 2.55 as will be shown in Chapter 4.

2.5 PVT Behavior of Methane-Propane Binary System

For the present research, experiments focussed on composition gradients with a methane-propane mixture. The reasons for selecting this particular binary pair will be described in Chapter 3. Here, the literature on this binary pair will be summarized. Several investigators have studied the methane-propane system throughout the temperature and pressure ranges commonly found in hydrocarbon reservoirs. This system may be considered as illustrating the behavior of a simplified case of near-critical reservoir fluids. Complete equilibrium data in the form of tables and graphs for various systems starting from pure propane to pure methane, including compositions very close to those used in this research methane-propane system are available in the literature (Sage and Lacey[47,65] and Reamer, et al.[66]). These data sets were very useful for checking equation of state calculations.

Pressure-temperature phase diagrams were constructed at different mole fractions of methane and propane as shown in Figures 2.5, 2.6, and 2.7. These pressure-temperature phase diagrams were constructed using a fluid phase equilibria package available in the internet site of Quest Consultants Inc (www.questconsult.com). The phase diagrams obtained using Quest Consultants package were checked using ASPEN package. Figure 2.8 shows the pressure-composition diagram for methane-propane system at different temperatures. These phase diagrams are important for selecting the right conditions to run centrifuge experiments as will be explained in Chapter 3.

Methane, CH4: fraction = 0.5
Propane, C3H8: fraction = 0.5
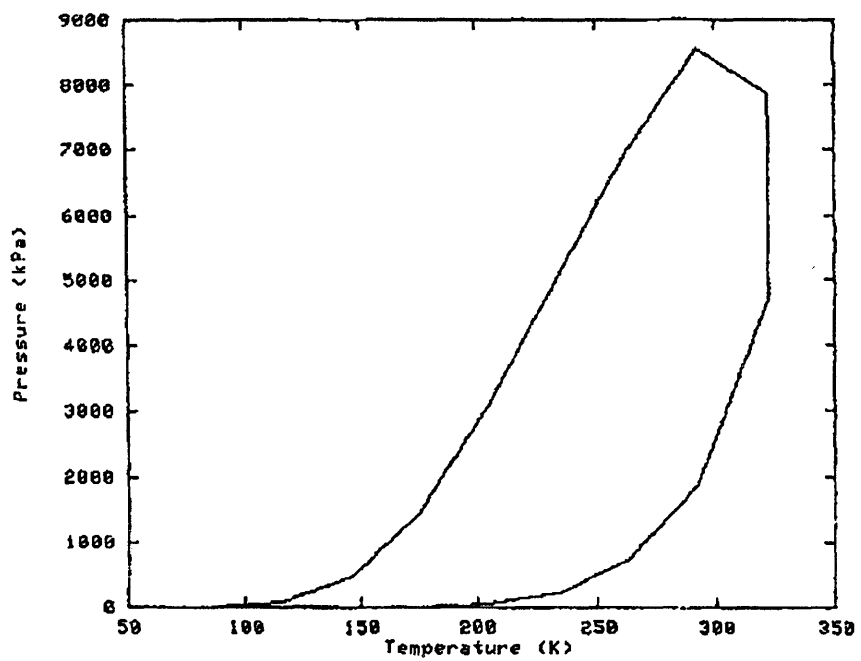
Figure 2.5 Pressure-Temperature Diagram for Methane-Propane System

(50% C1-50% C3)

Methane, CH4: fraction = 0.5832
Propane, C3H8: fraction = 0.4168
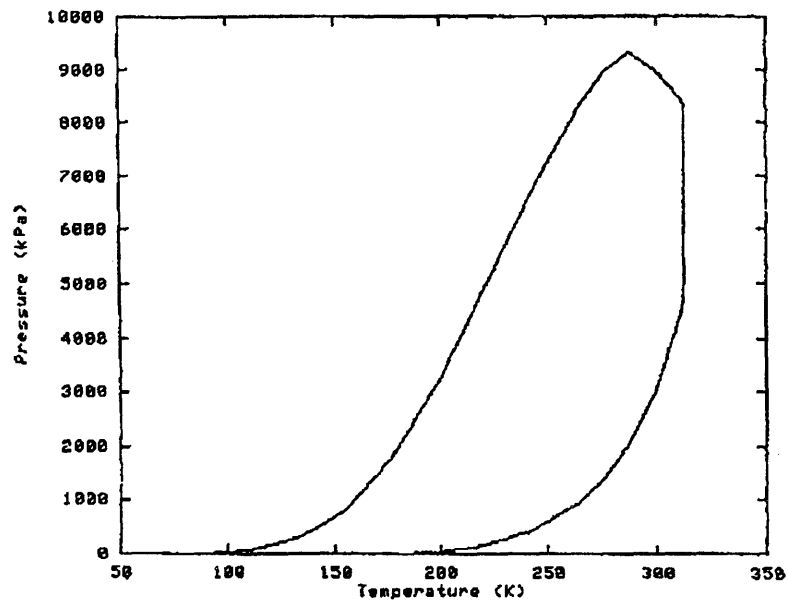
Figure 2.6 Pressure-Temperature Diagram for Methane-Propane System
(58.32% C1-41.68% C3)

Methane, CH4: fraction = 0.6
Propane, C3H8: fraction = 0.4
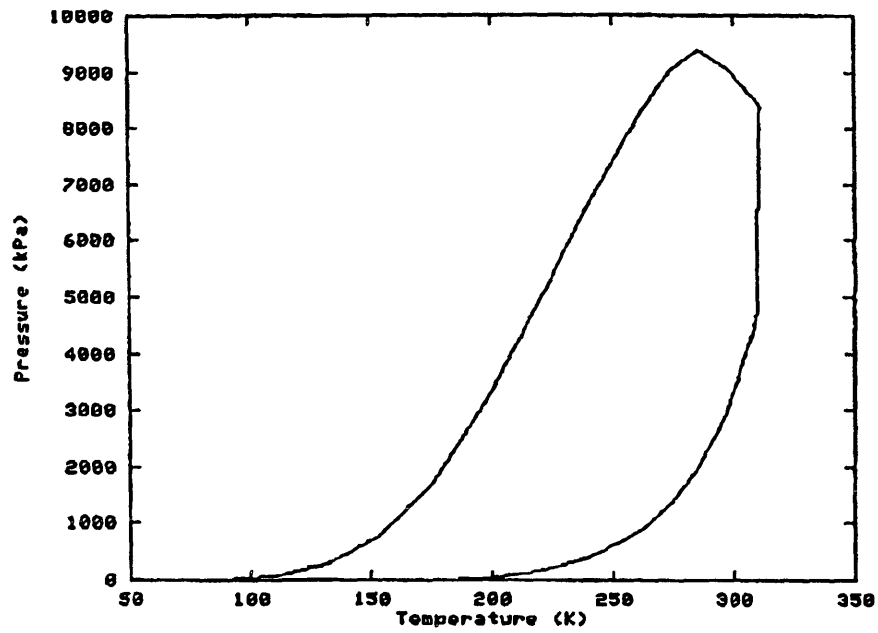
Figure 2.7 Pressure-Temperature Diagram for Methane-Propane System
(60% C1-40% C3)
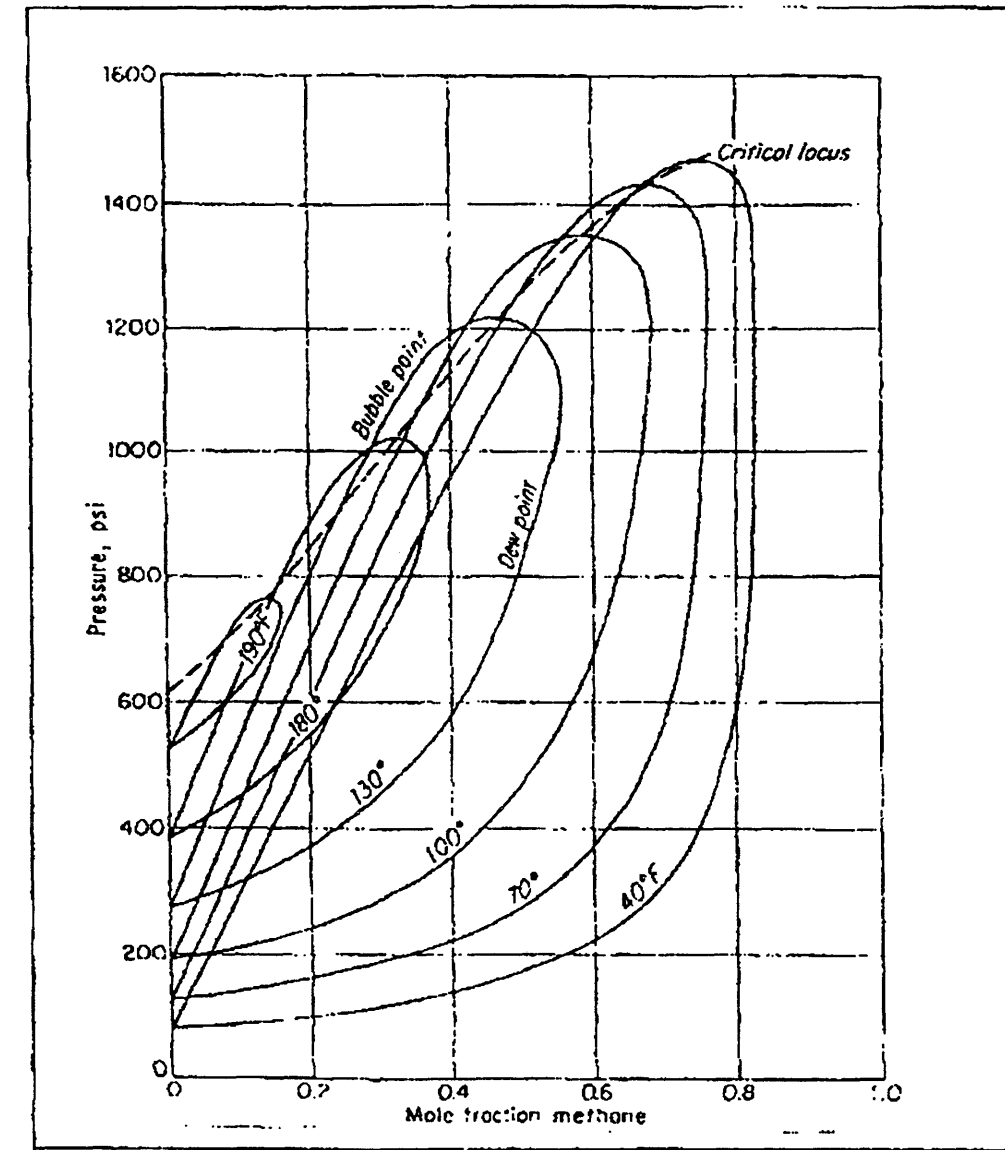
Figure 2.8 Pressure-Composition Diagram for Methane-Propane System

(Reamer, et al.[66])

CHAPTER 3

EXPERIMENTAL SETUP & PROCEDURES

Experiments using the centrifuge for simulating the effect of gravity and temperature gradient on the composition profile of a hydrocarbon fluid column are described in this chapter. The experimental apparatus is described in the first section followed by the steps in selecting and preparing the binary gas mixture in the second section. In the third section, a description of procedures for the experiments is given including centrifuge test, gas composition calculation, and temperature profile measurement.

3.1 Experimental Apparatus

The experimental apparatus consisted of a centrifuge, a profile-capture apparatus that attaches to the rotor of the centrifuge, and a gas chromatograph for measuring the compositions of gas samples.

3.1.1 Centrifuge

A Beckman J-6B centrifuge was used for all composition profile tests. The original rotor of this centrifuge was replaced with a rotor that facilitates mounting of the profile-capture apparatus, which is described in the following sub-section. The new rotor was described by Al-Omair[67]. It consists of a flat polycarbonate disk

(21-inch diameter, 1/4 inch thick) mounted on a flat aluminum disk (10-inch diameter, 1/4 inch thick), that is connected to an aluminum mount as shown in Figure 3.1. With this rotor, spin rates up to 6000 rpm are possible; however, the maximum allowable spin rate depends on the mass of items that are attached to the rotor.
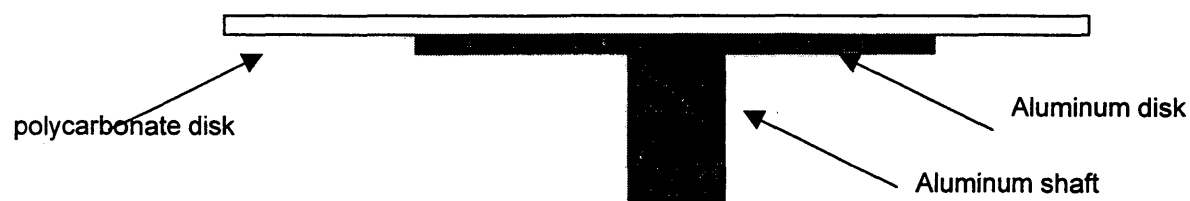
Figure 3.1 Side-view of the rotor assembly as described by Al-Omair[67]

The original refrigeration unit of the centrifuge was replaced with an external temperature bath (model RTE-210) that circulates water through tubing around the centrifuge chamber.

The original lid was replaced with a lid that allows visual observation of the profile-capture apparatus while the centrifuge is spinning. Visual observations were useful for qualitative measurement of the temperature profile. Also, visual checks of the spinning apparatus were helpful for safety purposes.

3.1.2 Profile-Capture Apparatus

In this section, the various profile-capture apparatus (PCA) that were used in this study will be described including low and high pressure PCAs. These profile-capture apparatus all consist of a series of eight valves with intervening tubing as shown in Figure 3.2a. Figure 3.2b shows a top view of PCA when it is mounted on the polycarbonate disk.

3.1.2.1 Low Pressure PCA

The first PCA that was used was built and described by Maan[48]. It consisted of 1/8 inch OD with 0.065 inch ID, polyetheretherketone PEEK 1544 tubing, and ETFE P-783 Blue shut-off valves and fittings obtained from Upchurch Scientific. Maan's PCA could be attached directly to the polycarbonate disk of the centrifuge rotor with machine screws. Spinning tests up to 4,000 rpm were possible with this PCA because of the low mass of the plastic valves (5 g each). This PCA was capable of operating up to about 200 psi. At pressures above that, the fittings could not seal sufficiently to prevent gas leakage.

(a)

Length=51 cm

Chamber
Lenth=6 cm

(b)

Steel sheet
support

Polycarbonate
disk

PCA
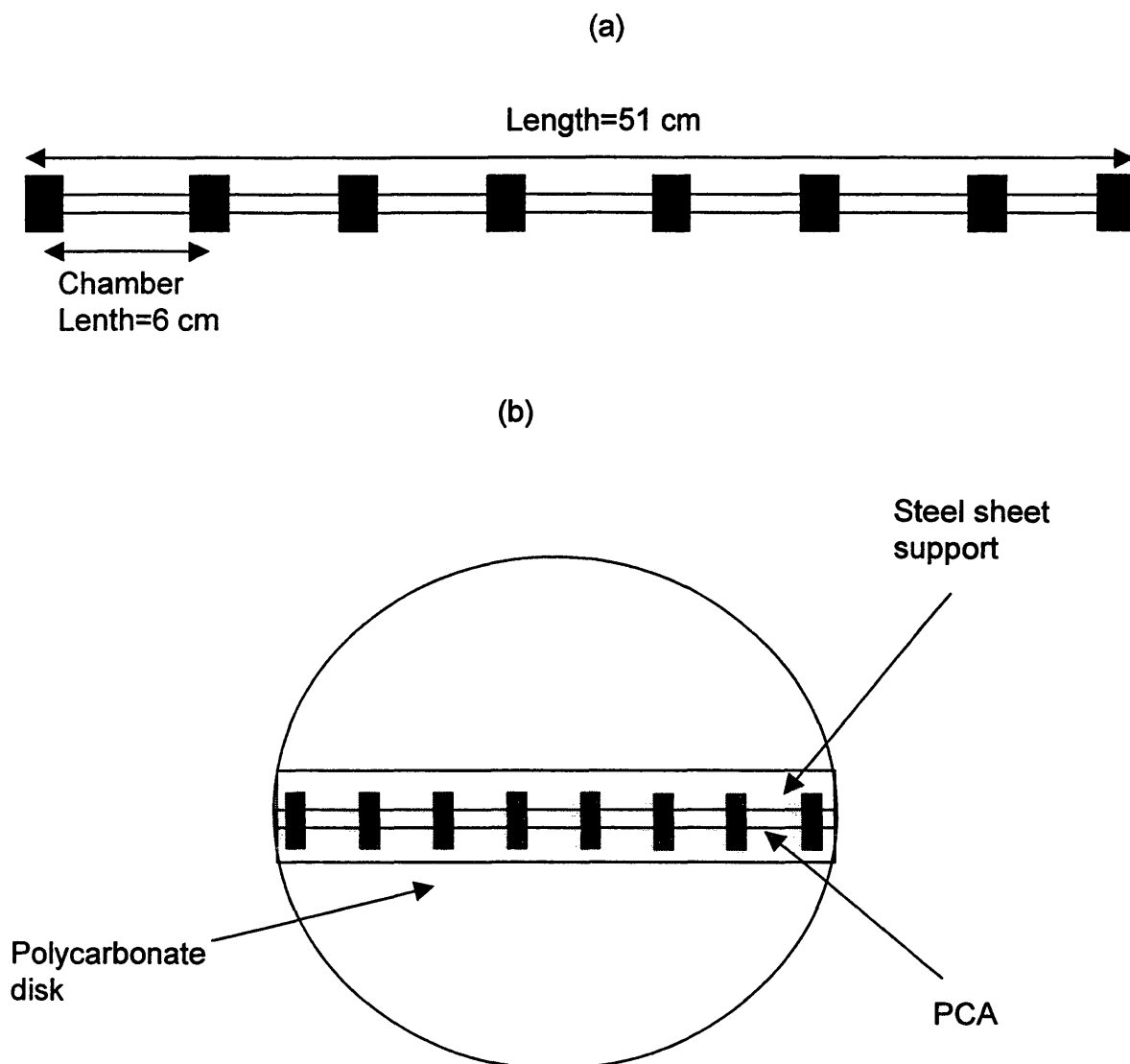
Figure 3.2 (a) A basic schematic for the various profile-capture apparatus. The black rectangles represent valves, which are connected by tubing. (b) Top view of profile-capture apparatus mounted on the polycarbonate disk.

3.1.2.2 High Pressure PCA

To allow for tests at higher pressures, some changes in the construction and design of the PCA were needed. The plastic components of Maan's PCA were replaced with 304SS stainless steel tubing, Whitey ball valves, and fittings which are capable of operating up to 2500 psi. Two diameters of tubing were used: 1/8 inch OD with 0.069 inch ID, and 1/4 inch OD with 0.180 inch ID. The larger OD tubing was selected initially to provide for larger gas volumes in the chambers between valves. With larger volumes, more reliable measurements of gas composition were anticipated. However, the 1/8-inch OD tubing provided sufficient gas sample size for operating pressures above 300 psi.

Replacing the light plastic components with heavy stainless steel components required changes in the mechanical support for the PCA. Two of the options that were used are described in the paragraphs immediately below. A description of the stress calculations for designing these options is included in the Section 3.1.2.3.

For non-isothermal experiments, the PCA was mounted in a manner to inhibit conduction of heat from valve to valve. A steel plate of 21 inch long, 2 inch wide, and 0.25 inch thick was used as a mechanical support and a plastic plate of the same dimensions as that of the steel one used as an insulator between the PCA and the steel plate. The arrangement of these plates with the PCA is shown in Figure 3.3. The same type of bolts used to mount the isothermal setup was used to mount the non-isothermal setup. During spinning tests with the non-isothermal arrangement, a temperature profile could be observed with stick-on temperature

labels and with direct temperature measurements at the conclusion of a test (after stopping the centrifuge).
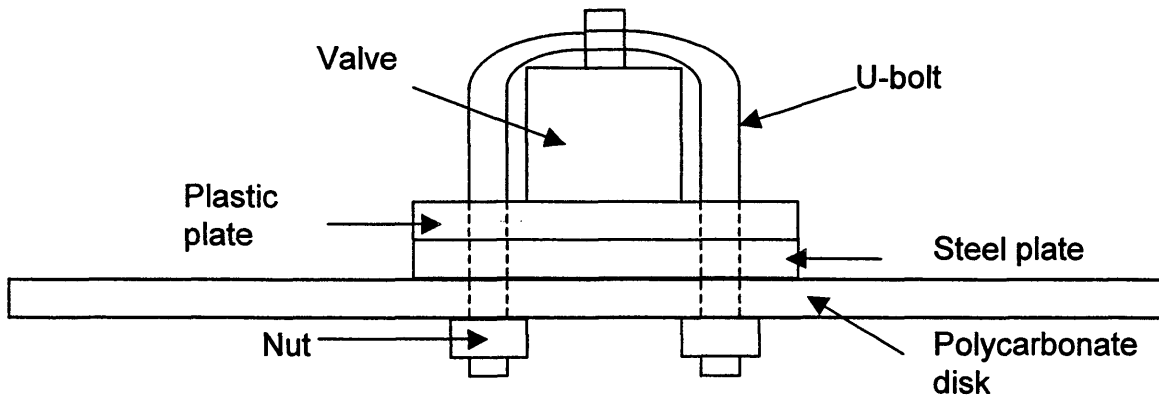
Figure 3.3 Side view of the non-isothermal setup of the PCA

For isothermal experiments, an aluminum channel 21 inch long, 2 inch wide, 1.25 inch high, and 0.25 inch thick was used to house the PCA in as shown in Figure 3.4. To mount the PCA inside the aluminum channel, several U-type bolts were used. Two U-type bolts were used to clamp every valve, so a total of 16 bolts were used. Figure 3.4 c shows a side view of the PCA sitting inside the aluminum channel and every valve is clamped in the channel and onto the polycarbonate disk by two U type bolts. During spinning tests, the temperature profile along the aluminum channel was observed (using stick-on temperature labels) to be fairly

uniform, as was expected because of the high thermal conductivity of the aluminum channel.

To be able to run the centrifuge at higher speeds, the balance of the setup has to be maintained. Therefore all the elements constituting the PCA (including valves, chambers, bolts and nuts) were weighed accurately and the weight was distributed evenly around the center of rotation. At some locations across the PCA, extra weights in forms of small nuts were added to achieve the balance. On each side of the center of rotation, there is a total of 371.955 g of mass. Figure 3.5 and Table 3.2 show the weight distribution around the axis of rotation.

3.1.2.3 Stress Calculation for High Pressure PCA

With the change from plastic to mostly-steel components for the high-pressure PCA, the mechanical support of the valves in particular was an important consideration. Stresses were calculated to make sure that the aluminum channel and the steel plate could stand the loads expected. Here, the calculation procedure is outlined and the results were tabulated in Table 3.1. For the aluminum channel and steel plate the following equations were used:

$$S = \frac{F}{A} \qquad (3.1A)$$

$$F = \int_{0}^{R_0} \rho A \omega^2 r\, dr = \frac{1}{2} \rho A \omega^2 R_o^{\,2} \qquad (3.1B)$$

$$S = \frac{1}{2}\rho\omega^2 R_o^2 \qquad \qquad (3.1C)$$

For Whitey ball valves the following equation was used:

$$S = \frac{F}{A} = \frac{M_v a}{A} = \frac{M_v \omega^2 R_o}{A} \qquad \qquad (3.2)$$

where

F = force applied, dynes

S = stress applied, dyne/cm^2 = 14.7 psi/(10^6 dyne/cm^2)

R_o = distance from the center of rotation, cm

A = cross-sectional area of the aluminum channel, cm^2 = 1 in^2 = 6.45 cm^2

ω = centrifuge speed = 400 rad/s^2

ρ = density of the metal, g/cm^3 (2.71 for aluminum, 7.83 for steel)

M_v = mass of the valve, g (82 g)

(a)

Length = 51 cm

1   2   3   4   Center   5   6   7   8

R_o R_o

(b)

1.25 in

2.0 in

0.25 in

(c)

U-type bolt

Valve

Polycarbonate disk

Aluminum channel

Nut
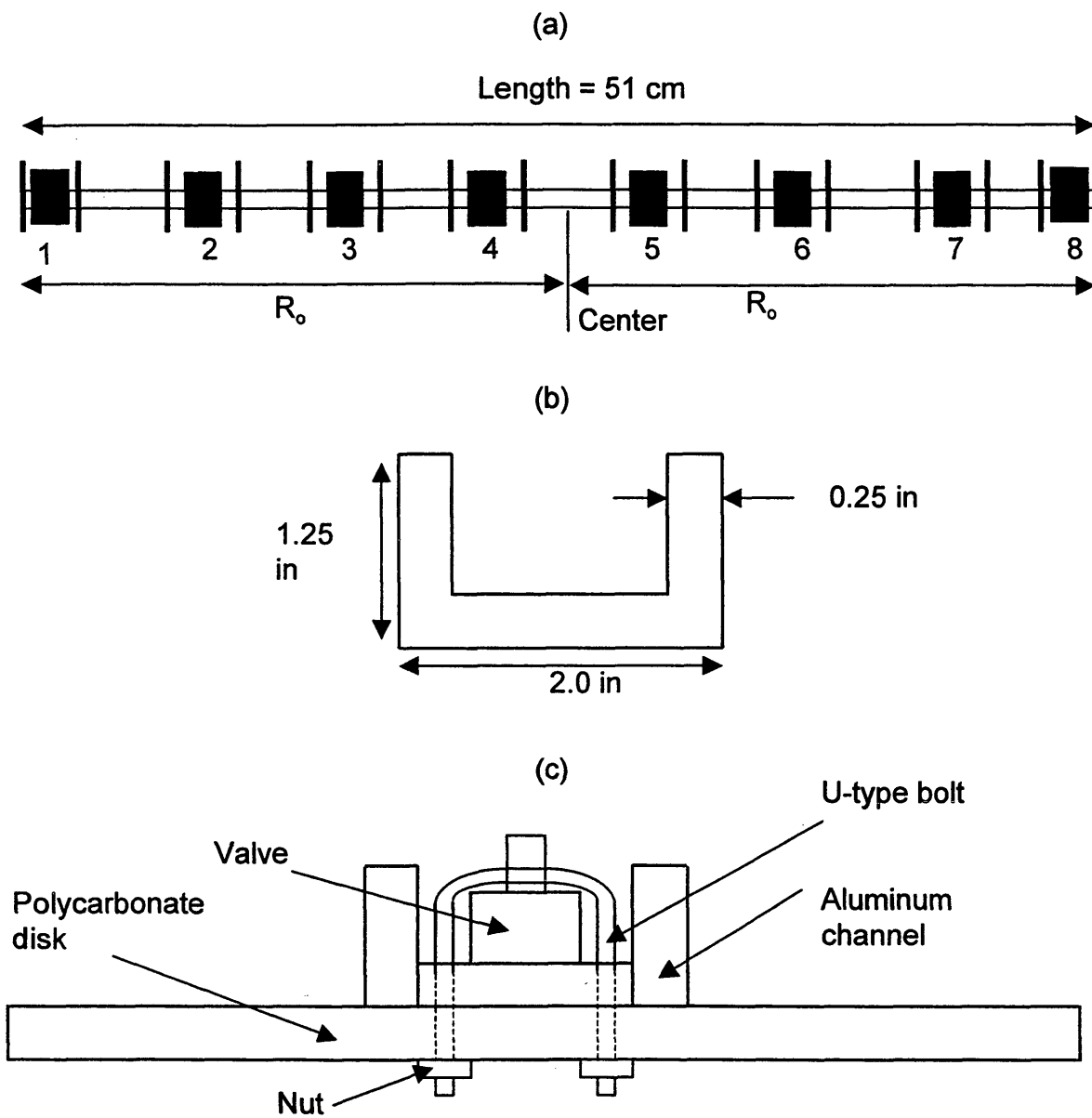
Figure 3.4 Mechanical supports including (a). front view of the PCA and (b). side view of the aluminum channel, (C). side view of the PCA sitting inside the aluminum channel and fixed on the polycarbonate disk

Table 3.1 Stress calculation for aluminum channel, steel plate, and valves

Components of PCA	Radius, R_o cm	Stress, S psi
Valves	25.5	1710
Channel	26.5	2238
Steel plate	26.5	6466

Bolt A1   Bolt A2

1 2 3 4 5 6 7 8

Bolt B1   Bolt B2
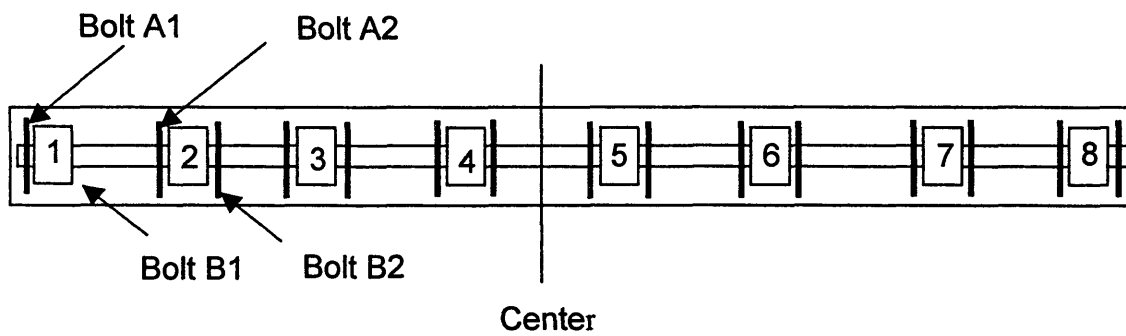
Center

Figure 3.5 Top view of the PCA showing the elements weighed for balance requirement

Table 3.2 Weight distribution around the center of rotation

Valve #	1	2	3	4	5	6	7	8
Bolt A	7.813	13.292	6.666	15.388	15.392	6.580	13.310	7.788
Bolt B	13.070	12.877	15.505	15.413	15.413	15.505	13.042	13.060
Total*	102.85	108.35	104.35	112.81	112.81	104.35	108.35	102.85

* weights of every valve, chamber, and additional nuts (82 g) were already included

3.1.3 Gas Chromatograph

An HP 5890 gas chromatograph (GC) as modified by Wasson ECE Instrumentation Inc. was used for all gas composition measurements. Procedures for composition measurements with the GC are described in the Wasson ECE manual. After finishing centrifuging the sample, the PCA (mounted on the polycarbonate disk) was connected to the GC for gas analysis as shown in Figure 3.4.

The GC output is sent to an integrator (HP Model No. 3396A) which calculates and reports areas of peaks. The integrator response was calibrated using the methane-propane binary gas mixture prepared for centrifuge experiments.

Pressure gauge
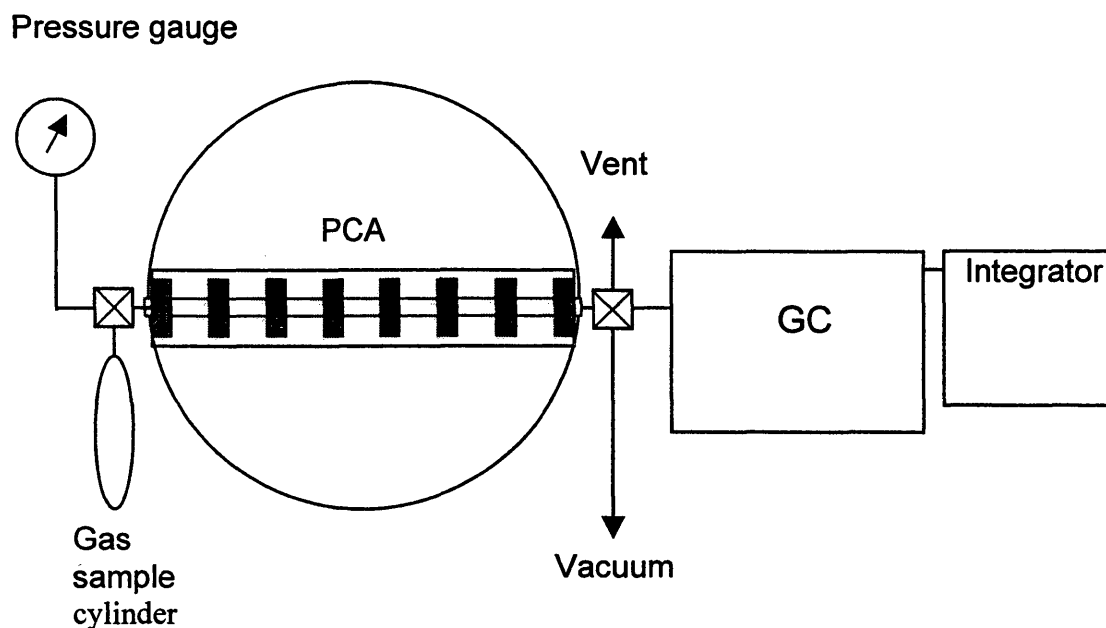
Figure 3.6 Schematic diagram showing the PCA connected to GC, sample cylinder, and vacuum pump

3.2 Sample Selection and Preparation

The following criteria were followed in selecting the candidate binary gas mixture for centrifuge tests:

1. The two components of the binary mixture should have a significant difference in their molecular weights.

2. The binary gas mixture must remain in a single phase during the course of the experiment.

3. The mole fractions of the two components should be near 0.5, in order to maximize sensitivity to any compositional variations.

4. The binary mixture should be easy to prepare in the lab.

Following the above criteria, Maan(1997) concluded that a blend of methane (59%) and propane (41%) was most appropriate. Calculations with an equation of state show that this blend will remain in the gas phase for temperatures above 50°C.

The following steps were followed for preparing the blend of methane and propane:

1. The amount of each component needed to make up the composition of the binary mixture was calculated as shown in Table 3.3.

2. Cylinders of high purity components were obtained (99.95%).

3. 70.00 g of propane was transferred to a 1000 ml Whitey cylinder with a pressure rating of 1800 psi.

4. Then, 35.63 g of methane was transferred to the Whitey cylinder.

5. The mixture was heated to 70 °C to make sure that the mixture was in a gaseous phase. At that temperature, the pressure was 1200 psi.

6. To check the composition of the binary mixture, some samples were injected into the GC and analyzed.

Table-3.3 Methane-propane binary mixture composition

Component	MW g/gmol	Mass g	Moles	Mole Fraction by Mass	Mole Fraction by GC
Methane	16.043	35.63	2.2209	0.5832	0.5823
Propane	44.097	70.00	1.5874	0.4168	0.4177
Sum			3.8083	1.0000	1.0000

Using my numerical model under isothermal condition, I have compared the composition gradient produced by different possible combination of methane and propane that can be used to make the binary gas mixture. In Figure 3.7, the mole percent change in methane, as it segregates to the center of the PCA, was plotted against the initial composition of methane used to make the binary gas mixture. From Figure 3.7, I concluded that the binary system having 58.32% methane and 41.68% propane to be the most suitable system to produce a considerable composition gradient. The calculation of composition gradient was done at isothermal condition at spinning rate of 2500 rpm, a pressure of 1500 psig and a temperature of 50 °C.

Methane mole fraction in the Binary gas mixture

| 0.45 | 0.5 | 0.55 | 0.6 | 0.65 | 0.7 | 0.75 |
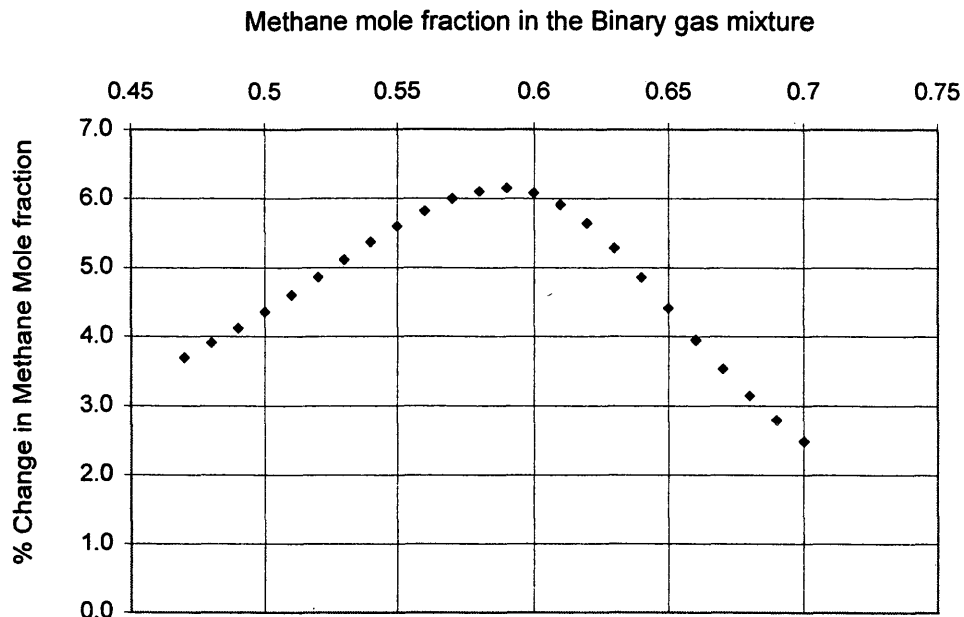
Figure 3.7 % Change in Methane Mole Fraction vs. Methane Mole Fraction
in the Bianry Gas Mixture at 2500 rpm, 1500 psig, 50 °C
(Isothermal)

3.3 Experimental Procedures

This section contains the steps for a complete centrifuge test and the steps for calculating the composition of the binary gas in each chamber of the PCA.

3.3.1 Test Procedures

A binary gas mixture (58% methane, 42% propane) was prepared in the lab and stored in a Whitey cylinder as described in section 3.2. That sample was charged to the PCA and subjected to a centrifugal field as outlined in the procedure below.

Charging the Sample to PCA

1. Connect the PCA to the heated sample cylinder (70 °C) as shown in Figure 3.6.
2. Check all lines including the PCA for leakage.
3. Then, flush all lines including the PCA with sample gas to eliminate air contamination.
4. Heat all lines and PCA using heating tapes to 70 °C to eliminate condensation.
5. Evacuate all lines and PCA.
6. Charge the sample to the PCA to the desired operating pressure.
7. Close the end valves (Valves 1 & 8) and keep others open (Valves 2 through 7).
8. Disconnect the PCA from the sample cylinder.

Running a Centrifuge Test

1. Mount the PCA inside the centrifuge chamber.
2. Set the water bath temperature at 50 °C.
3. Run the centrifuge at a specific test speed for a specific duration.
4. Stop the centrifuge and immediately close valves 2 through 7 in the following order: 2 & 7 simultaneously, 3 & 6 simultaneously, and 4 & 5 simultaneously.

5. Remove the PCA from the centrifuge and connect it to the GC as shown in Figure 3.6.

6. Heat all lines and PCA using heating tapes to 50 °C.

7. Evacuate all lines connecting to the PCA and GC and the GC sample valves.

8. Inject the gas sample starting with chamber 1 to the GC in the following order: chamber 1, chamber 7, chamber 6, chamber2, chamber 3, chamber 5, chamber 4.

9. The time needed for GC analysis of each chamber is approximately 20 min.

The signals from the GC are converted to areas of peaks by HP 3396A Integrator. Usually for binary mixture, three peaks are obtained: one for air and the other two for the two components of the binary mixture. Every component has its own peak and every peak has an area %. The integrator also converts peak areas for each chamber to composition as outlined in the following section.

3.3.2 Gas Composition Calibration

The GC and integrator were calibrated with a sample of the binary gas mixture (58.32% methane, 41.68% propane) as prepared in Section 3.2. This calibration sample was injected ten times to get average response factors. The average response factors were used for calculation of mole fractions in the samples from the PCA. With these response factors, the integrator reports mole fractions as well as areas of each peak for each component in the binary sample.

The ratio of methane mole fraction x_1 to propane mole fraction x_2 is a more sensitive indicator of change in composition of the samples. This ratio was used throughout this research as an additional indicator of composition gradients.

Table 3.4 shows the compositional results for a centrifuge test that was conducted at a pressure of 600 psia and a temperature of 50 °C.

Table 3.4 An example of methane-propane mole fractions and ratios for all PCA chambers.

Chamber	x_1	x_2	x_1/x_2
1-2	0.5705	0.4294	1.3285
2-3	0.5837	0.4162	1.4025
3-4	0.5919	0.4081	1.4505
4-5	0.5924	0.4076	1.4536
5-6	0.5849	0.4151	1.4092
6-7	0.5838	0.4162	1.4026
7-8	0.5662	0.4338	1.3053

3.3.3 Temperature Profile Measurement

Temperatures along the PCA were measured using an Omega HH82 digital thermometer and stick-on temperature labels also obtained from Omega. Using stick-on temperature labels, it was possible to observe the temperatures along the PCA while it was spinning in the centrifuge. Table 3.5 shows eight sets of temperature measurements at 2500 rpm. Figure 3.8 shows the six profiles from Table 3.5.

The measured temperature data were fit as a function of r^2 and r^4 using a regression routine. The following two equations are good candidates that can reasonably fit data.

$$T = 1.3E - 2\, r^2 + 316.0251 \qquad\qquad (3.3A)$$

$$T = 2.8642E - 5\, r^4 + 316.6149 \qquad\qquad (3.3B)$$

The calculated temperature profiles with these two equations are shown in Figure 3.8.

Equation 3.3A was found to fit the measured temperature data better than equation 3.3B. On the other hand equation 3.3B fits the measured composition data at low and high pressure better than equation 3.3A as will be shown in Chapter 4. Therefore I decided to use equation 3.3B for T and $\dfrac{dT}{dr}$ in my

numerical model (equations 2.49 and 2.52) for calculating composition gradient under non-isothermal condition.

Table 3.5 Measured Temperature Profile Along the PCA

Profile	1	2	3	4	5	6	7	8
r, cm	T, K	T, K	T, K	T, K	T, K	T, K	T, K	T, K
0	315.93	316.59	316.04	316.37	315.87	316.04	316.2	316.3
6.85	316.26	317.21	317.21	316.76	316.26	316.48	316.6	316.8
13.7	318.43	318.71	319.54	318.93	318.48	318.98	318.8	318.7
20.55	320.93	321.76	320.87	321.93	321.98	322.04	322.1	321.7

Table 3.6 Calculated Temperature Profile Along the PCA

r cm	T, calc.,K r^2 fit	T, calc.,K r^4 fit
0	316.03	316.61
6.85	316.64	316.68
13.7	318.47	317.62
20.55	321.52	321.72

Figure 3.8 Measured and Calculated Temperature along the PCA
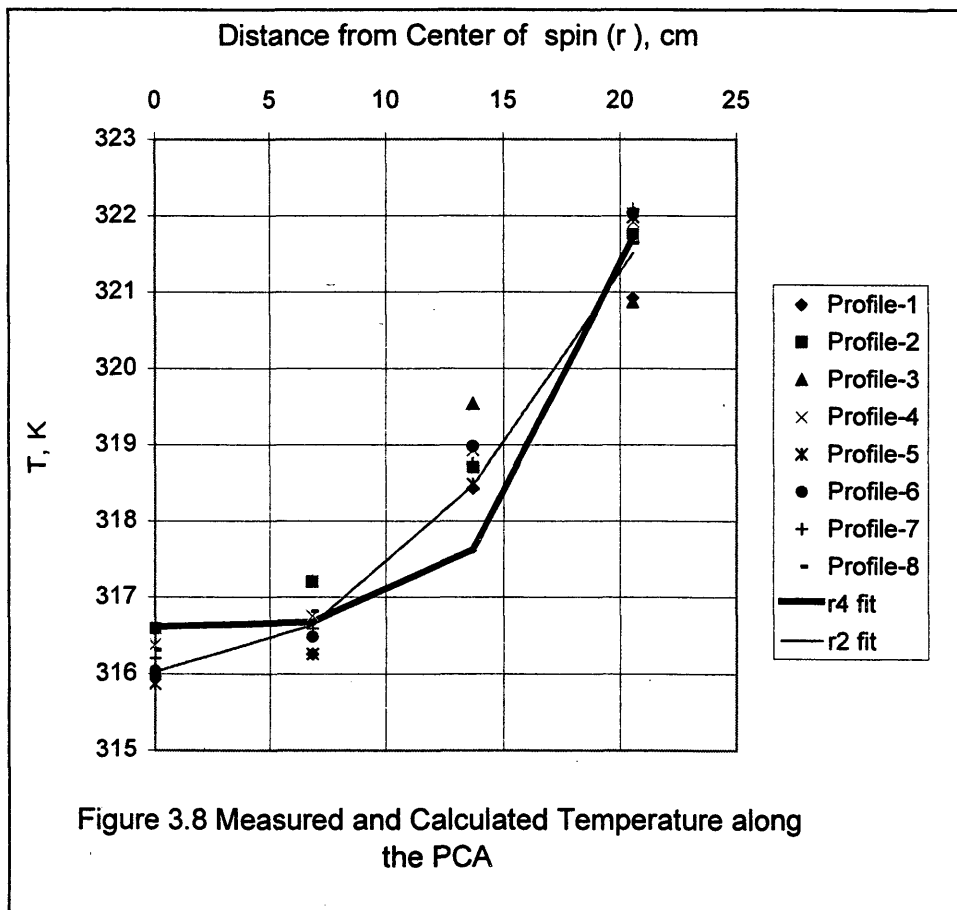
According to the hydrostatic head equation in Chapter 2, equation 2.25, an equivalent height h in ft can be defined by equating potential changes in the experiment and in the hydrocarbon fluid column from some arbitrary datum as follows:

$$gdh = \omega^2 rdr \tag{3.4}$$

Integrating equation 3.4 from a reference depth h_0 in the reservoir and a reference distance along the PCA r_0 gives

$$g\int_{h_0}^{h} dh = \omega^2 \int_{r_0}^{r} rdr \tag{3.5}$$

$$g(h - h_0) = \frac{\omega^2}{2}\left(r^2 - r_0^2\right) \tag{3.6}$$

From equation 3.6 the corresponding height in reservoir h is

$$h = h_0 + \frac{\omega^2}{2g}\left(r^2 - r_0^2\right) \tag{3.7}$$

At a centrifuge speed of 2500 rpm and a distance r from the center of spin ($r_0 = 0$) equal to 22 cm which is half of the length of the PCA, the fluid column in the lab is equivalent to 500 ft of a fluid column in the reservoir.

The measured temperature difference between the center of spin and the edge is 11 °F which corresponds to 0.022 °F/ft in a petroleum reservoir. With the available equipment this temperature gradient was the maximum we can create. In all of the above experiments, a temperature gradient of 0.022 °F/ft was used. This is comparable to an average geothermal gradient of 0.015 °F/ft published for some reservoirs in the Middle East, North Sea, and North America.

CHAPTER 4

RESULTS AND DISCUSSION

Results obtained for the centrifuge experiments under isothermal and non-isothermal conditions at low and high pressure are presented and discussed in this chapter. Accordingly, this chapter will be divided into four main sections. In the first section, I will describe the numerical model I have set up to calculate the compositional gradient using thermodynamic and transport approaches. The second section will focus on the compositional evolution with time under isothermal conditions. In the third section the results obtained for seven experiments conducted under isothermal conditions where the gravitational field is the only factor influencing the composition of the binary gas mixture of methane and propane are presented and discussed. Also a comparison of the experimental data with the calculated data using the numerical model are included. The fourth section will focus on the results for ten experiments conducted under non-isothermal conditions where both gravity and temperature fields are acting on the composition of the binary gas mixture. Under non-isothermal conditions, the calculations were done for constant value of the thermal diffusion ratio k_T. Again the experimental data will be compared with the calculated data using the numerical model. In the final section, discussion of the observations and the calculations are presented.

4.1 Numerical Model

A numerical program was written to calculate the composition gradient in the binary gas mixture of methane and propane. In this program I use both thermodynamic and transport approaches for calculating the composition gradient for four sets of conditions:

- Isothermal and non-ideal gas behavior (equations 2.25 and 2.26),
- Isothermal and ideal gas behavior (equations 2.32 and 2.33),
- Non-isothermal and non-ideal gas behavior (equations 2.49 and 2.50),
- Non-isothermal and ideal gas behavior (equations 2.52 and 2.53).

Also, the program allows the option of using either Peng-Robinson[68]or Redlich-Kwong[69] equations of state to calculate partial molar volumes, densities, and fugacities for the binary system. The program solves two first order differential equations using Runge-Kutta methods. Their solution provides the pressure P and the composition x_1.

The numerical model was written in FORTRAN-77 using IMSL codes for differentiating functions such as z-factor, mole fraction, and fugacity.

To check the performance of the model, its predictions for isothermal conditions with ideal gas behavior were compared with the predictions of the Sage and Lacey[1] model. The results of the two approaches are nearly identical as shown in Table 4.1.

Table 4.1 Comparison of Composition Gradient Prediction
By Numerical Model and Sage and Lacey Model

			This work	Sage&Lacey
r, cm	x_1	x_2	x_1/x_2	x_1/x_2
0	0.58432	0.41568	1.40571	1.40571
1	0.58431	0.41569	1.40566	1.40566
2	0.58429	0.41571	1.40551	1.40551
3	0.58424	0.41576	1.40526	1.40526
4	0.58418	0.41582	1.40491	1.40491
5	0.58410	0.41590	1.40445	1.40445
6	0.58401	0.41599	1.40390	1.40390
7	0.58390	0.41610	1.40324	1.40324
8	0.58376	0.41624	1.40248	1.40248
9	0.58362	0.41638	1.40163	1.40163
10	0.58345	0.41655	1.40067	1.40067
11	0.58327	0.41673	1.39961	1.39961
12	0.58307	0.41693	1.39846	1.39846
13	0.58285	0.41715	1.39720	1.39720
14	0.58261	0.41739	1.39585	1.39585
15	0.58236	0.41764	1.39439	1.39439
16	0.58209	0.41791	1.39284	1.39284
17	0.58180	0.41820	1.39119	1.39119
18	0.58149	0.41851	1.38944	1.38944
19	0.58117	0.41883	1.38759	1.38759
20	0.58083	0.41917	1.38565	1.38565

In Table 4.1, the calculation was done at a pressure of 300 psig, temperature of 50 °C and a speed of 2500 rpm, using the ideal-gas option in the numerical algorithm. Throughout my thesis, I used the pressure and composition at the center of the PCA (center of the spin, r=0 cm) as initial conditions in the numerical program. In all tables in this thesis, the row having the initial conditions of methane mole fraction and the ratio is shaded.

As another check on the model, especially the phase-behavior portion of the model, predictions of partial molar volume for the methane-propane system at 1500 psia and 460 °F were compared with measured values reported by Sage and Lacey[65,66]. The comparison is shown in Figure 4.1.

Mole Fraction
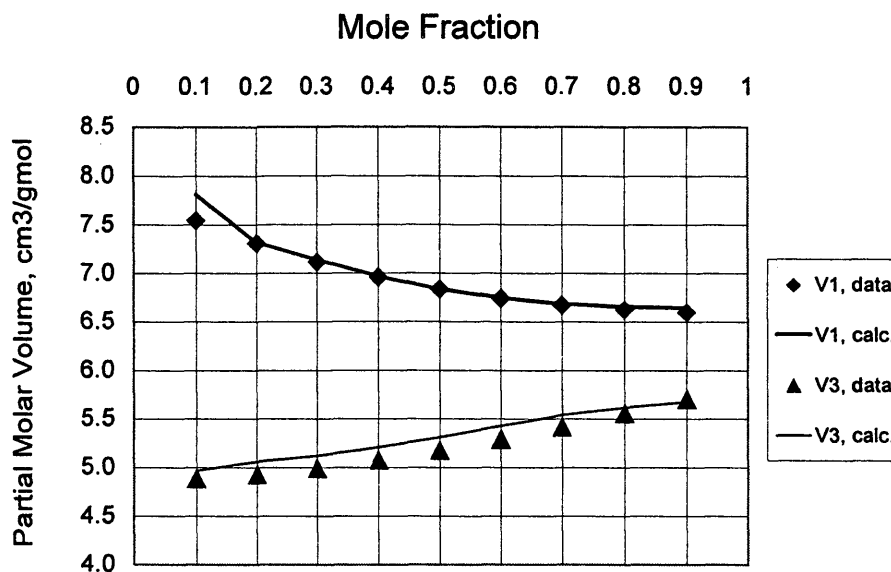
Figure 4.1 Measured and Calculated Partial Molar Volumes
of Methane and Propane

As a further check of the program performance, the predictions of composition gradient for isothermal and non-ideal gas behavior were compared with a model written independently by Professor Christiansen using the Redlich-Kwong[70] equation of state. The two predictions are essentially identical.

The variation of density from the spin axis to the outside radius of the PCA was examined for a wide variety of operating conditions. This examination showed that density increased with radius for the present binary system at 50 °C and all pressures considered. So, density driven convection was not expected in the

experiments. As mentioned in Chapter 2, Ghorayeb et al.[22] reported composition gradient predictions including gravity and thermal diffusion effects for a gas reservoir in Japan. They predicted a density inversion for that system.

4.2 Compositional Evolution with Time

To estimate the time t needed to achieve steady-state equilibrium condition, the following simple relation was used, which specifies time for 90% completion of a diffusion process (Bird *et al.*[53]):

$$t = \frac{l^2}{D_{AB}}$$

(4.1)

where D_{AB} is the molecular diffusion coefficient of methane and propane in cm^2/sec and l is the characteristic length of the diffusion path in cm. D_{AB} was estimated to be 0.02 cm^2/sec and the characteristic length is 1/2 of the total length of the PCA, or about 22 cm. The time for 90% completion of the process should be, using equation 4.1, about 6 hours.

This estimated time to reach steady-state is important for indicating how long an experiment needs to run to establish a composition gradient. It is also important in figuring out how much time is needed for the composition gradient to collapse after the centrifuge is turned off. Since the time elapsed from the moment I turned the centrifuge off to when the valves are completely closed is approximately one

minute, the composition gradient that is established during the experiment does not have time to collapse before the samples are captured.

To observe the development of the steady-state condition in the lab, centrifugal experiments at different time periods (2, 3, 4, 5, and 6 hours) at a pressure of 300 psig, temperature of 50 °C and a speed of 2500 rpm were conducted. Table 4.2A and 4.2B show the methane/propane ratio and methane mole fraction respectively on each side of the center of spin for the time periods mentioned above. Plots of the methane mole fraction and the ratio of methane to propane vs. the distance from the center of spin (r) are shown in Figure 4.2. For comparison, I included in Figure 4.2 the measured composition of the binary gas mixture before spinning in the centrifuge as a base line at time equal to zero. The conclusion that can be drawn from Figures 4.2 is that 6 hours duration is a fair amount of time to run all experiment to observe reasonable composition gradient for isothermal and non-isothermal conditions and for all pressures of interest.

The ratio of methane mole fraction x_1 to propane mole fraction x_2 is a more sensitive indicator of change in composition of the samples. This ratio was used throughout this research as an additional indicator of composition gradients. At low pressure and for isothermal conditions, for instance, the compositional gradient is quite small and therefore plotting mole fraction of methane will not clearly express the amount of change in composition.

Table 4.2A Composition Evolution with Time (Isothermal)
Experimental Methane/Propane Ratio
2500 rpm, 300 psig, 50°C

Time, hr	0	2	3	4	5	6
r, cm	x_1/x_2	x_1/x_2	x_1/x_2	x_1/x_2	x_1/x_2	x_1/x_2
20.55	1.4007	1.3882	1.3872	1.3865	1.3855	1.3858
13.70	1.4033	1.3969	1.3957	1.3955	1.3952	1.3958
6.85	1.4016	1.4040	1.4032	1.4048	1.4022	1.4018
0.00	1.4010	1.4082	1.4067	1.4074	1.4069	1.4037
-6.85	1.4045	1.4073	1.4025	1.4091	1.4024	1.4073
-13.70	1.4041	1.4048	1.4044	1.4074	1.4035	1.4067
-20.55	1.4035	1.3984	1.3876	1.3866	1.3878	1.3939

Table 4.2B Composition Evolution with Time (Isothermal)
Experimental Methane Mole Fraction
2500 rpm, 300 psig, 50°C

Time, hr	0	2	3	4	5	6
r, cm	x_1	x_1	x_1	x_1	x_1	x_1
20.55	0.5834	0.5813	0.5811	0.5810	0.5808	0.5809
13.70	0.5839	0.5828	0.5826	0.5825	0.5825	0.5826
6.85	0.5836	0.5840	0.5839	0.5842	0.5837	0.5837
0.00	0.5835	0.5847	0.5845	0.5846	0.5845	0.5840
-6.85	0.5841	0.5846	0.5838	0.5849	0.5838	0.5846
-13.70	0.5840	0.5842	0.5841	0.5846	0.5839	0.5845
-20.55	0.5839	0.5831	0.5812	0.5810	0.5812	0.5823

Distance from the spin, cm
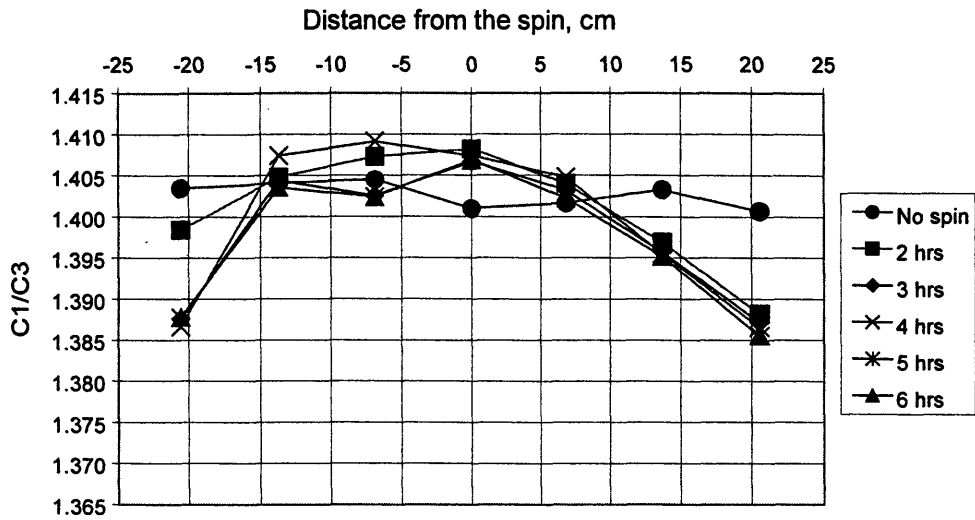
Figure 4.2A Compositional Evolution with Time (Isothermal)
Experimental Methane/Propane Ratio
2500 rpm, 300 psig, 50°C

Distance from Center of Spin, cm
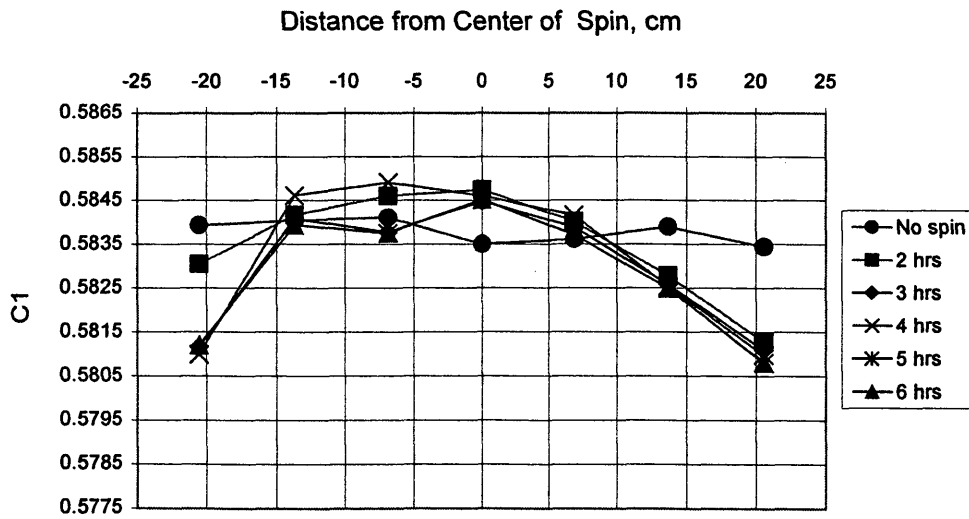
Figure 4.2B Compositional Evolution with Time (Isothermal)
Experimental Methane Mole Fraction
2500 rpm, 300 psig, 50°C

4.3   Compositional Variation under the Effect of Gravity Alone

Extensive efforts were spent on designing an experimental setup and procedures to produce an observable compositional gradient in the lab. Under isothermal conditions, many laboratory experiments were conducted using methane/propane binary gas mixture to reproduce the effect of gravity on a thick hydrocarbon zone by applying large accelerations on a short fluid loop in a centrifuge as described in Chapter 3. To confirm the thermodynamic theory and experimental techniques, these experiments were performed at low pressures (< 200 psi) and at high pressures (≥ 300 psi). The results will be discussed accordingly below. For all of the tests discussed below, observations indicated that temperature was fairly uniform across the PCA; that is, the temperature varied less than 1°F.

4.3.1 Low Pressure Results

I started centrifuge experiments at low pressure (about 150 psig) to test the equipment, to confirm the theory for ideal gases, and to develop a feel for how much change in composition can be achieved. Tests at pressures less than 150 psig were not possible because the volume of gas in the sample chambers at lower pressures was insufficient for GC analysis. Even at 150 psig, there is some difficulty in achieving reliable results.

At 150 psig, the gas behaves approximately as an ideal gas. So, the results at this pressure should be compared with the predictions of Sage and Lacey[1] and with

the predictions of the numerical program for ideal gas behavior for isothermal conditions, equation 2.32.

The results obtained for three centrifuge experiments are shown in Table 4.3 in terms of methane mole fraction x_1 and the ratio of methane to propane x_1/x_2. Comparing the composition gradient in Table 4.3 expressed as ratio of methane to propane and as a mole fraction of methane, one sees that the ratio is a more sensitive indicator of change in composition of the samples. A plot of the ratio of methane to propane is shown in Figure 4.3A. The methane mole fraction is plotted in Figure 4.3B.

From these two figures, it can be concluded that the maximum observable change in composition gradient is quite small, less than two percent of the mole ratio. This small gradient is expected at low pressure and isothermal condition. Figure 4.3 shows the symmetry of the data relative to the center of the PCA. Except for inevitable scatter in the GC results, the compositions on one side of the PCA should be similar to the other side of the PCA.

It is clear that the data are not fully symmetric, but they are partially symmetric. Some of the data show more symmetry. For instance, for Runs 2 and 3, the ratios as well as the mole fraction for the end chambers, which are located at 20.55 cm from the center of spin, are very nearly equal. The symmetry of the data will be improved as we go higher in pressure since the volume of gas in the sample chambers at higher pressures will be sufficient for reproducible GC analysis.

Methane to propane ratio and methane mole fraction obtained for these three experiments are compared with the prediction from Sage-Lacey model and the numerical program. The comparison for every run is shown in Figure 4.4 for the ratios of and in Figure 4.5 for the methane mole fractions. The predictions from Sage and Lacey and from the numerical model are identical so I just presented them as one line in all figures. As it is clear from those figures, predicted compositional gradients are slightly larger than measured gradients.

Much effort was directed to improving and maintaining good experimental technique in order to generate high quality data. For example, all of the tubing and vessels were heated to avoid condensation of liquids during transfers to the PCA and from the PCA to the GC. But, for lack of funds and time, some issues were not fully resolved. For example, instead of manually closing the valves on the PCA after stopping the centrifuge, automatically closing valves would eliminate the potential for mixing of gases between sample chambers. Perhaps, this issue will be solved in future experimentation.

Table 4.3 Experimental Methane/Propane Ratio and Methane Mole Fraction
2500 rpm, 6 hrs, 150 psig, 50°C
Isothermal

Run #	1	1	2	2	3	3
r, cm	x_1	x_1/x_2	x_1	x_1/x_2	x_1	x_1/x_2
20.55	0.5832	1.3991	0.5820	1.3925	0.5819	1.3920
13.70	0.5838	1.4026	0.5826	1.3958	0.5824	1.3946
6.85	0.5843	1.4058	0.5832	1.3994	0.5838	1.4025
0.00	0.5845	1.4070	0.5840	1.4038	0.5843	1.4057
-6.85	0.5845	1.4067	0.5851	1.4101	0.5850	1.4095
-13.70	0.5837	1.4018	0.5843	1.4053	0.5839	1.4033
-20.55	0.5827	1.3962	0.5819	1.3917	0.5820	1.3923
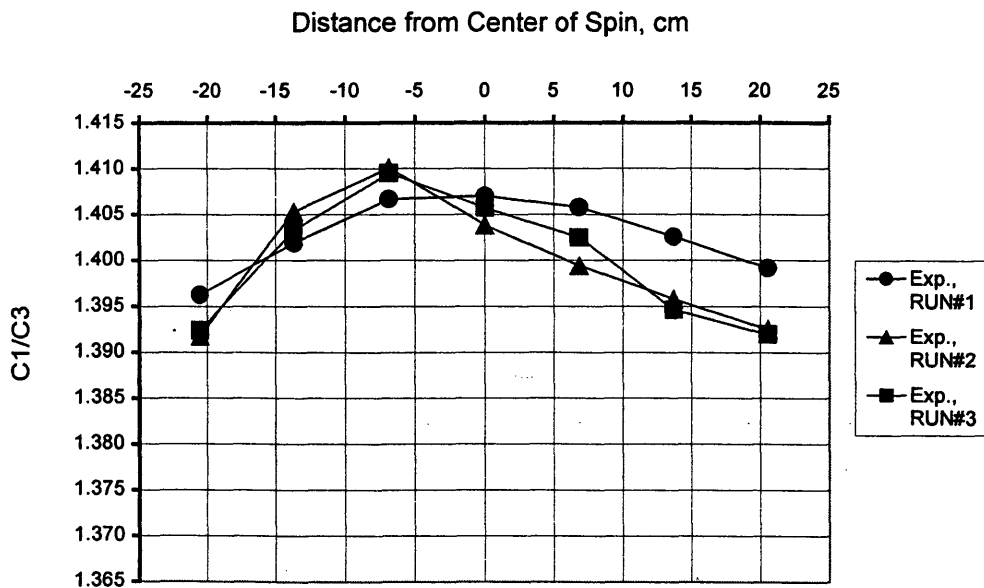
Figure 4.3A: Experimental Methane/Propane Ratio
2500 rpm, 6 hrs, 150 psi, 50°C
Isothermal

Distance from Center of Spin, cm

| | -25 | -20 | -15 | -10 | -5 | 0 | 5 | 10 | 15 | 20 | 25 |
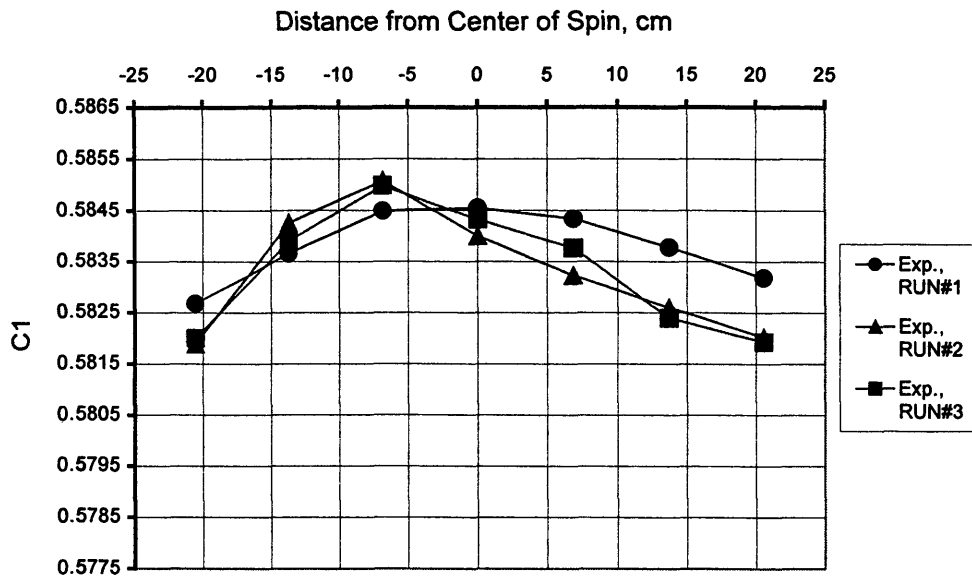
Figure 4.3B: Experimental Methane Mole Fraction
2500 rpm, 6 hrs, 150 psi, 50°C
Isothermal

Distance from Center of Spin, cm
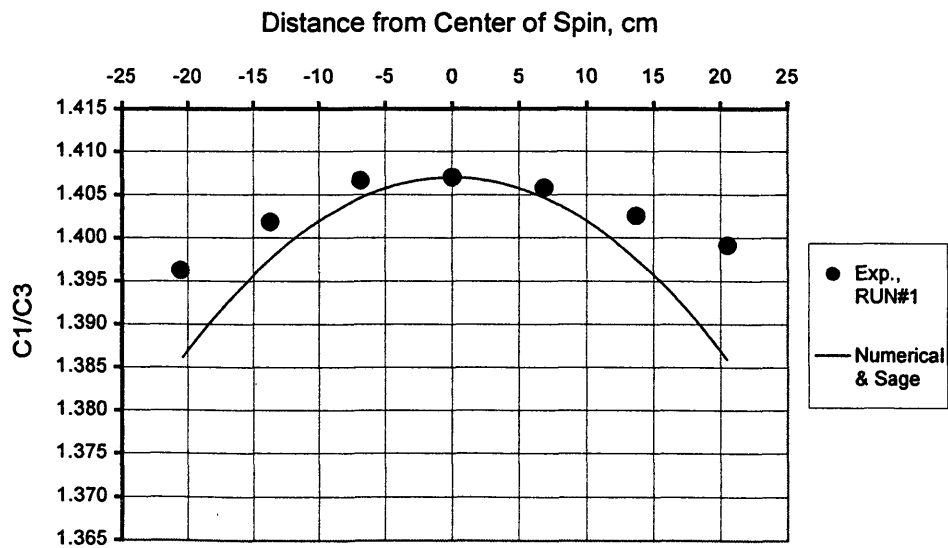
Figure 4.4A : Experimental & Theoretical Methane/Propane Ratio
2500 rpm, 6 hrs, 150 psi, 50°C
Isothermal

Distance from Center of Spin, cm
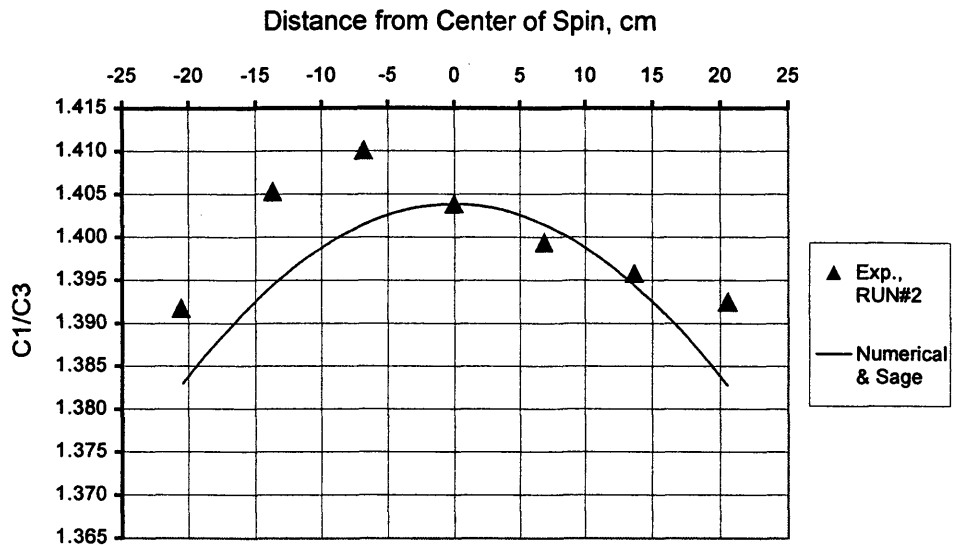
Figure 4.4B : Experimental & Theoretical Methane/Propane Ratio
2500 rpm, 6 hrs, 150 psi, 50°C
Isothermal

Distance from Center of Spin, cm
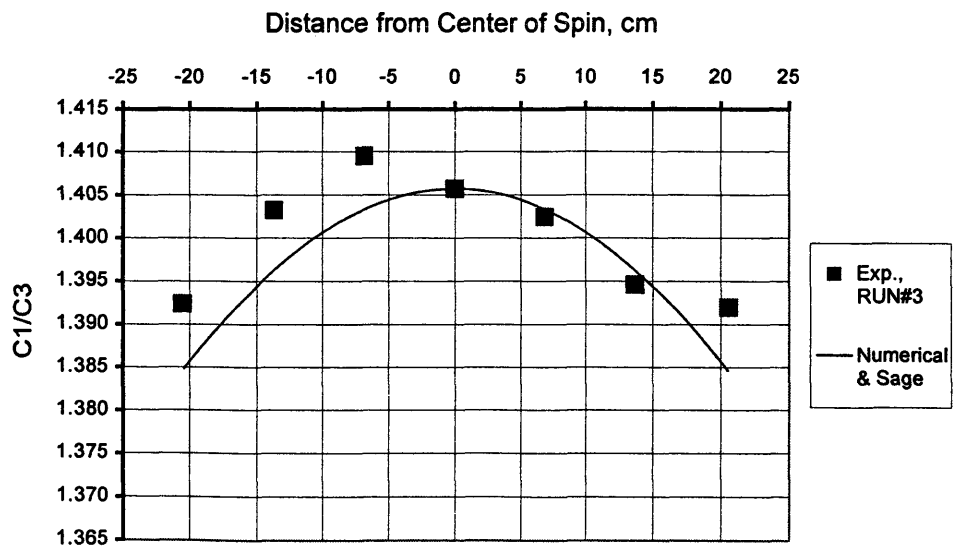
Figure 4.4C : Experimental & Theoretical Methane/Propane Ratio
2500 rpm, 6 hrs, 150 psi, 50°C
Isothermal

Distance from Center of Spin, cm

-25   -20   -15   -10   -5   0   5   10   15   20   25

C1
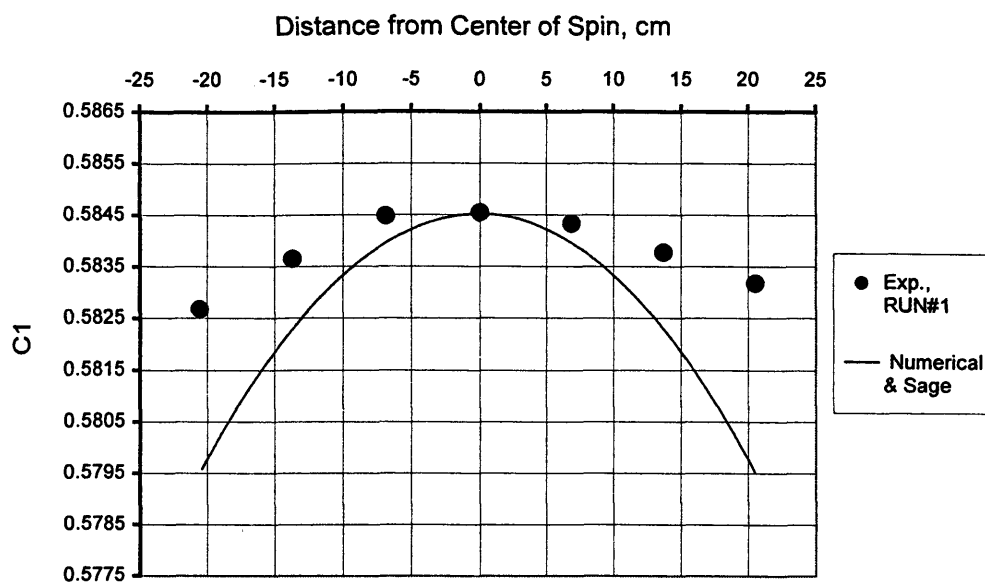
Figure 4.5A : Experimental & Theoretical Methane Mole Fraction
2500 rpm, 6 hrs, 150 psi, 50°C
Isothermal

Distance from Center of Spin, cm

-25   -20   -15   -10   -5   0   5   10   15   20   25

C1
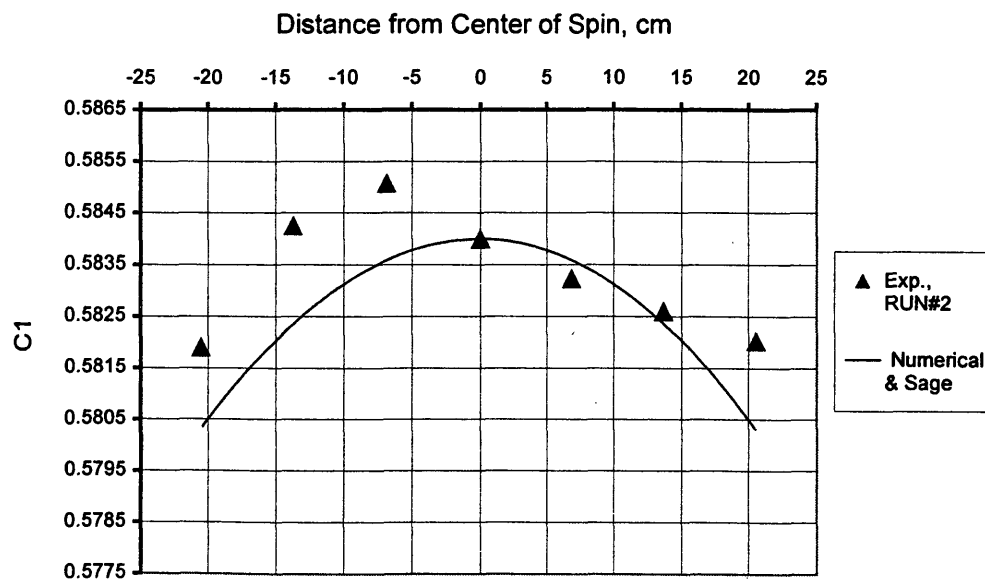
Figure 4.5B : Experimental & Theoretical Methane Mole Fraction
2500 rpm, 6 hrs, 150 psi, 50°C
Isothermal

Distance from Center of Spin, cm
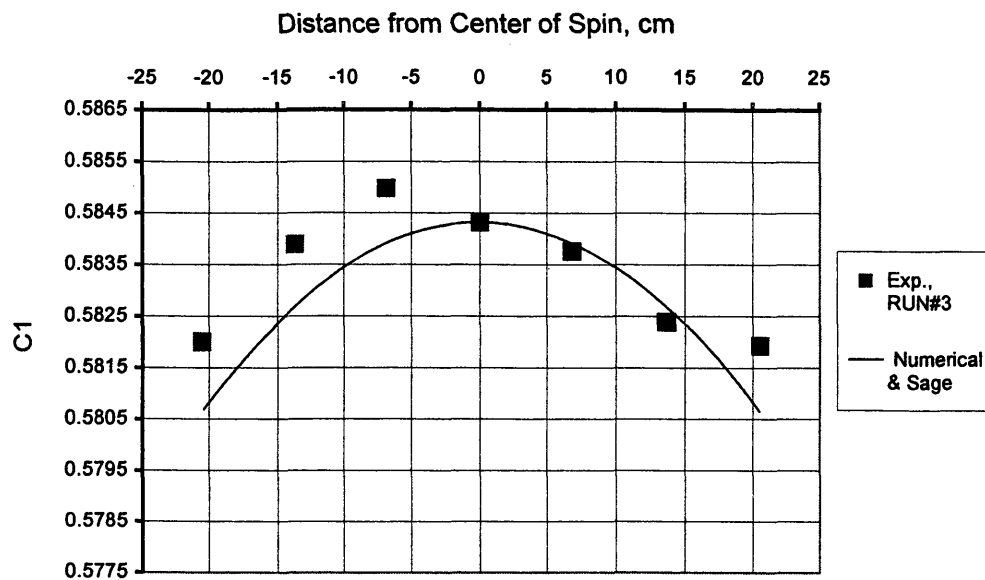
Figure 4.5C : Experimental & Theoretical Methane Mole Fraction
2500 rpm, 6 hrs, 150 psi, 50°C
Isothermal

4.3.2 High Pressure Results

The results of seven isothermal experiments are presented in this section. These isothermal experiment were conducted at centrifuge speed of 2500 rpm, temperature of 50 °C, time duration of 6 hrs, and at different pressures: three experiments at 300 psig, two experiments at 600 psig, one experiment at 900 psig, and one experiment at 1500 psig.

The results for three experiments at 300 psig are tabulated in Table 4.4. Methane mole fractions for the three runs are plotted in Figure 4.6A. The ratios are plotted in Figure 4.6B.

Table 4.4 Experimental Methane/Propane Ratio and Methane Mole Fraction
2500 rpm, 6 hrs, 300 psig, 50°C
Isothermal

Run #	1	1	2	2	3	3
r, cm	x_1	x_1/x_2	x_1	x_1/x_2	x_1	x_1/x_2
20.55	0.5808	1.3855	0.5810	1.3868	0.5812	1.3880
13.70	0.5825	1.3952	0.5828	1.3967	0.5822	1.3936
6.85	0.5837	1.4022	0.5848	1.4083	0.5838	1.4028
0.00	0.5845	1.4069	0.5852	1.4107	0.5846	1.4073
-6.85	0.5838	1.4024	0.5846	1.4076	0.5830	1.3978
-13.70	0.5839	1.4035	0.5842	1.4051	0.5821	1.3927
-20.55	0.5812	1.3878	0.5823	1.3939	0.5815	1.3895

Distance from Center of Spin, cm

-25 -20 -15 -10 -5 0 5 10 15 20 25

C1/C3

1.415
1.410
1.405
1.400
1.395
1.390
1.385
1.380
1.375
1.370
1.365

—■— Exp.,
RUN#1

—▲— Exp.,
RUN#2

—●— Exp.,
RUN#3
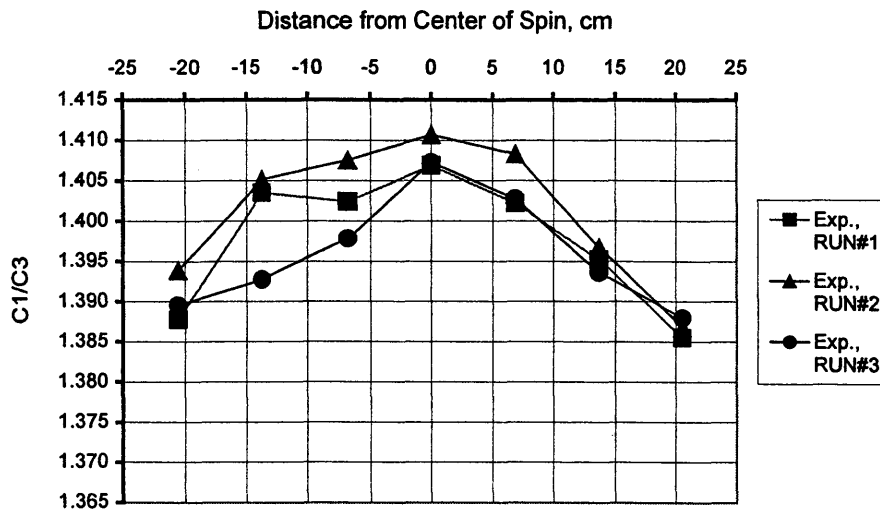
Figure 4.6A: Experimental Methane/Propane Ratio
2500 rpm, 6 hrs, 300 psi, 50°C
Isothermal

Distance from Center of Spin, cm

-25 -20 -15 -10 -5 0 5 10 15 20 25

C1

0.5865
0.5855
0.5845
0.5835
0.5825
0.5815
0.5805
0.5795
0.5785
0.5775

—■— Exp.,
RUN#1

—▲— Exp.,
RUN#2

—●— Exp.,
RUN#3
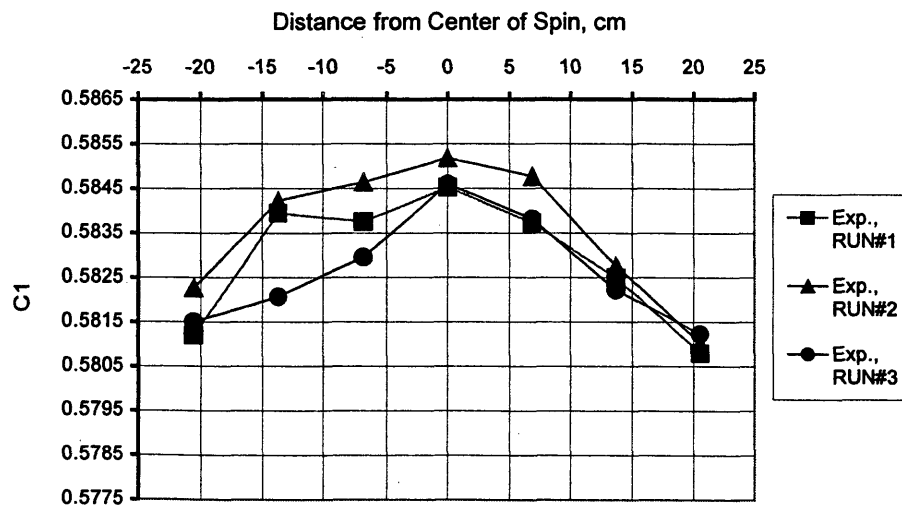
Figure 4.6B: Experimental Methane Mole Fraction
2500 rpm, 6 hrs, 300 psi, 50°C
Isothermal

Comparing this composition gradient with that obtained at 150 psig one can conclude that as the pressure increases, the gradient increases. Still, the magnitude of the change in composition is quite small -- less than two percent in the mole ratio. This is expected since the experiments were conducted at isothermal condition and quite low pressure.

The methane mole fraction and the ratio for each run were compared with the predicted values from the numerical program, using equation 2.25, as shown in Figures 4.7 and 4.8 respectively. Looking to these figures, one finds again that the predicted gradient is larger than the measured gradient.

As mentioned earlier, the symmetry of the data would improve with higher pressure. Comparing the symmetry of the data at 300 psig to that at 150 psig, there is some improvement, which indicates increased quality of the data. One reason for this is that the volume of gas in the sample chambers at this pressure was sufficient for reproducible GC analysis.

Distance from Center of Spin, cm
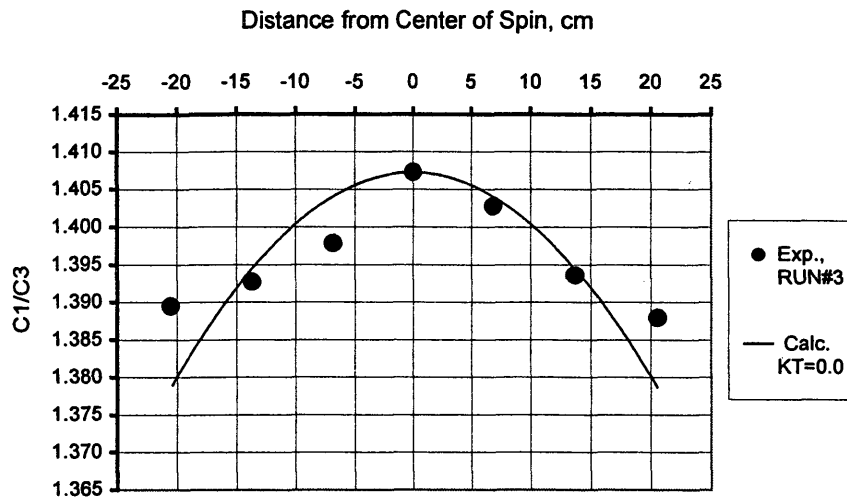
Figure 4.7A : Experimental & Theoretical Methane/Propane Ratio
2500 rpm, 6 hrs, 300 psi, 50°C
Isothermal

Distance from Center of Spin, cm
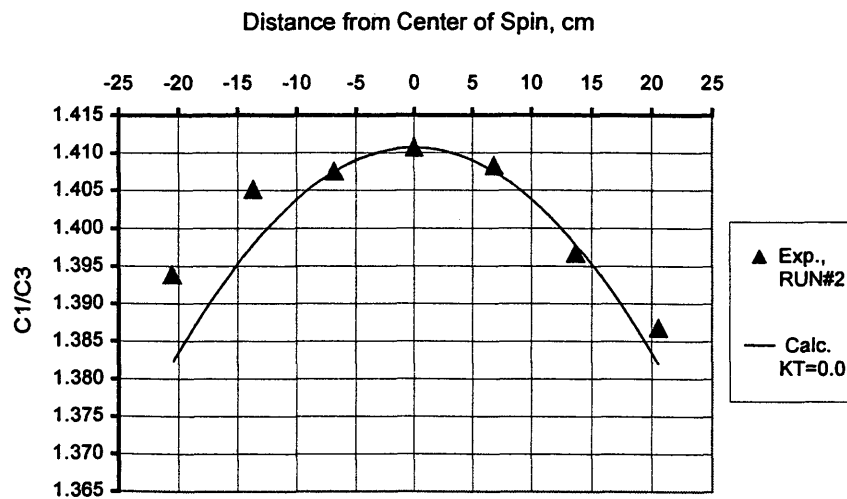
Figure 4.7B : Experimental & Theoretical Methane/Propane Ratio
2500 rpm, 6 hrs, 300 psi, 50°C
Isothermal

Distance from Center of Spin, cm
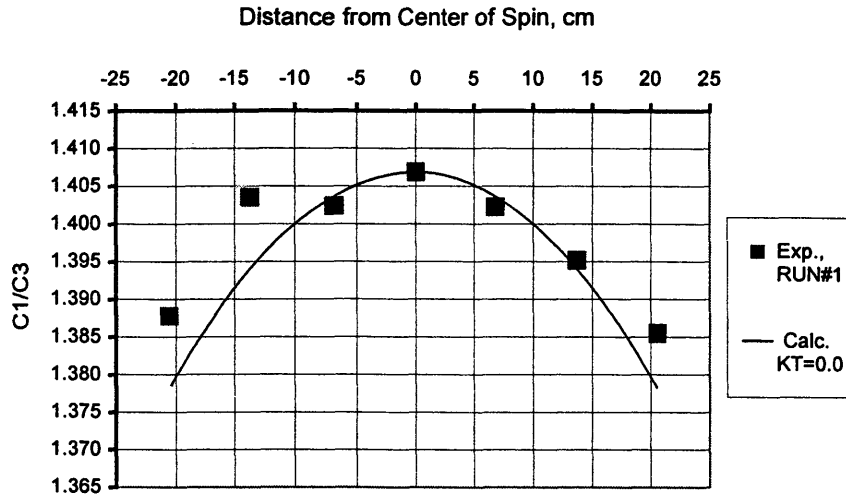
Figure 4.7C : Experimental & Theoretical Methane/Propane Ratio
2500 rpm, 6 hrs, 300 psi, 50°C
Isothermal

Distance from Center of Spin, cm
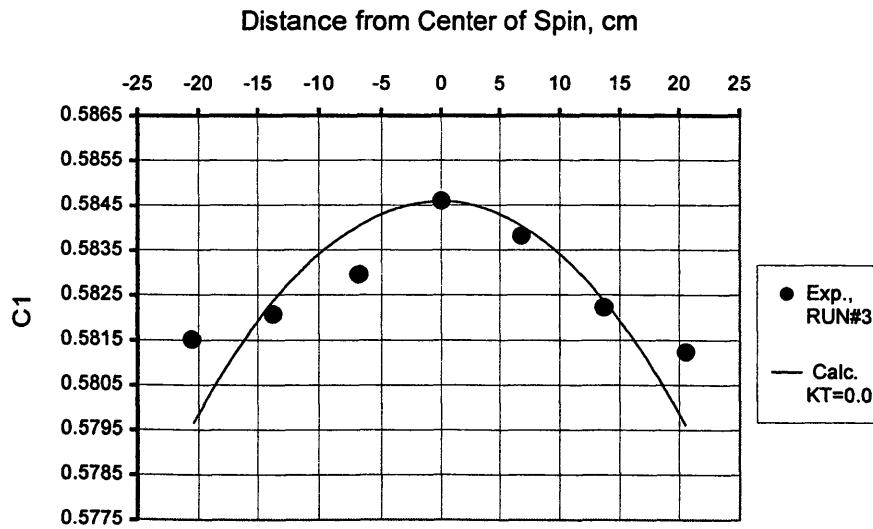
Figure 4.8A : Experimental & Theoretical Methane Mole Fraction
2500 rpm, 6 hrs, 300 psi, 50°C
Isothermal

Distance from Center of Spin, cm
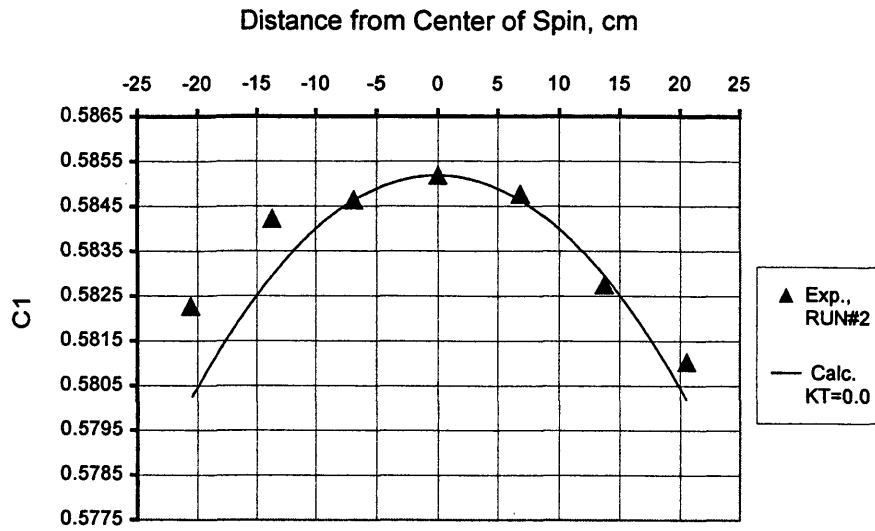
Figure 4.8B : Experimental & Theoretical Methane Mole Fraction
2500 rpm, 6 hrs, 300 psi, 50°C
Isothermal

Distance from Center of Spin, cm
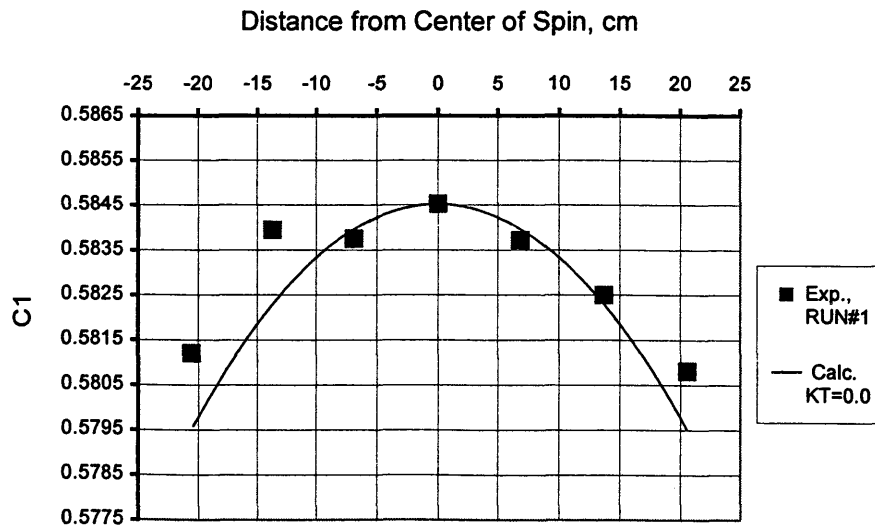
Figure 4.8C : Experimental & Theoretical Methane Mole Fraction
2500 rpm, 6 hrs, 300 psi, 50°C
Isothermal

Two centrifuge experiments were performed at 600 psig at temperature of 50 °C and a spin rate of 2500 rpm. The results are presented in Table 4.5 below. The data in Table 4.5 are plotted in Figure 4.9. The magnitude of composition gradient for these experiments is similar to that obtained for previous experiments at 300 psig.

Table 4.5 Experimental Methane/Propane Ratio and Methane Mole Fraction
2500 rpm, 6 hrs, 600 psig, 50°C
Isothermal

Run #	1	1	2	2
r, cm	x_1	x_1/x_2	x_1	x_1/x_2
20.55	0.5807	1.3849	0.5812	1.3878
13.70	0.5824	1.3948	0.5824	1.3944
6.85	0.5833	1.3996	0.5830	1.3983
0.00	0.5828	1.3969	0.5837	1.4024
-6.85	0.5799	1.3802	0.5819	1.3919
-13.70	0.5829	1.3975	0.5826	1.3958
-20.55	0.5791	1.3761	0.5813	1.3884

Distance from Center of Spin, cm
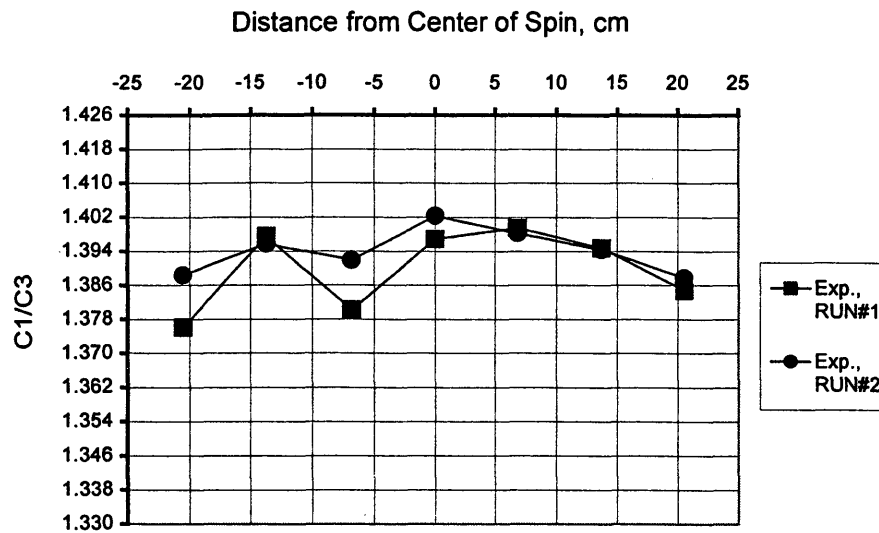
Figure 4.9A: Experimental Methane/Propane Ratio
2500 rpm, 6 hrs, 600 psi, 50°C
Isothermal

Distance from Center of Spin, cm
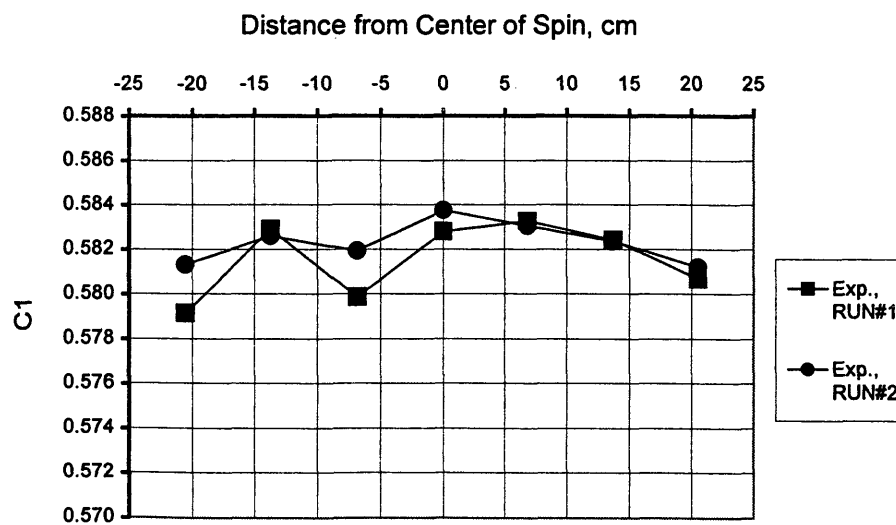
Figure 4.9B: Experimental Methane Mole Fraction
2500 rpm, 6 hrs, 600 psi, 50°C
Isothermal

Composition gradients predicted using the numerical program are compared with the data for the tests at 600 psig in Figures 4.10 and 4.11. As observed at lower pressures, the predicted composition gradient is larger than the measured gradient. But, the difference between the predicted and the measured gradient is larger at 600 psig than at the lower pressures.

Distance from Center of Spin, cm
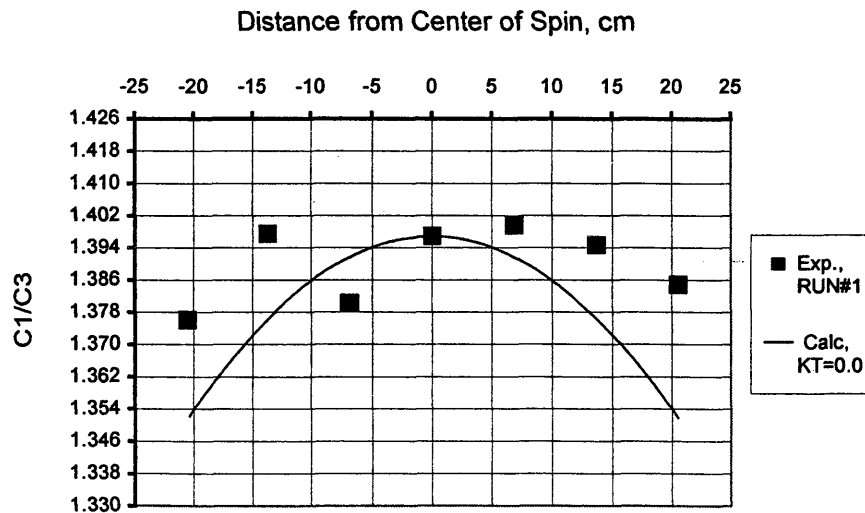
Figure 4.10A : Experimental & Theoretical Methane/Propane Ratio
2500 rpm, 6 hrs, 600 psi, 50°C
Isothermal

Distance from Center of Spin, cm

-25 -20 -15 -10 -5 0 5 10 15 20 25

1.426
1.418
1.410
1.402
1.394
1.386
1.378
1.370
1.362
1.354
1.346
1.338
1.330

C1/C3

● Exp., RUN#2

— Calc. KT=0.0

Figure 4.10B : Experimental & Theoretical Methane/Propane Ratio
2500 rpm, 6 hrs, 600 psi, 50°C
Isothermal

Distance from Center of Spin, cm

-25 -20 -15 -10 -5 0 5 10 15 20 25

0.588
0.586
0.584
0.582
0.580
0.578
0.576
0.574
0.572
0.570

C1

■ Exp., RUN#1

— Calc. KT=0.0

Figure 4.11A : Experimental & Theoretical Methane Mole Fraction
2500 rpm, 6 hrs, 600 psi, 50°C
Isothermal

Distance from Center of Spin, cm

Figure 4.11B : Experimental & Theoretical Methane Mole Fraction
2500 rpm, 6 hrs, 600 psi, 50°C
Isothermal

Two experiments were successfully completed at higher pressures: 900 psig, and 1500 psig. Each lasted for 6 hours at 2500 rpm and 50 °C. Table 4.6 shows the results. It is clear at these levels of pressure that the composition gradient is much larger than at lower pressures. The reason for this enhanced gradient is that the system is closer to the critical condition for the binary system. The change in mole ratio for the 900 psig data is about 10% whereas the change at 1500 psig is about 20%. Therefore, compared to the gradients at lower pressures, the gradients at 900 psig and 1500 psig are much more significant.

Table 4.6 Experimental Methane/Propane Ratio and Methane Mole Fraction
2500 rpm, 6 hrs, 900 psig and 1500 psig, 50°C
Isothermal

P, psig	900	900	1500	1500
r, cm	x_1	x_1/x_2	x_1	x_1/x_2
20.55	0.5632	1.2892	0.5328	1.1403
13.70	0.5823	1.3940	0.5791	1.3758
6.85	0.5869	1.4210	0.5861	1.4161
0.00	0.5941	1.4639	0.5962	1.4764
-6.85	0.5917	1.4491	0.5862	1.4168
-13.70	0.5869	1.4205	0.5689	1.3198
-20.55	0.5639	1.2930	0.4992	0.997

This considerable effect of gravity on the composition of methane and propane is clearly illustrated in Figure 4.12 for the data generated at 900 psig. The data for 900 psig were compared to the predicted composition gradient using the numerical program as shown in Figure 4.13. As is clear from these two figures, the numerical model is underestimating the gradient rather than overestimating it as it did for lower pressures.

Distance from Center of Spin, cm
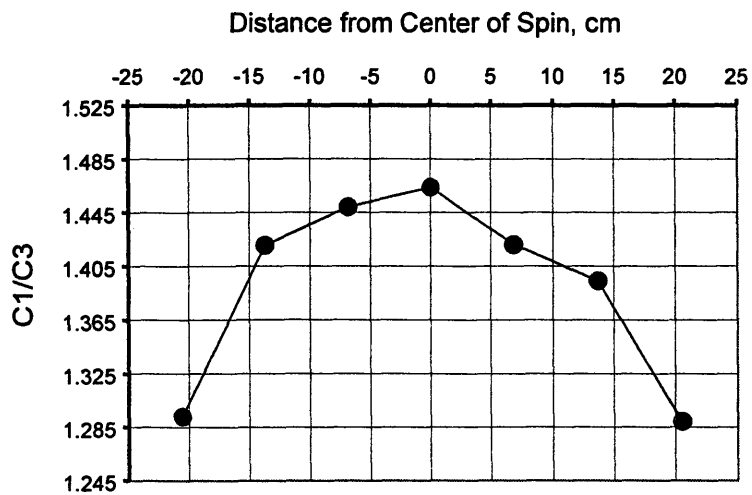
Figure 4.12A: Experimental Methane/Propane Ratio
2500 rpm, 6 hrs, 900 psi, 50 °C
Isothermal

Distance from Center of Spin, cm
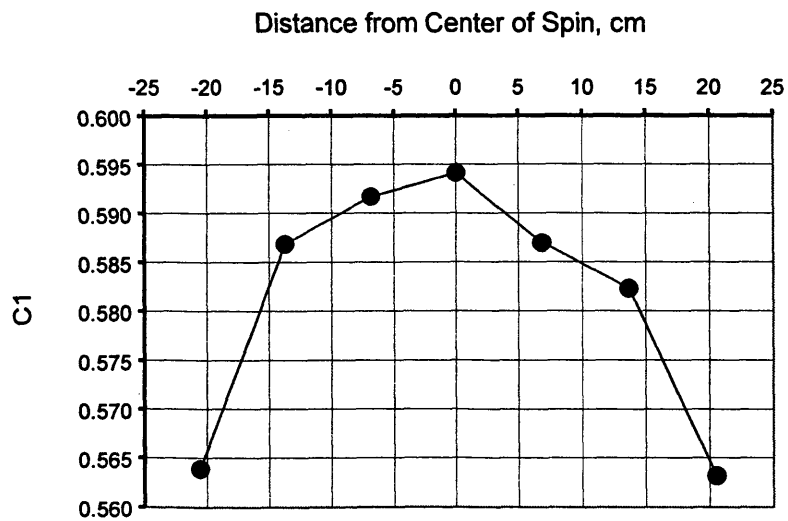
Figure 4.12B: Experimental Methane Mole Fraction
2500 rpm, 6 hrs, 900 psi, 50 °C
Isothermal

Distance from Center of Spin, cm
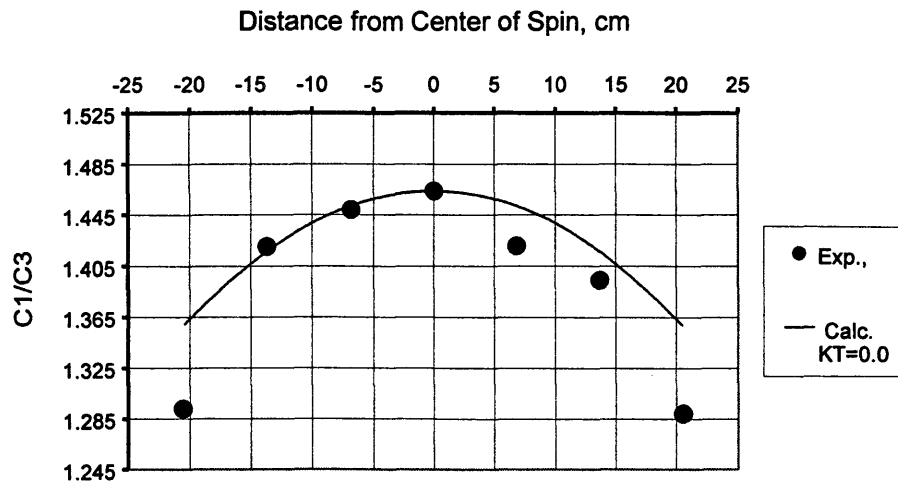
Figure 4.13A : Experimental & Theoretical Methane/Propane Ratio
2500 rpm, 6 hrs, 900 psi, 50 °C
Isothermal

Distance from Center of Spin, cm
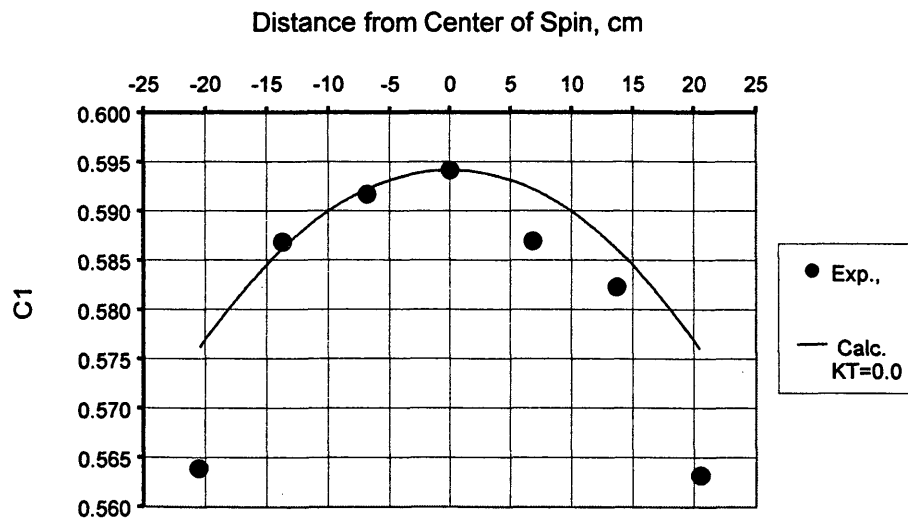
Figure 4.13B : Experimental & Theoretical Methane Mole Fraction
2500 rpm, 6 hrs, 900 psi, 50 °C
Isothermal

The composition gradient resulted at 1500 psig is larger than at 900 psig, as shown in Figure 4.14. Figures 4.15A and 4.15B are plots of the data and the predicted composition from the numerical program. As was the case for 900 psig, the numerical program underestimates the gradient.

Distance from Center of Spin, cm
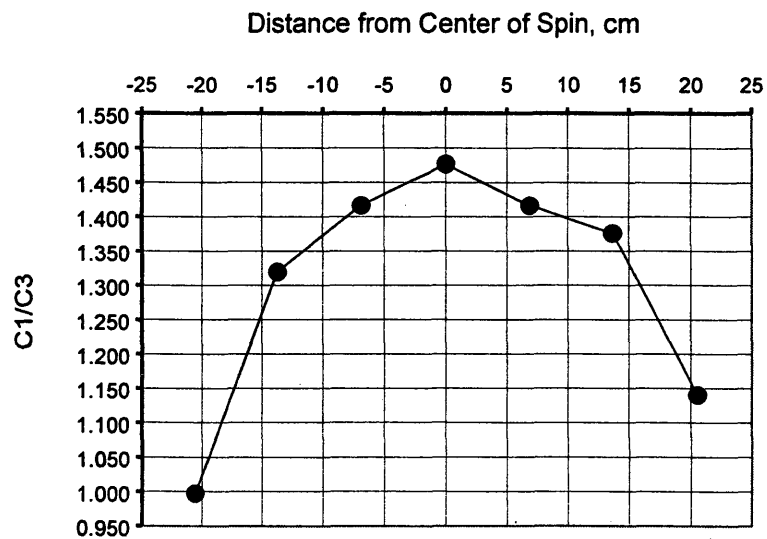
Figure 4.14A: Experimental Methane/Propane Ratio
2500 rpm, 6 hrs, 1500 psi, 50°C
Isothermal

Distance from Center of Spin, cm
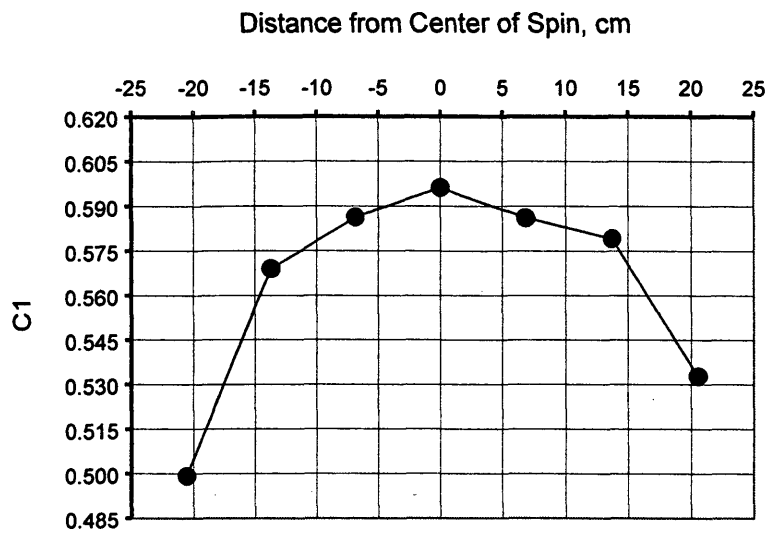
Figure 4.14B: Experimental Methane Mole Fraction
2500 rpm, 6 hrs, 1500 psi, 50 °C
Isothermal

Distance from Center of Spin, cm
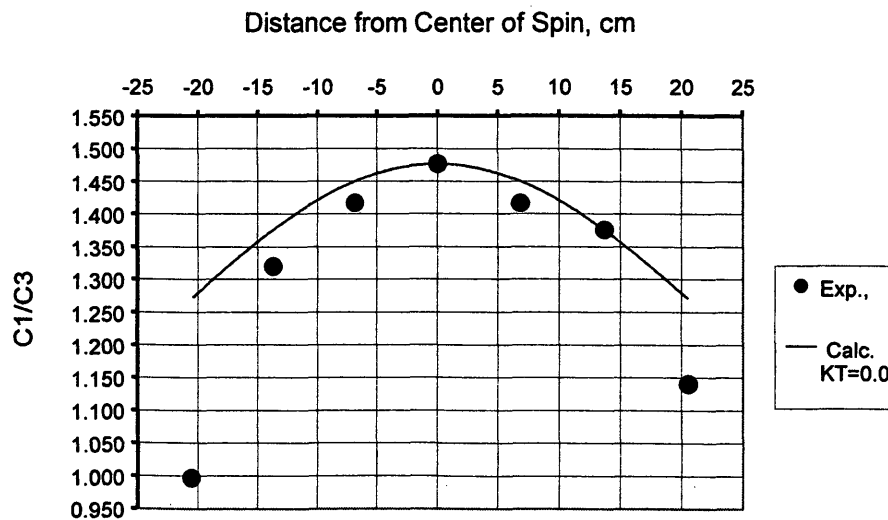
Figure 4.15A : Experimental & Theoretical Methane/Propane Ratio
2500 rpm, 6 hrs, 1500 psi, 50C
Isothermal

Distance from Center of Spin, cm
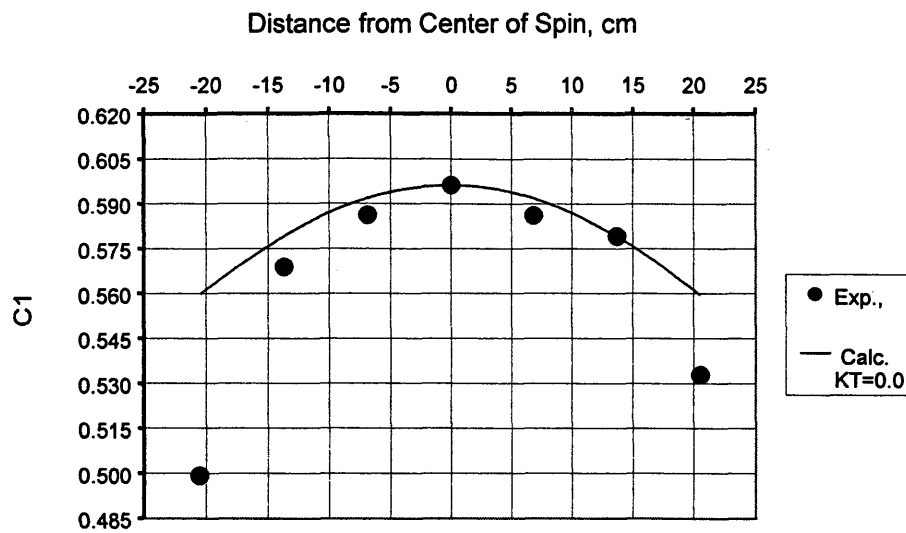
Figure 4.15B : Experimental & Theoretical Methane Mole Fraction
2500 rpm, 6 hrs, 1500 psi, 50 °C
Isothermal

4.4 Compositional Variation under the Effect of Gravity and Temperature Gradients

In an effort to reproduce more closely the real conditions of pressure and temperature in petroleum reservoirs, ten centrifugal experiments with temperature gradients were performed in the lab. (About 20 other experiments were attempted, but because of a variety of problems, the tests were aborted. In some tests, gas leaks occurred. In some tests, the centrifuge stopped spinning because of overheating.) In these non-isothermal tests, the binary gas mixture of methane and propane was charged to the PCA at pressures from 300 psig to 1500 psig. In all of these experiments, the PCA was spun at 2500 rpm for 6 hours.

The temperature difference from the outside sample cell to the center sample cell was about 11 °F. This difference in temperature corresponds approximately to 500 feet of elevation difference for a temperature gradient of 0.022 °F/ft. The average geothermal gradient published for some reservoirs in the Middle East[4], North Sea[40], and North America[30], is 0.015°F/ft.

In calculations for the non-isothermal experiments, the effect of the temperature field on composition gradient is controlled by the thermal diffusion ratio. The thermal diffusion ratio is known to depend on temperature, pressure, and composition. Here, however, the thermal diffusion coefficient is assumed to be constant. This may be a reasonable assumption since for the temperature gradient obtained in this research, but much further testing is required to fully assess it.

The data for the following ten successful non-isothermal experiments are discussed below:

Three experiments at 300 psig,

Two experiments at 600 psig,

Three experiments at 900 psig,

Two experiments at 1500 psig.

The composition gradient data at 300 psig are listed in Table 4.7 and plotted in Figure 4.16.

Table 4.7 Experimental Methane/Propane Ratio and Methane Mole Fraction
2500 rpm, 6 hrs, 300 psig, 50°C
Non-Isothermal

Run #	1	1	2	2	3	3
r, cm	x_1/x_2	x_1	x_1/x_2	x_1	x_1/x_2	x_1
20.55	1.3806	0.5799	1.3806	0.5799	1.3816	0.5801
13.70	1.4010	0.5835	1.3946	0.5824	1.3890	0.5814
6.85	1.4041	0.5841	1.4034	0.5839	1.3941	0.5823
0.00	1.4075	0.5846	1.4045	0.5841	1.3969	0.5828
-6.85	1.4052	0.5842	1.4025	0.5838	1.3909	0.5818
-13.70	1.4043	0.5841	1.3950	0.5825	1.3877	0.5812
-20.55	1.3807	0.5799	1.3771	0.5793	1.3814	0.5801

Distance from Center of Spin, cm

-25 -20 -15 -10 -5 0 5 10 15 20 25

C1/C3

1.415
1.410
1.405
1.400
1.395
1.390
1.385
1.380
1.375
1.370
1.365

Exp., RUN#1

Exp., RUN#2

Exp., RUN#3
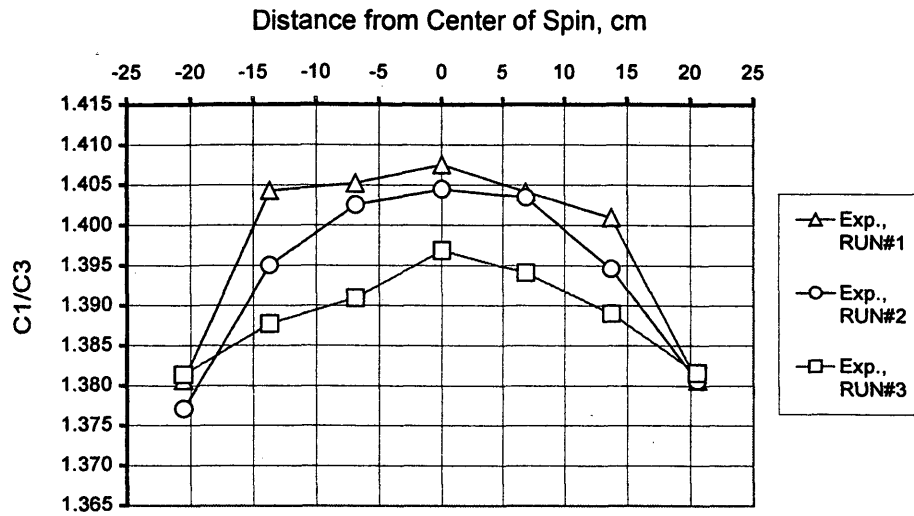
Figure 4.16A : Experimental Methane/Propane Ratio
2500 rpm, 6 hrs, 300 psi, 50°C
Non-isothermal

Distance from Center of Spin, cm

-25 -20 -15 -10 -5 0 5 10 15 20 25

C1

0.5865
0.5855
0.5845
0.5835
0.5825
0.5815
0.5805
0.5795
0.5785
0.5775

Exp., RUN#1

Exp., RUN#2

Exp., RUN#3
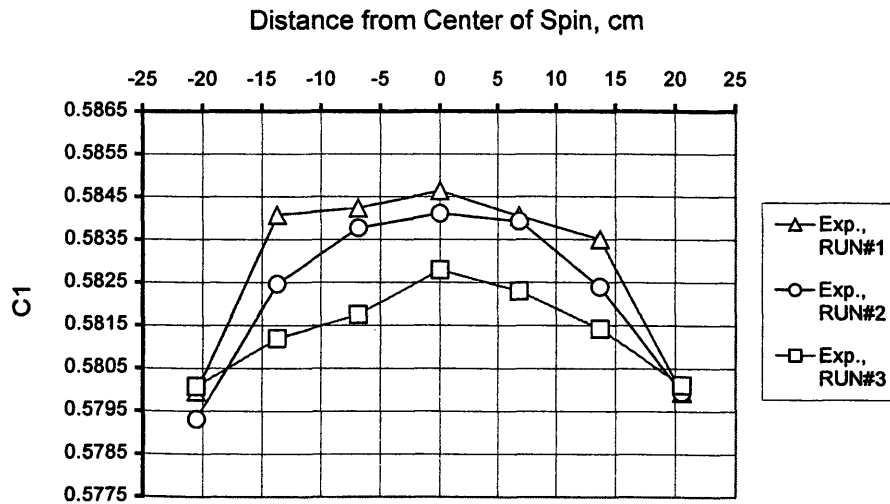
Figure 4.16B : Experimental Methane Mole Fraction
2500 rpm, 6 hrs, 300 psi, 50°C
Non-isothermal

Now having both gravity and temperature effects on composition in these experiments, one might expect a larger composition gradient compared to the isothermal experiments. As a matter of fact, looking to Figure 4.16, this is not the case. The magnitude of the change in composition is still quite small -- about two percent in the mole ratio, or slightly higher than that for isothermal runs. So, the conclusion at this point is that there is no remarkable change in composition gradient in going from isothermal to non-isothermal conditions at these conditions. This is clearly illustrated in Figure 4.16, which compare the non-isothermal with the isothermal data at 300 psig. Considerable change in composition was encountered at higher pressures as will be explained later.
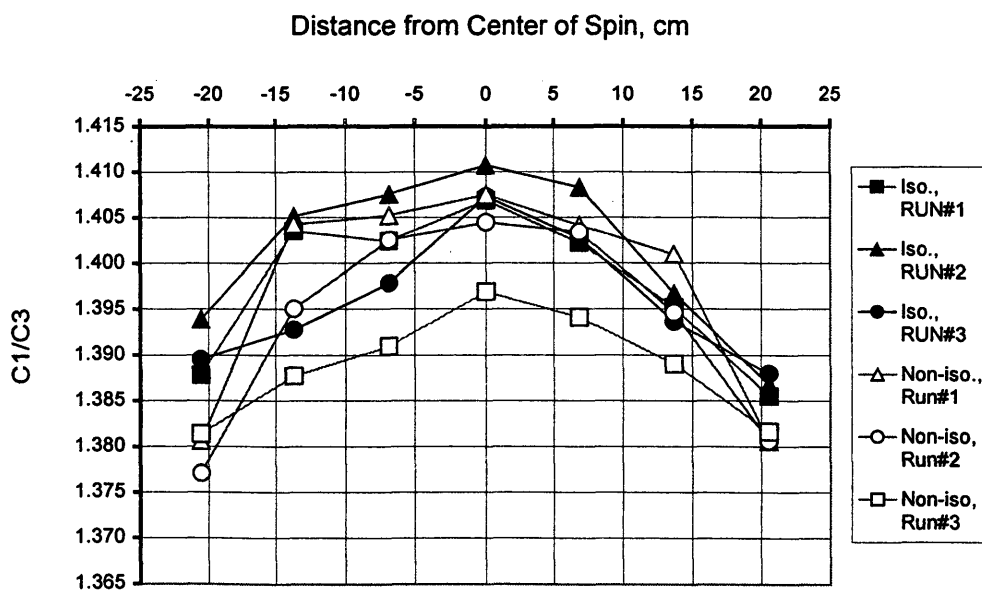
Figure 4.16C : Experimental Methane/Propane Ratio
2500 rpm, 6 hrs, 300 psi, 50°C
Isothermal & Non-isothermal

Distance from Center of Spin, cm
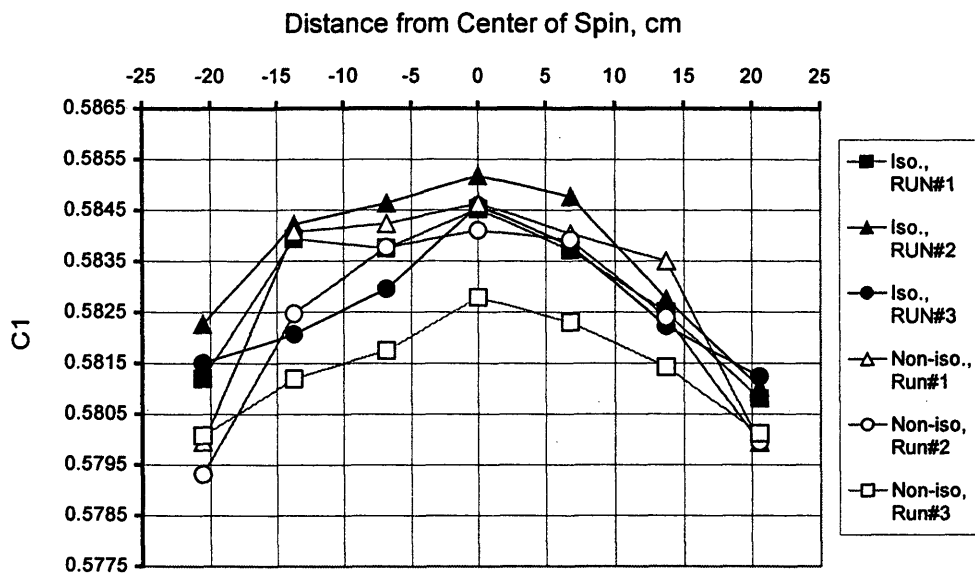
Figure 4.16D : Experimental Methane Mole Fraction
2500 rpm, 6 hrs, 300 psi, 50°C
Isothermal & Non-isothermal

In the numerical program, equation 2.49 is used to calculate the composition gradient for non-isothermal condition. In equation 2.49, the last term in the right hand side, the thermal diffusion term, takes care of the temperature effect. The thermal diffusion ratio k_T is a parameter in the model that can change to fit the non-isothermal data. For each set of data, I started with $k_T=0$, which represents the isothermal case, and gradually increased it until I obtained the best fit. The resulting fits are shown in Figures 4.17 and 4.18.

The predicted composition profile for the isothermal case k_T=0.0 is also included in these figures. The best-fit k_T for all three data sets are all very nearly equal to zero (from -0.012 to 0.0015). This supports the conclusion drawn earlier that isothermal and non-isothermal data at 300 psig look similar. For the same condition, the predicted value of the thermal diffusion ratio by Firoozabadi[25] is k_T = 0.05. I have coded Hirschfelder[55] approximation of thermal diffusion ratio for low density gases using FORTRAN-77. Using Hirschfelder[55] approximation, the predicted thermal diffusion ratio for the methane-propane system used in this research, is -0.025.

Distance from Center of Spin, cm
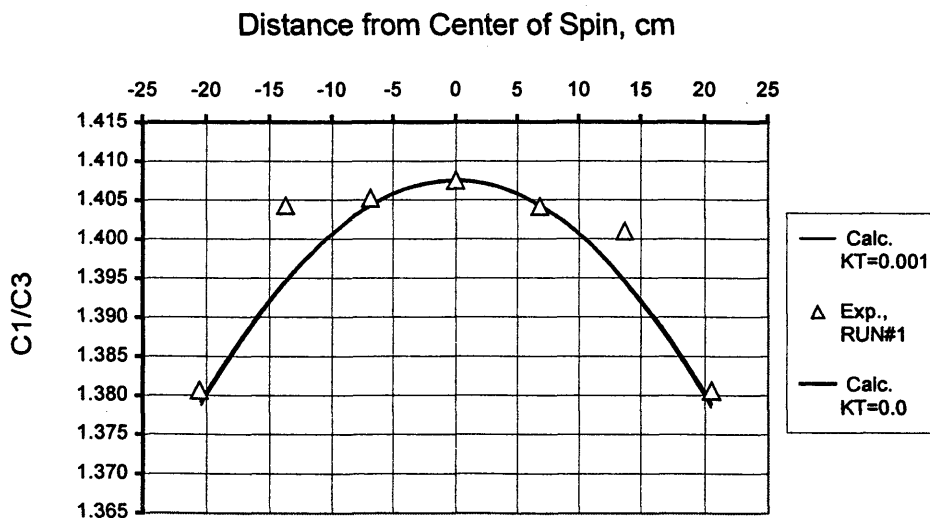
Figure 4.17A : Experimental & Theoretical Methane/Propane Ratio
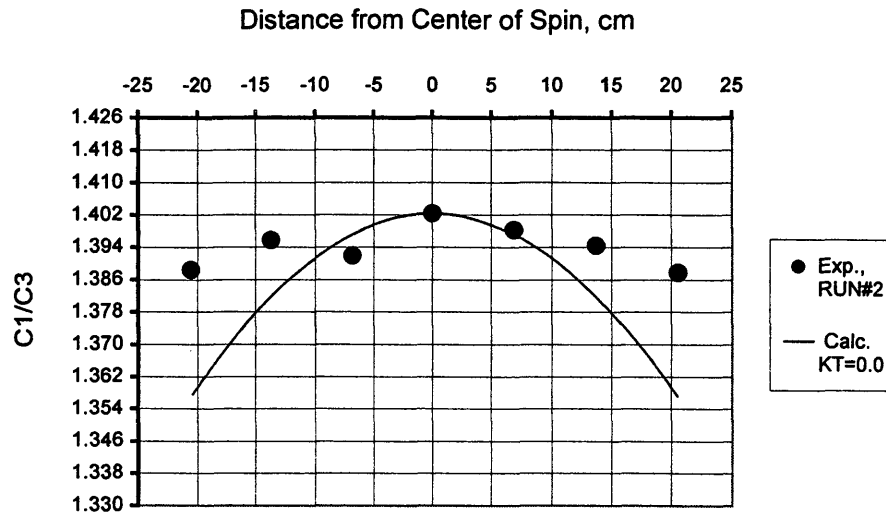2500 rpm, 6 hrs, 300 psi, 50°C
Non-isothermal
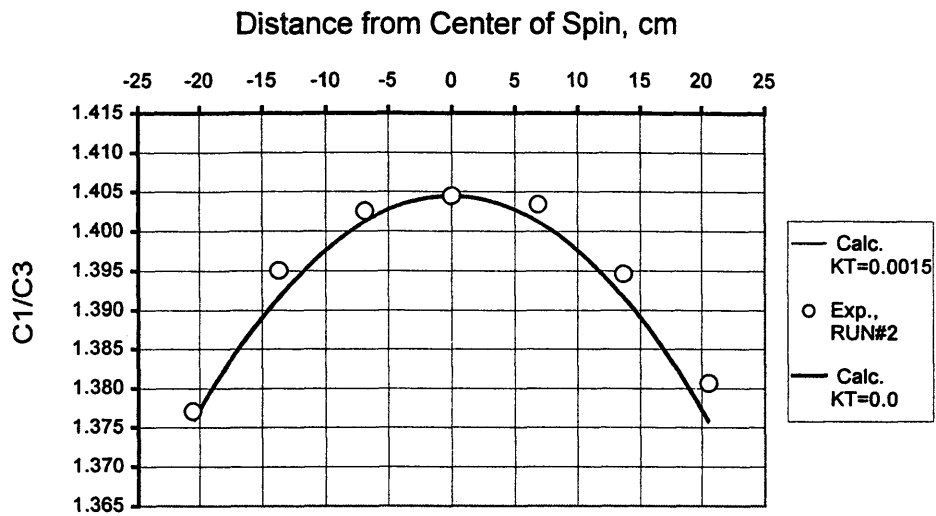
Figure 4.17B : Experimental & Theoretical Methane/Propane Ratio
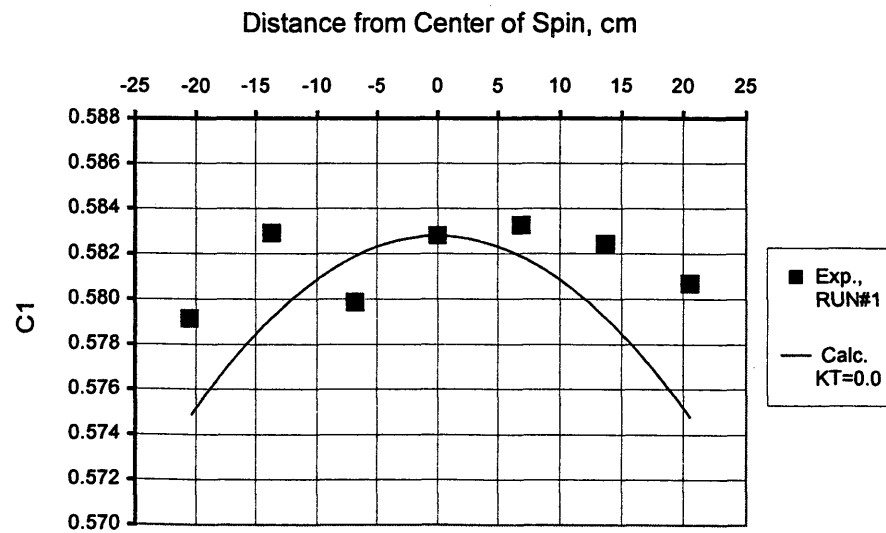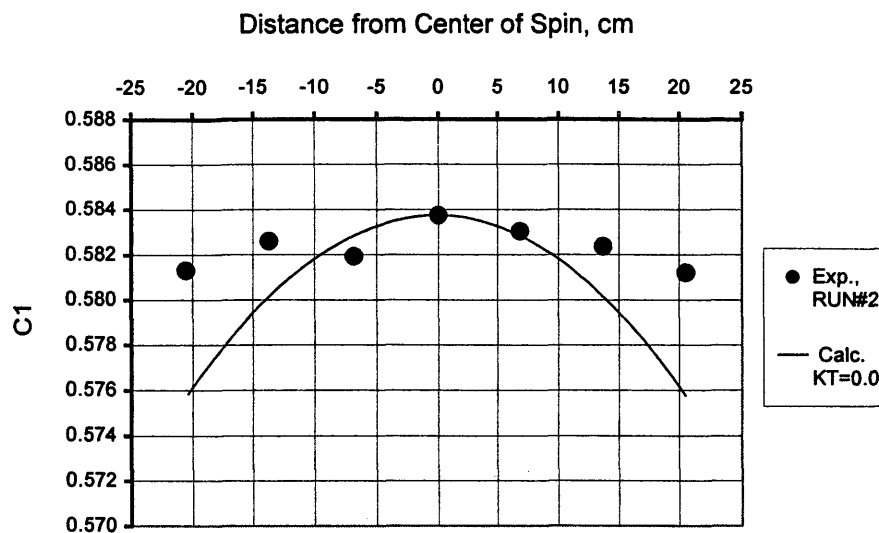2500 rpm, 6 hrs, 300 psi, 50°C
Non-isothermal
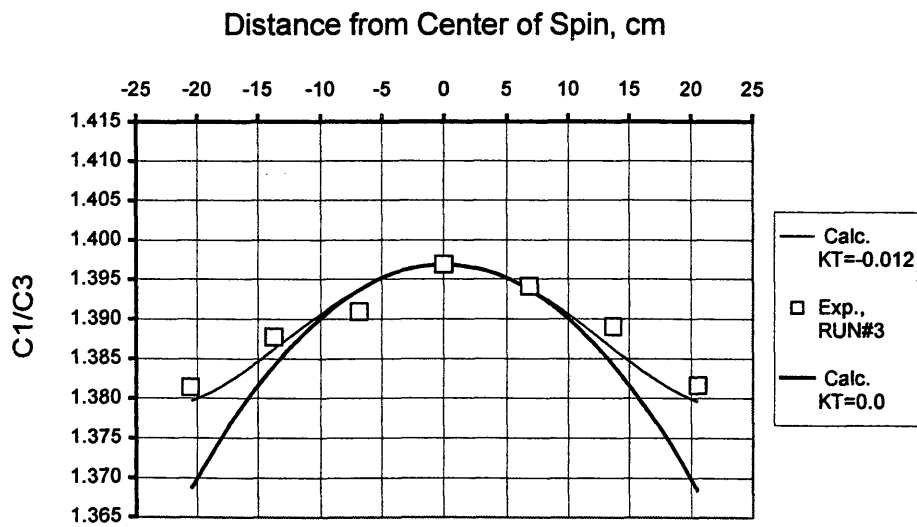
Figure 4.17C : Experimental & Theoretical Methane/Propane Ratio
2500 rpm, 6 hrs, 300 psi, 50°C
Non-isothermal

Distance from Center of Spin, cm
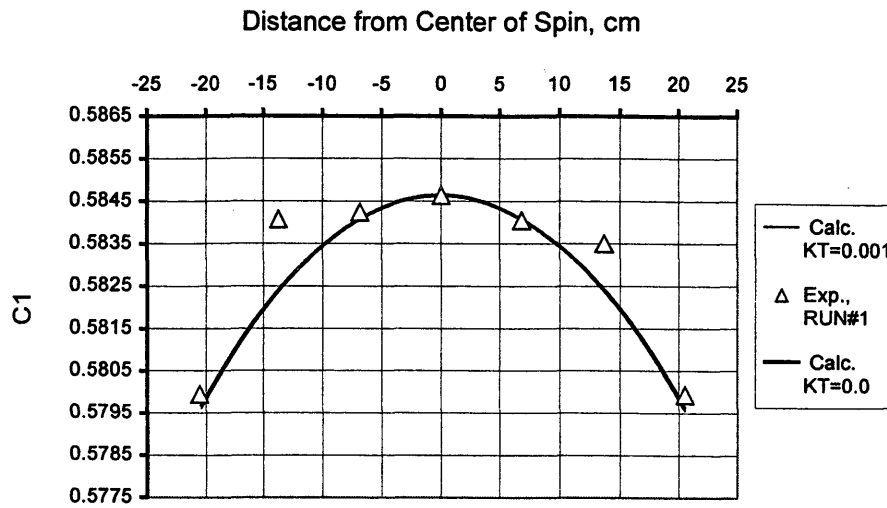
Figure 4.18A : Experimental & Theoretical Methane Mole Fraction
2500 rpm, 6 hrs, 300 psi, 50°C
Non-isothermal

Distance from Center of Spin, cm
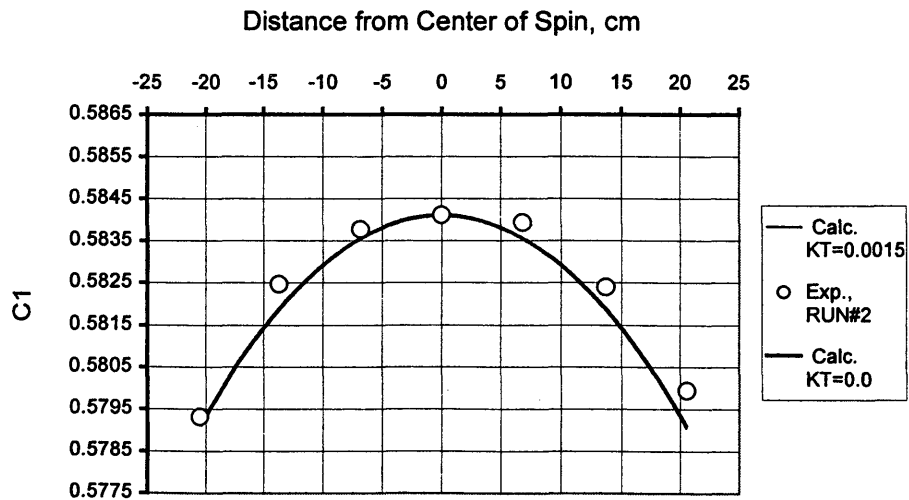
Figure 4.18B : Experimental & Theoretical Methane Mole Fraction
2500 rpm, 6 hrs, 300 psi, 50°C
Non-isothermal

Distance from Center of Spin, cm
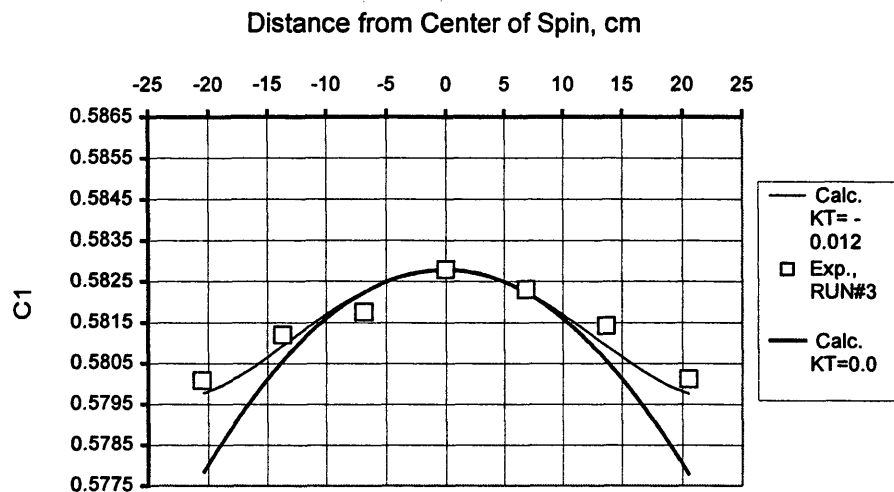
Figure 4.18C : Experimental & Theoretical Methane Mole Fraction
2500 rpm, 6 hrs, 300 psi, 50°C
Non-isothermal

Interestingly, the best-fit value of k_T for data set 3 is negative. Negative value of thermal diffusion ratio means that methane migrates toward higher temperatures. This migration downwards is opposite to the segregation of methane under gravity. The net result will be a reduced methane concentration gradient, and possibly even a gradient reversal. Apparently, negative thermal diffusion ratios of methane are not uncommon (Whitson[15]). Some investigators observed such

unique behavior in some reservoirs around the world as was mentioned earlier in Chapter 2.

Significant methane movement downward, as a result of negative thermal diffusion ratios, will tend to create a mechanically unstable condition. The consequence may be convection. If convection occurs, the equilibrium problem is no longer one-dimensional and another approach must be used for studying the compositional gradient problem. Firoozabadi[58] theoretically considers compositional gradients with the effect of convection.

Figure 4.19 reflects the effect of thermal diffusion on composition grading. The composition grading increases with increasing value of thermal diffusion ratio k_T.

Distance from Center of Spin, cm
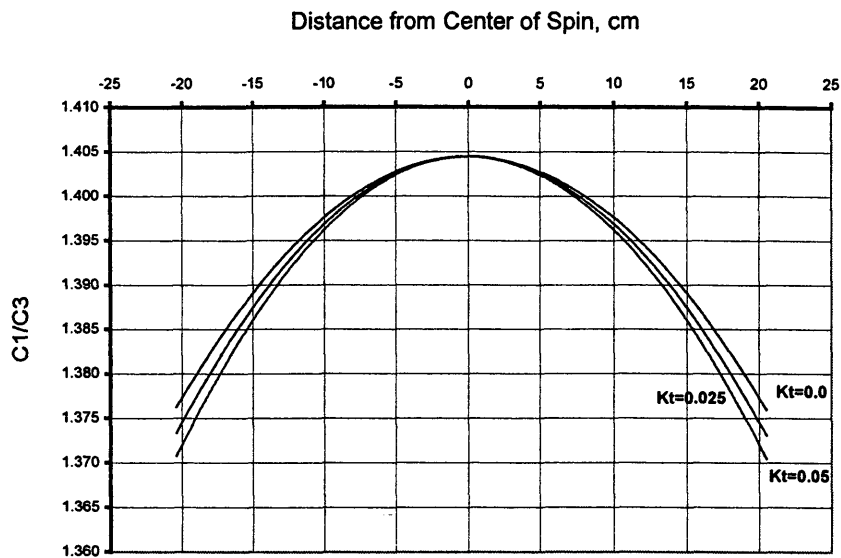
Figure 4.19A : Theoretical Methane/Propane Ratio at Different k_T

2500 rpm, 6 hrs, 300 psi,50°C

Distance from Center of Spin, cm
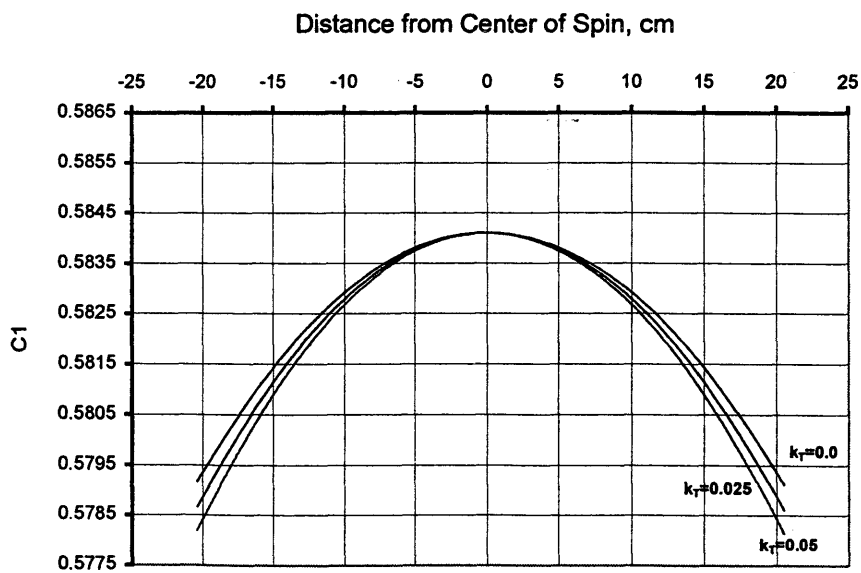
Figure 4.19B : Theoretical Methane Mole Fraction at Different k_T

2500 rpm, 6 hrs, 300 psi,50°C

According to Firoozabadi's calculations, the thermal diffusion ratio should increase to about 0.5 at pressures between 1000 psi and 1500 psi. Hoping to observe a larger composition gradient under the effect of both gravity and temperature fields, more experiments were conducted at higher pressures. The results for two non-isothermal experiments at 600 psig are presented in Table 4.8. The data are plotted in Figure 4.20.

Table 4.8 Experimental Methane/Propane Ratio and Methane Mole Fraction
2500 rpm, 6 hrs, 600 psig, 50°C
Non-Isothermal

Run #	1	1	2	2
r, cm	x_1	x_1/x_2	x_1	x_1/x_2
20.55	0.5718	1.3356	0.5725	1.3392
13.70	0.5849	1.4093	0.5847	1.4077
6.85	0.5854	1.4117	0.5852	1.4108
0.00	0.5865	1.4182	0.5861	1.4159
-6.85	0.5863	1.4172	0.5861	1.4158
-13.70	0.5854	1.4118	0.5853	1.4115
-20.55	0.5728	1.3406	0.5823	1.3939

For isothermal experiments, there was little difference in the composition gradients for 300 and 600 psi. But, for non-isothermal experiments, there is a very noticeable difference as shown in Figure 4.20.

Distance from Center of Spin, cm
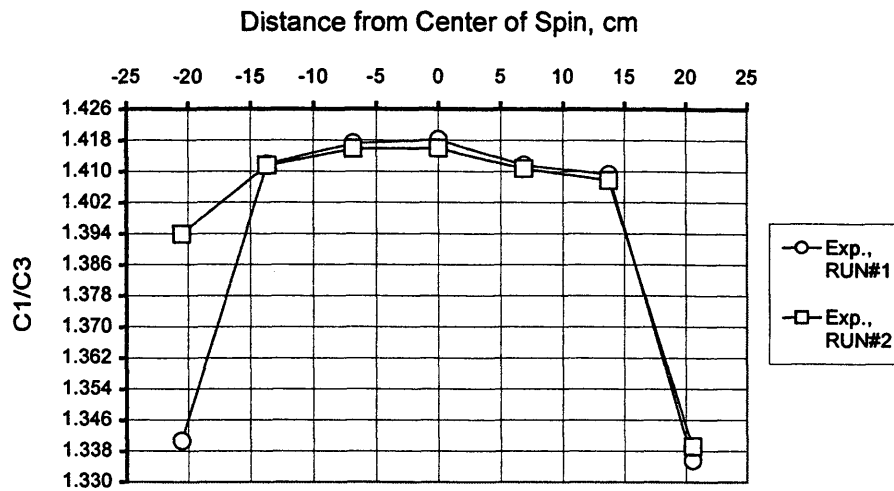
Figure 4.20A: Experimental Methane/Propane Ratio
2500 rpm, 6 hrs, 600 psi, 50°C
Non-isothermal

Distance from Center of Spin, cm
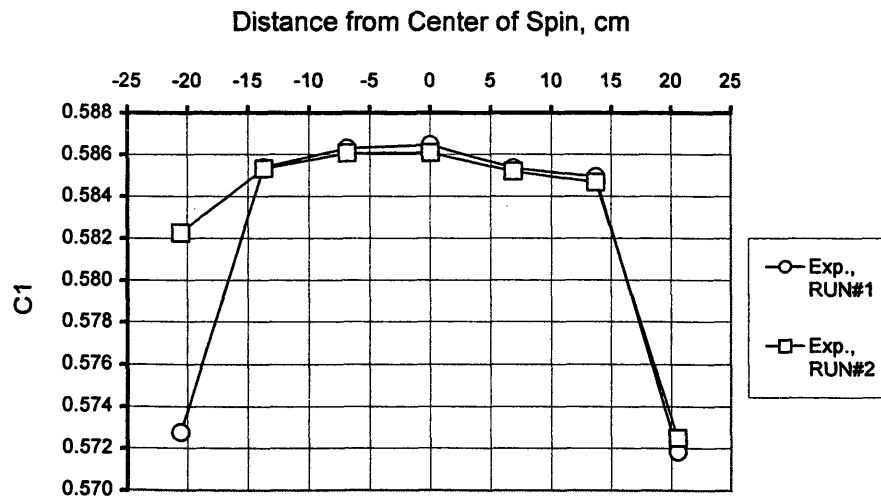
Figure 4.20B: Experimental Methane Mole Fraction
2500 rpm, 6 hrs, 600 psi, 50°C
Non-isothermal

In Figure 4.21, composition gradients at 600 psig for isothermal and non-isothermal conditions are compared. The magnitude of the composition change with radius for the non-isothermal condition is very significant. The magnitude of composition gradient, in terms of the ratio, at this pressure is 6% compared to 2% at the same pressure for isothermal condition. Therefore, it can be concluded that the effect of thermal diffusion on composition gradient does indeed increase with pressure.
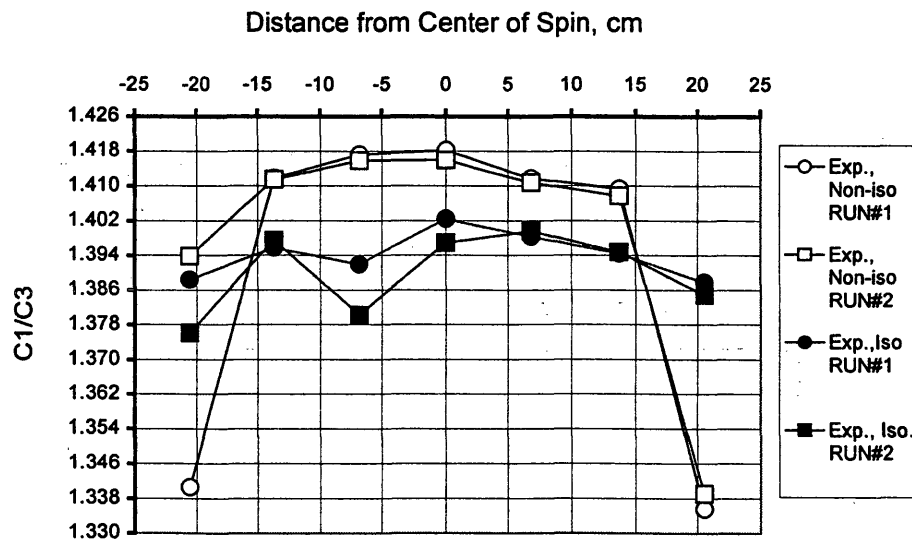
Figure 4.21A: Experimental Methane/Propane Ratio
2500 rpm, 6 hrs, 600 psi, 50°C
Isothermal & Non-isothermal
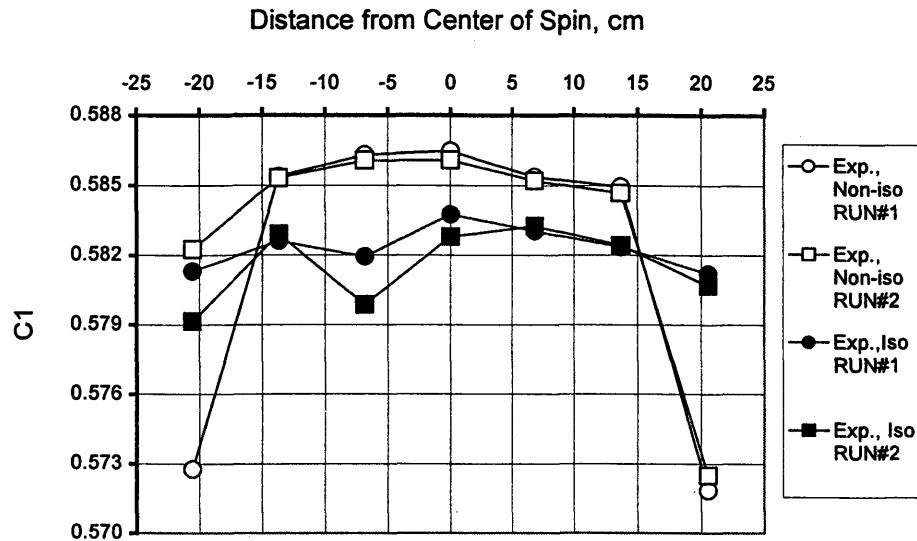
Figure 4.21B: Experimental Methane Mole Fraction
2500 rpm, 6 hrs, 600 psi, 50°C
Isothermal & Non-isothermal

Using the numerical program to fit the data, the thermal diffusion ratios obtained for 600 psi are k_T = 0.30 and 0.26 for data sets 1 and 2 respectively as shown in Figures 4.22 and 4.23. So k_T is larger than that at 300 psig. For this condition, the predicted value of k_T by Firoozabadi is 0.147. To illustrate the role of thermal diffusion on composition grading, the predicted composition profile at k_T = 0, which corresponds for isothermal case, and at larger values of k_T are plotted in Figure 4.24.

Distance from Center of Spin, cm
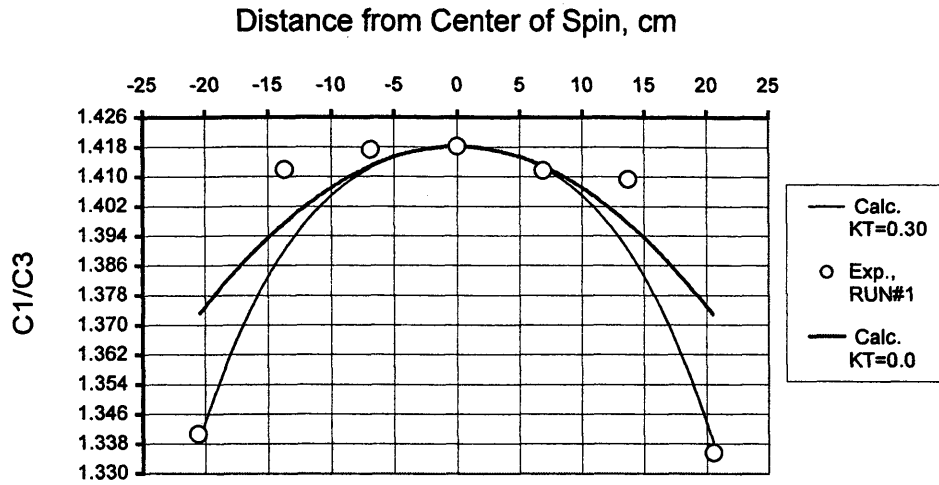
Figure 4.22A : Experimental & Theoretical Methane/Propane Ratio
2500 rpm, 6 hrs, 600 psi, 50°C
Non-isothermal

Distance from Center of Spin, cm
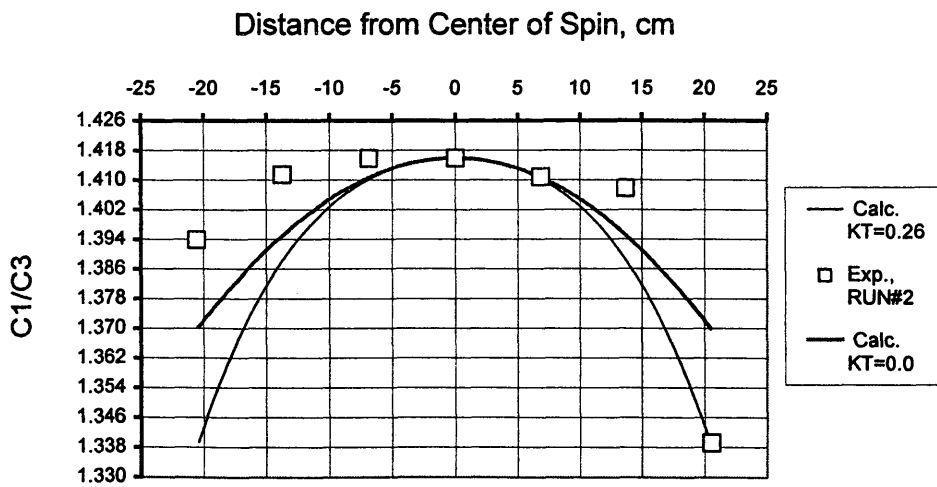
Figure 4.22B : Experimental & Theoretical Methane/Propane Ratio
2500 rpm, 6 hrs, 600 psi, 50°C
Non-isothermal

Distance from Center of Spin, cm
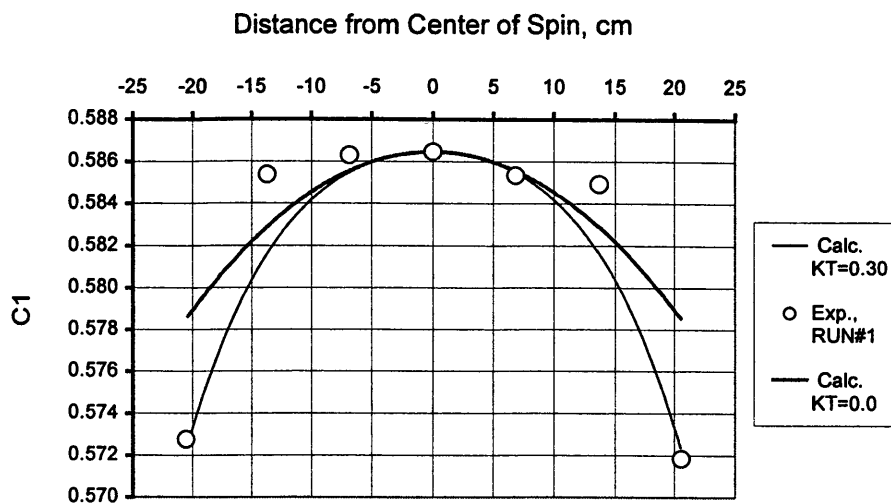
Figure 4.23A : Experimental & Theoretical Methane Mole Fraction
2500 rpm, 6 hrs, 600 psi, 50°C
Non-isothermal

Distance from Center of Spin, cm
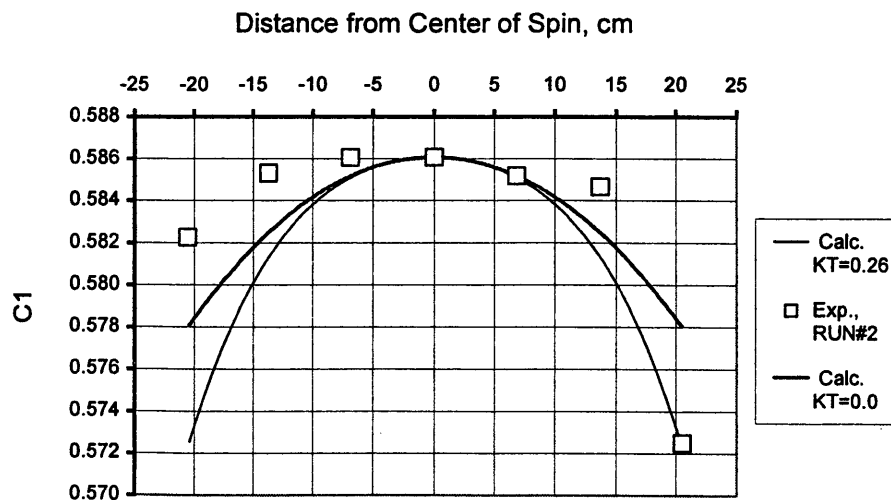
Figure 4.23B : Experimental & Theoretical Methane Mole Fraction
2500 rpm, 6 hrs, 600 psi, 50°C
Non-isothermal

Distance from Center of Spin, cm
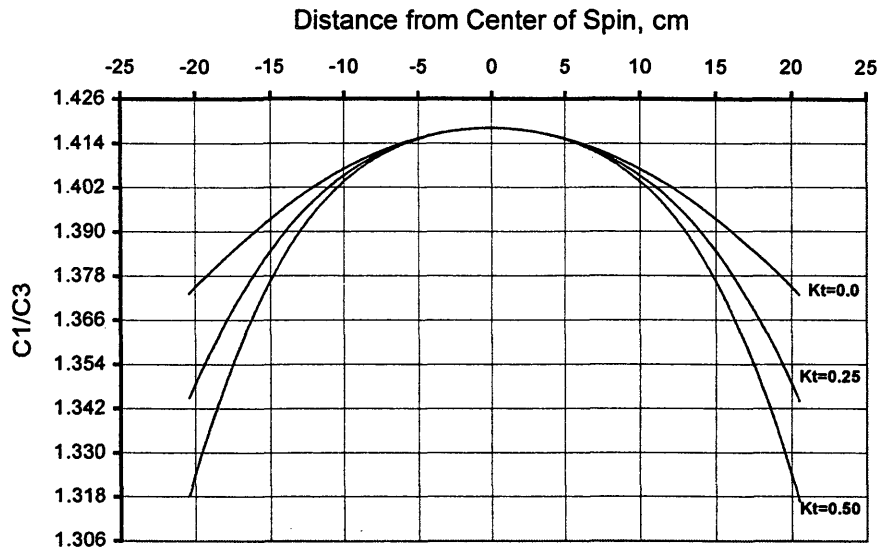
Figure 4.24A: Theoretical Methane/Propane Ratio at Different k_T
2500 rpm, 6 hrs, 600 psi,50°C

Distance from Center of Spin, cm
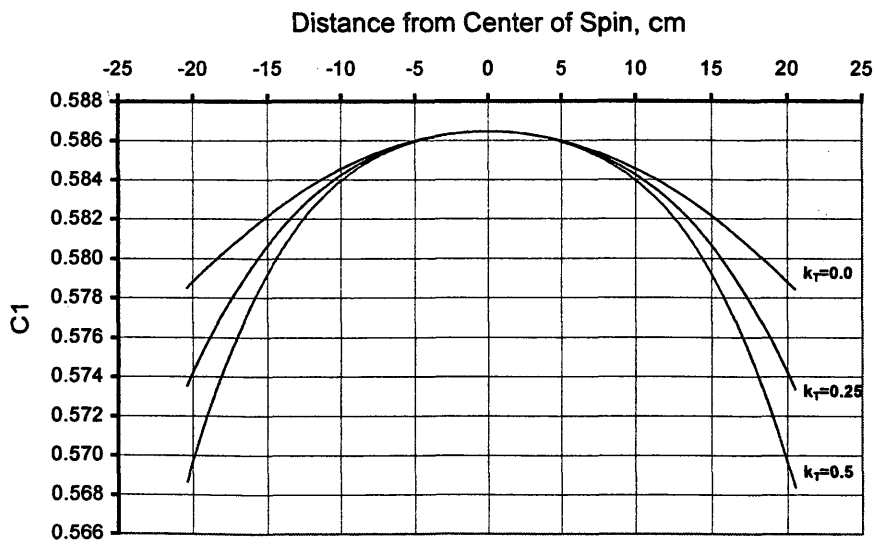
Figure 4.24B: Theoretical Methane Mole Fraction at Different k_T
2500 rpm, 6 hrs, 600 psi,50°C

Continuing the investigation of non-isothermal compositional grading at higher pressures, three experiments were conducted at 900 psig. The composition gradient data at 900 psig are listed in Table 4.9 and plotted in Figure 4.25.

Table 4.9 Experimental Methane/Propane Ratio and Methane Mole Fraction
2500 rpm, 6 hrs, 900 psig, 50°C
Non-Isothermal

Run #	1	1	2	2	3	3
r, cm	x_1/x_2	x_1	x_1/x_2	x_1	x_1/x_2	x_1
20.55	1.1275	0.5300	1.1769	0.5406	0.9728	0.4931
13.70	1.4313	0.5887	1.4457	0.5911	1.5173	0.6028
6.85	1.5323	0.6051	1.4432	0.5907	1.5195	0.6031
0.00	1.5646	0.6101	1.4846	0.5975	1.5461	0.6072
-6.85	1.5445	0.6070	1.4785	0.5965	1.5487	0.6076
-13.70	1.4851	0.5976	1.4611	0.5937	1.5273	0.6043
-20.55	1.1429	0.5333	1.1980	0.5450	1.1317	0.5309

Just by looking at the numbers in the above table, one sees that the change in compositional grading at this pressure is very significant compared to the same pressure at isothermal conditions and to 600 psig for the non-isothermal condition. The percentage increase in compositional grading, in terms of the ratio, is 25%, approximately 2.5 times the increase encountered at the same pressure for isothermal condition and four times the increase obtained at 600 psig for non-isothermal condition. It is indeed very remarkable change in composition as a result of the combined effect of gravity and temperature gradients. Deeper insight can be obtained by looking to the plots in Figures 4.25 and 4.26.

Distance from Center of Spin, cm
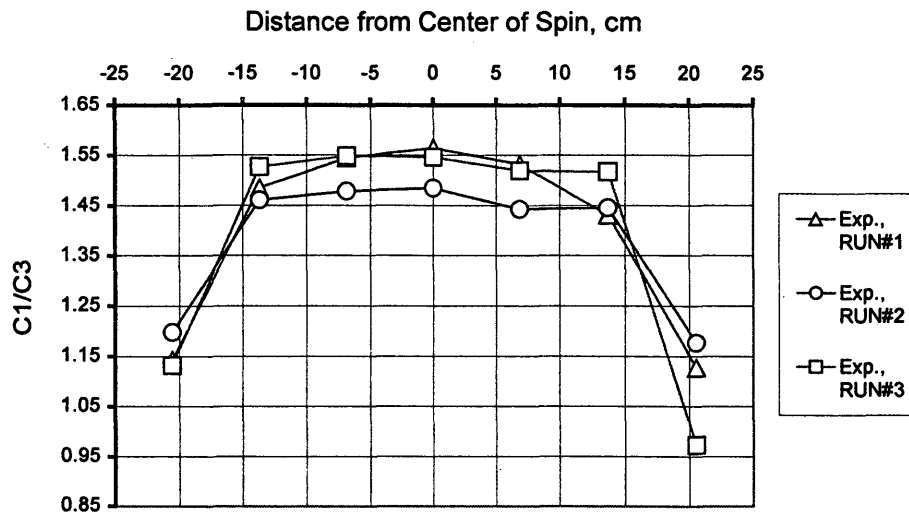
Figure 4.25A : Experimental Methane/Propane Ratio
2500 rpm, 6 hrs, 900 psi, 50°C
Non-isothermal

Distance from Center of Spin, cm
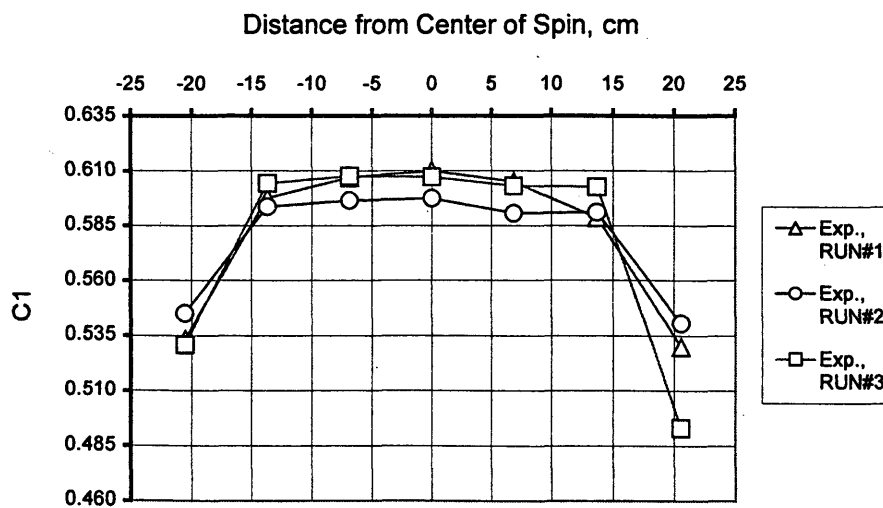
Figure 4.25B : Experimental Methane Mole Fraction
2500 rpm, 6 hrs, 900 psi, 50°C
Non-isothermal

Distance from Center of Spin, cm
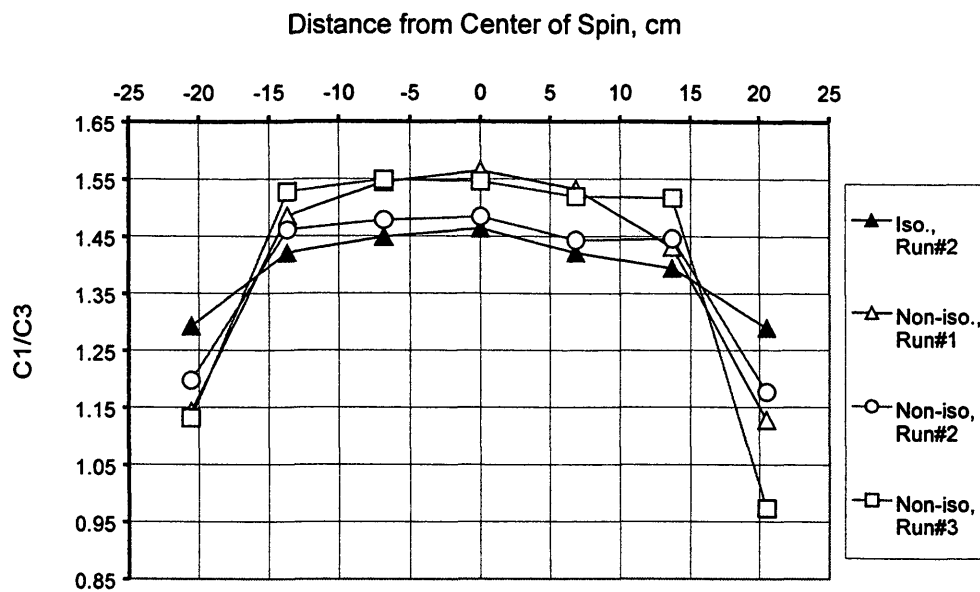
Figure 4.26A: Experimental Methane/Propane Ratio
2500 rpm, 6 hrs, 900 psi, 50°C
Isothermal & Non-isothermal

Distance from Center of Spin, cm
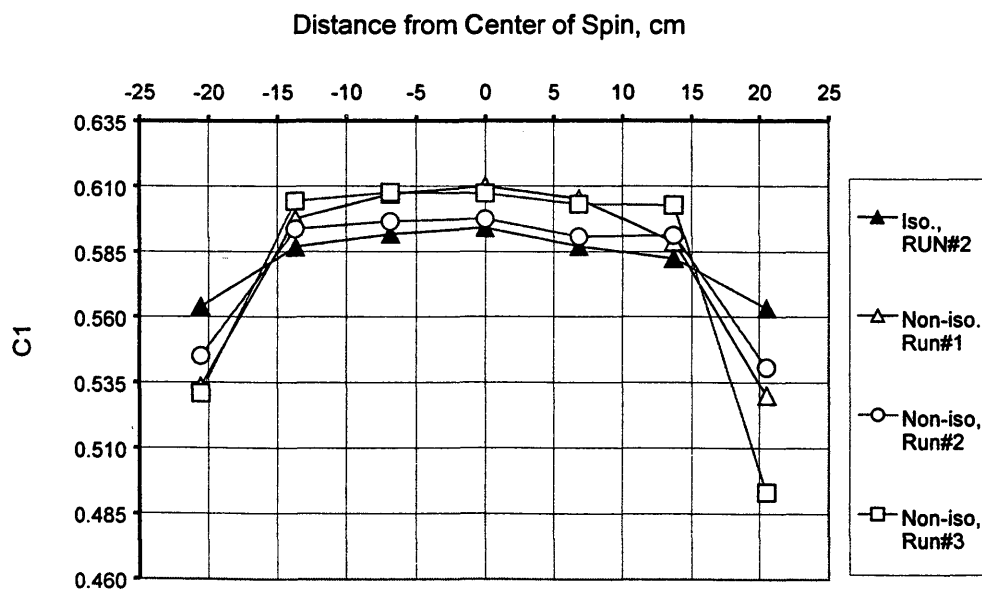
Figure 4.26B: Experimental Methane Mole Fraction
2500 rpm, 6 hrs, 900 psi, 50°C
Isothermal & Non-isothermal

The best-fit values of thermal diffusion ratio k_T using the numerical program were
1.8, 1.65, and 1.1 for data sets 1, 2, and 3 respectively as shown in Figures 4.27
and 4.28.

Distance from Center of Spin, cm
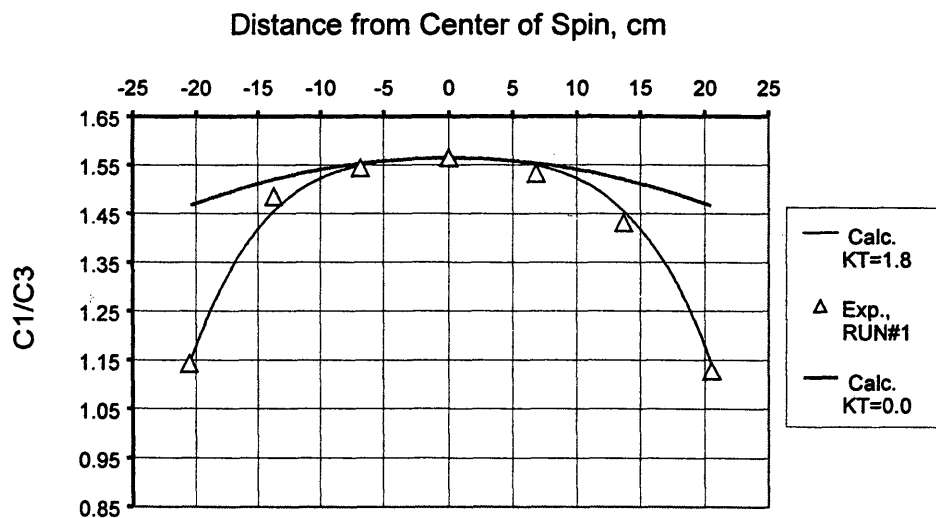
Figure 4.27A : Experimental & Theoretical Methane/Propane Ratio
2500 rpm, 6 hrs, 900 psi, 50°C
Non-isothermal

Distance from Center of Spin, cm
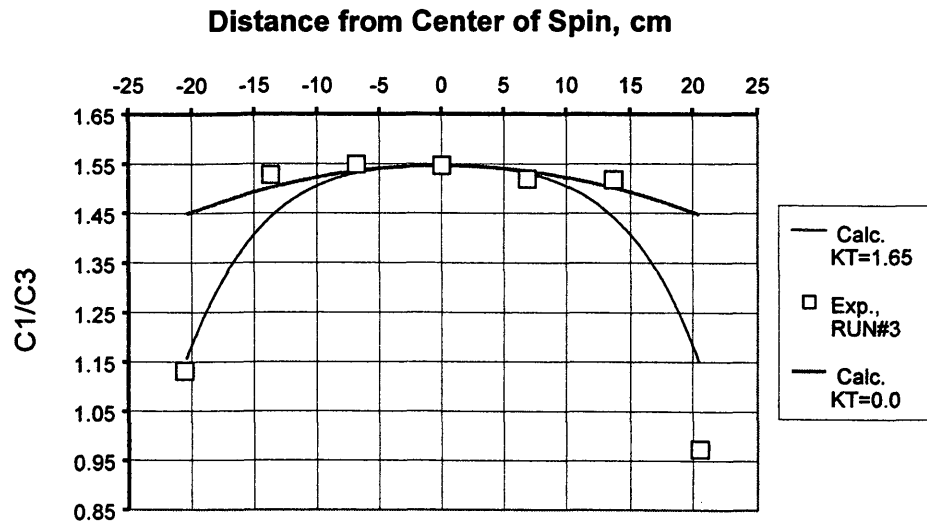
Figure 4.27B : Experimental & Theoretical Methane/Propane Ratio
2500 rpm, 6 hrs, 900 psi, 50°C
Non-isothermal

Distance from Center of Spin, cm
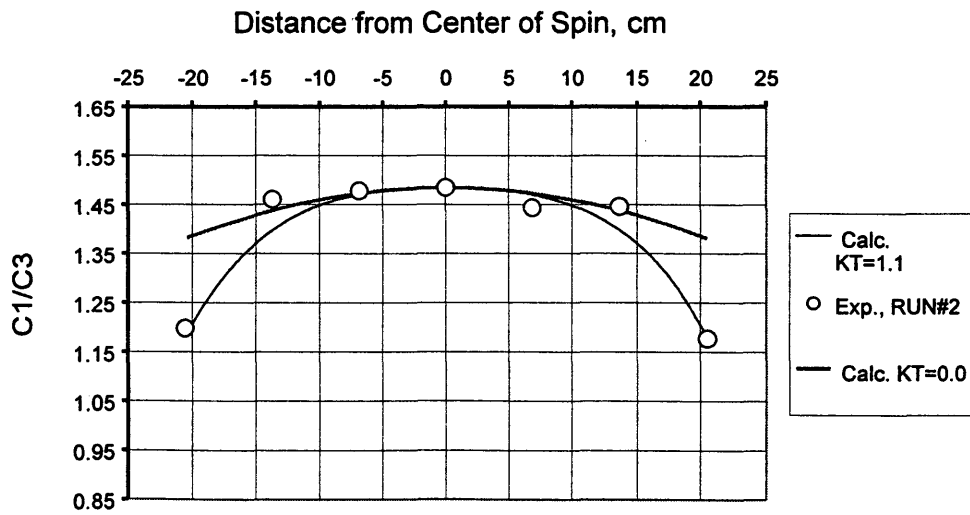
Figure 4.27C : Experimental & Theoretical Methane/Propane Ratio
2500 rpm, 6 hrs, 900 psi, 50°C
Non-isothermal

Distance from Center of Spin, cm
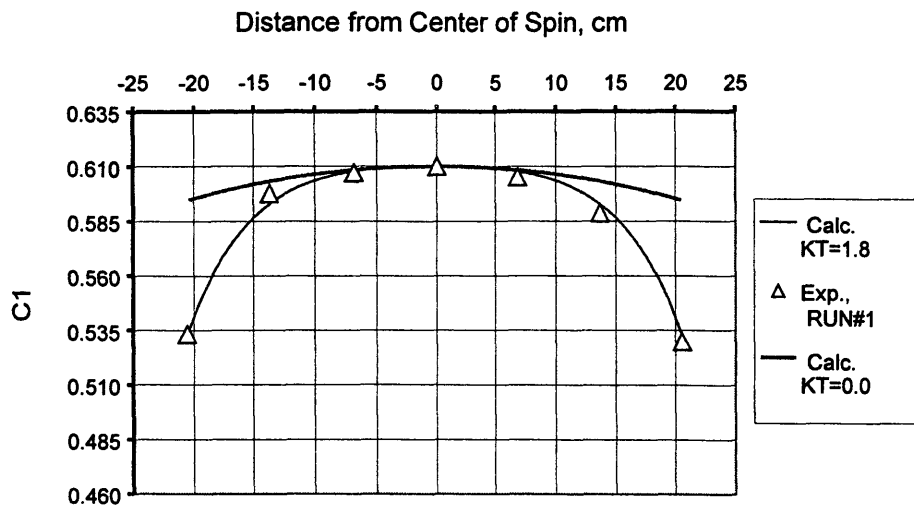
Figure 4.28A : Experimental & Theoretical Methane Mole Fraction
2500 rpm, 6 hrs, 900 psi, 50°C
Non-isothermal

Distance from Center of Spin, cm
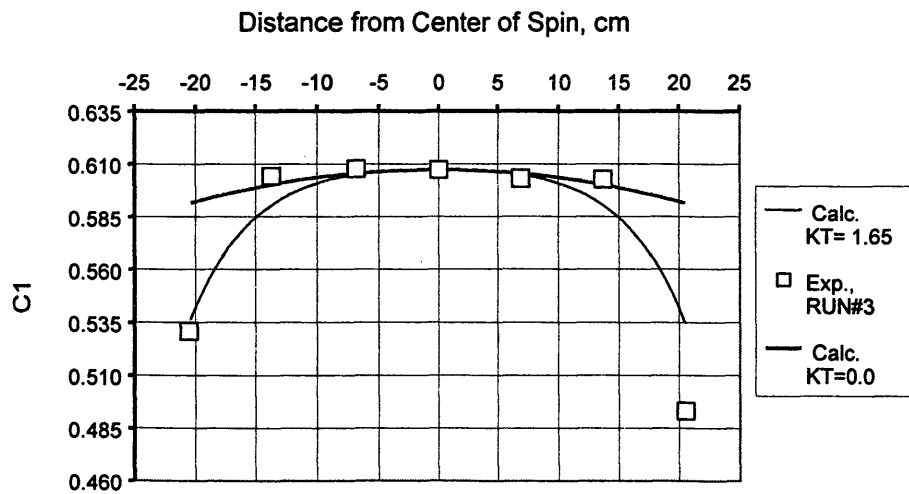
Figure 4.28B : Experimental & Theoretical Methane Mole Fraction
2500 rpm, 6 hrs, 900 psi, 50°C
Non-isothermal

Distance from Center of Spin, cm
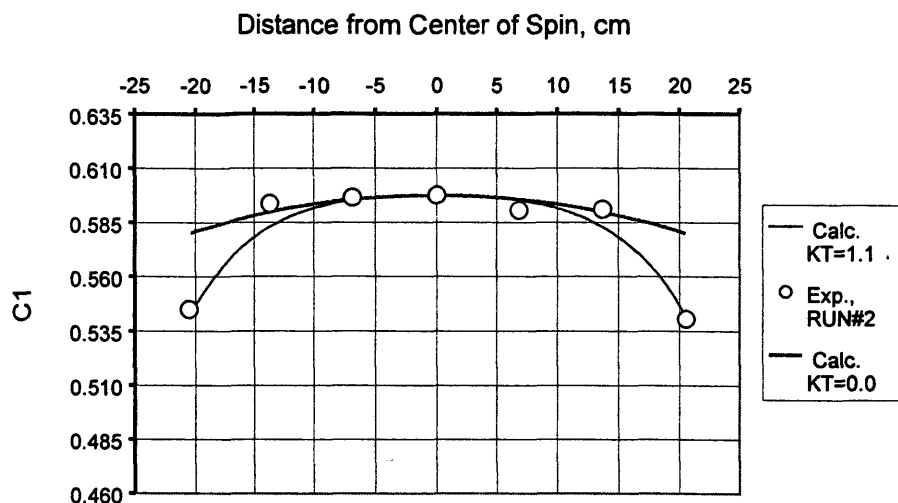
Figure 4.28C : Experimental & Theoretical Methane Mole Fraction
2500 rpm, 6 hrs, 900 psi, 50°C
Non-isothermal

The average value of k_T for the three data sets is approximately 1.5 which is five times greater than the average value of k_T at 600 psig. This large value of thermal diffusion ratio supports the conclusion of several investigators mentioned in Chapter 2 that thermal diffusion could significantly contribute to mass transport in hydrocarbon reservoirs. The Firoozabadi prediction of thermal diffusion ratio at the condition of this experiment is approximately k_T = 0.34. To see how the best-fit values and the Firoozabadi prediction differ, plots of composition grading as a function of distance from center of spin for isothermal case and for non-isothermal case with different values of k_T are shown in Figure 4.29.

Distance from Center of Spin, cm
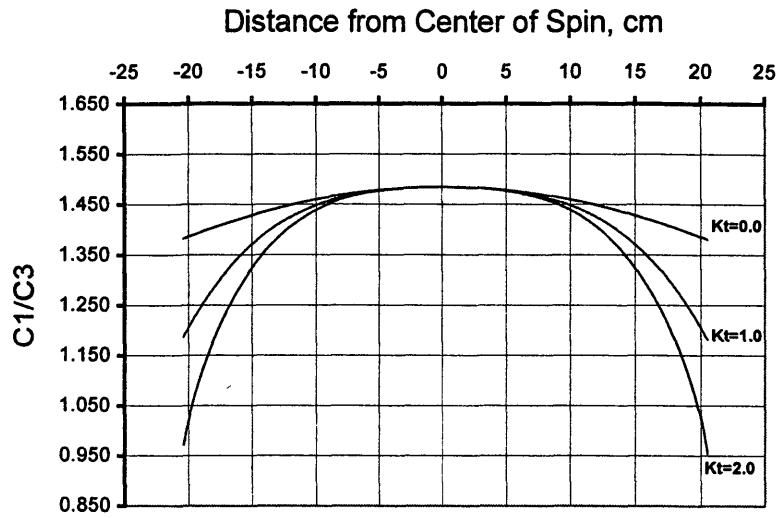
Figure 4.29A: Theoretical Methane/Propane Ratio at Different k_T
2500 rpm, 6 hrs, 900 psi, 50°C

Distance from Center of Spin, cm
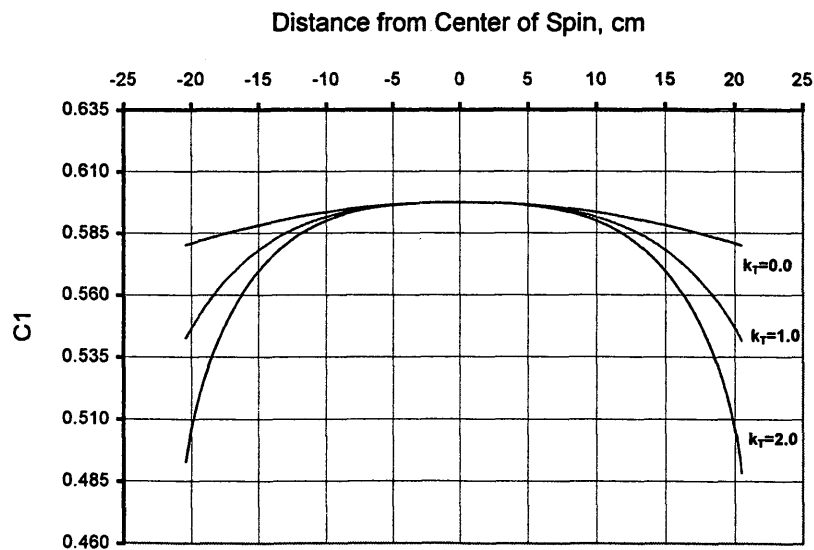
Figure 4.29B: Theoretical Methane Mole Fraction at Different k_T
2500 rpm, 6 hrs, 900 psi, 50°C

Non-isothermal centrifuge experiments were also conducted at a pressure of 1500 psig. Two successful experiments were completed. Their results are shown in Table 4.10 and plotted in Figure 4.30.

Table 4.10 Experimental Methane/Propane Ratio and Methane Mole Fraction
2500 rpm, 6 hrs, 1500 psig, 50°C
Non-Isothermal

Run #	1	1	2	2
r, cm	x_1	x_1/x_2	x_1	x_1/x_2
20.55	0.5155	1.0639	0.4791	0.9197
13.70	0.5884	1.4293	0.5954	1.4715
6.85	0.5923	1.4529	0.5949	1.4684
0.00	0.6000	1.5000	0.6030	1.5187
-6.85	0.5947	1.4674	0.5954	1.4718
-13.70	0.5913	1.4466	0.5925	1.4539
-20.55	0.5233	1.0976	0.4599	0.8517

Going in pressure from 900 psig to 1500 psig did not produce as much change in composition grading as was observed in going from 600 psig to 900 psig. The change in methane-propane ratio at this pressure is 30% compared to 25% at 900 psig. This is also reflected by the magnitude of best-fit thermal diffusion ratio for this condition. The composition gradient is large at 900 psig and 1500 psig because the system is in the vicinity of the critical condition.

Distance from Center of Spin, cm
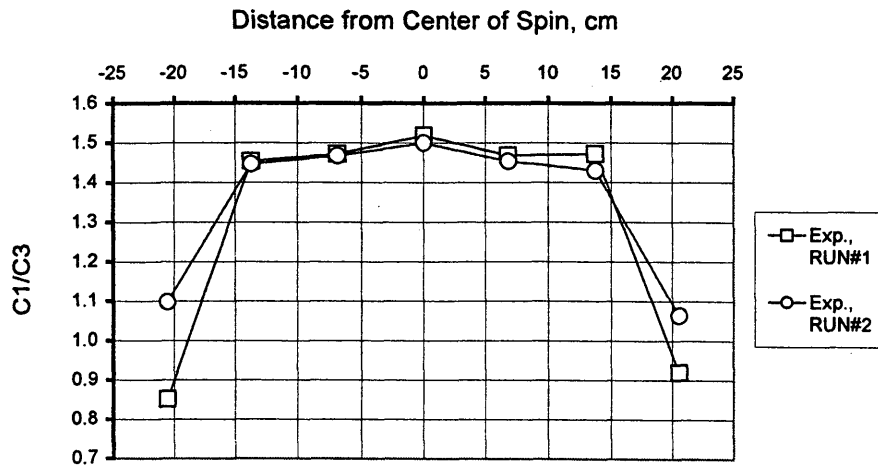
Figure 4.30A: Experimental Methane/Propane Ratio
2500 rpm, 6 hrs, 1500 psi, 50°C
Non-isothermal

Distance from Center of Spin, cm
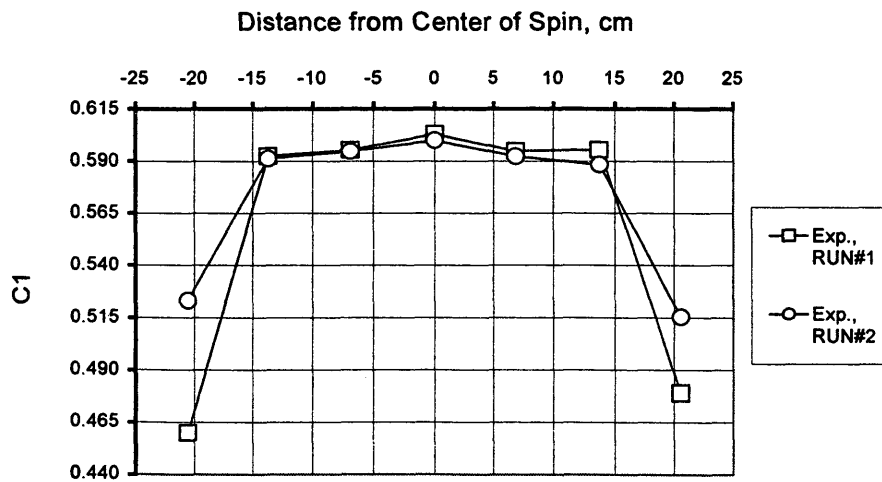
Figure 4.30B: Experimental Methane Mole Fraction
2500 rpm, 6 hrs, 1500 psi, 50oC
Non-isothermal

Figure 4.31 shows a comparison of isothermal data with the non-isothermal data at 1500 psig. The difference between the two conditions is not big compared to the change attained for 900 psig case. The reason for this is that the change in composition gradient obtained at 900 psig, for a step in pressure of 300 psi going from 600 psig, is significant compared to the gradient obtained at 1500 psig for a step in pressure of 600 psi going from 900 psig. If the expected increase in gradient at 1500 psig obtained, then the difference between isothermal data and non-isothermal data would be large.

Distance from Center of Spin, cm
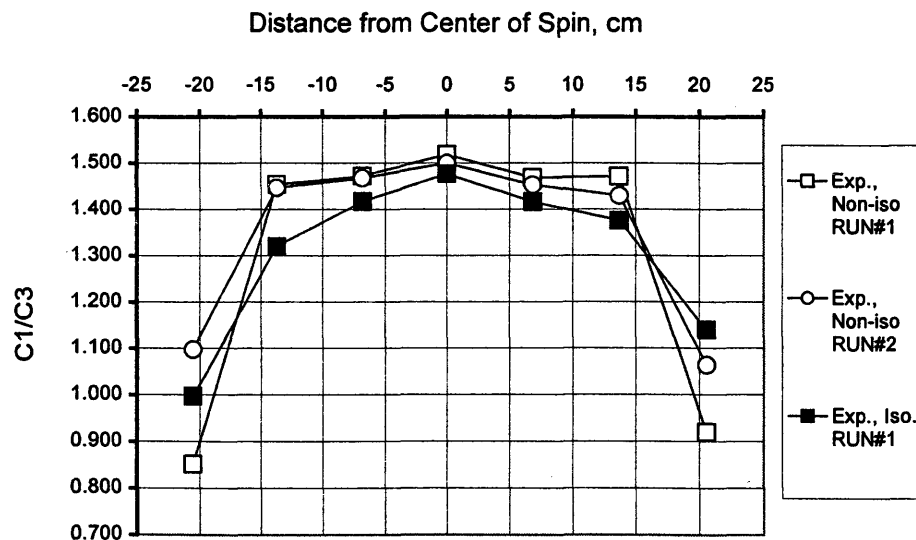
Figure 4.31A: Experimental Methane/Propane Ratio
2500 rpm, 6 hrs, 1500 psi, 50°C
Isothermal & Non-isothermal

Distance from Center of Spin, cm
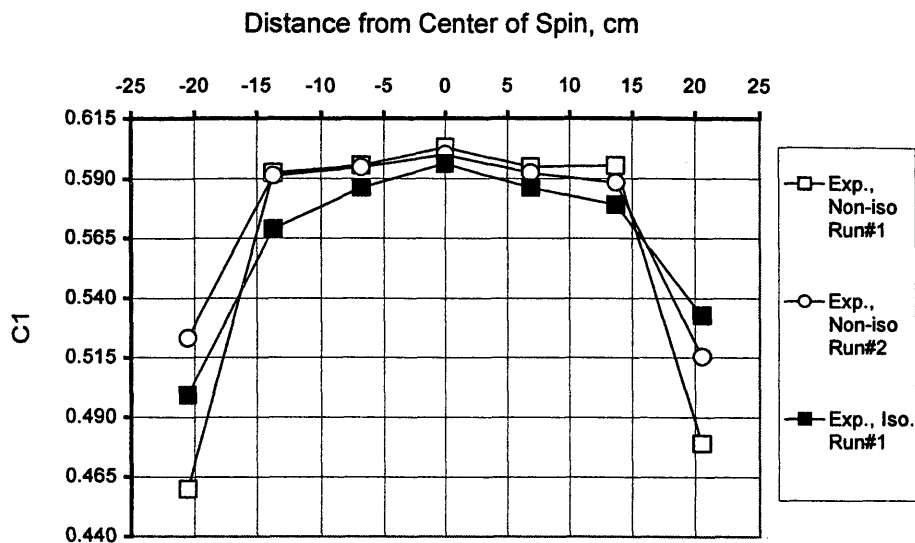
Figure 4.31B: Experimental Methane Mole Fraction
2500 rpm, 6 hrs, 1500 psi, 50°C
Isothermal & Non-isothermal

The predicted composition gradient at 1500 psig is shown in Figures 4.32 and 4.33. The predicted thermal diffusion ratios are 2.1 and 1.5 for Run 1 and 2. An average k_T of 2 is obtained. At this condition the predicted value of k_T with Firoozabadi model is 0.66.
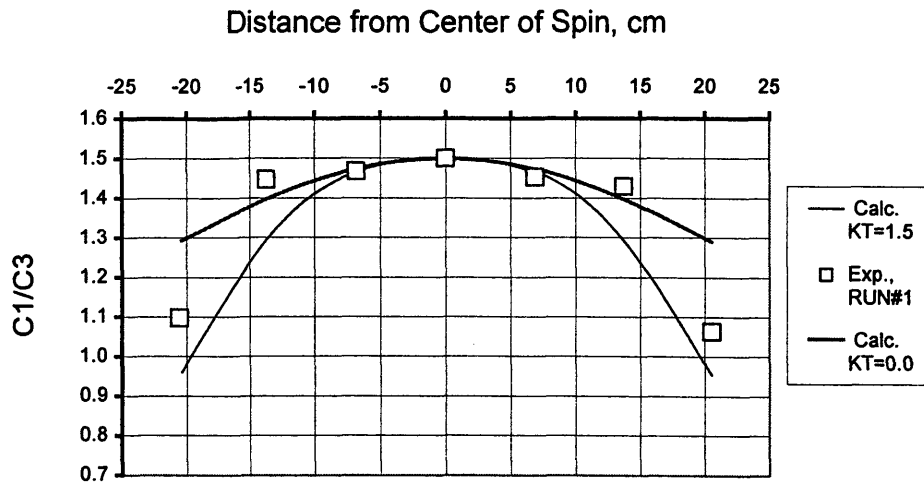
Figure 4.32A : Experimental & Theoretical Methane/Propane Ratio
2500 rpm, 6 hrs, 1500 psi, 50°C
Non-isothermal
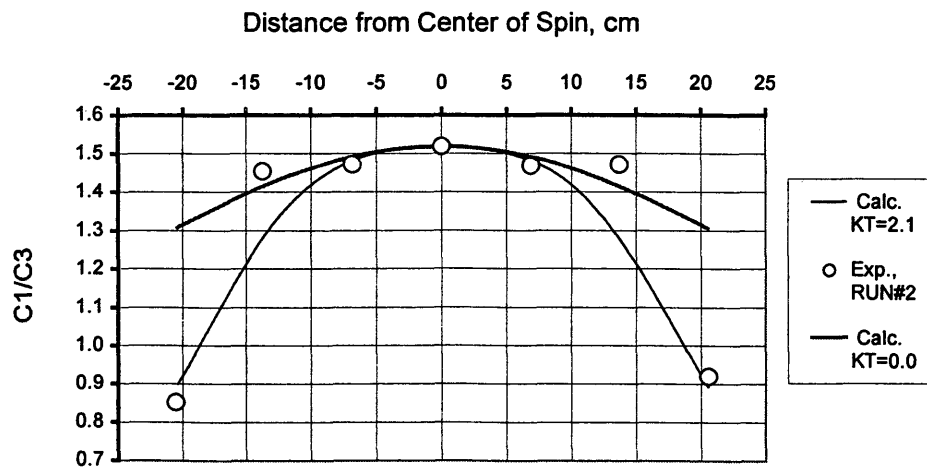
Figure 4.32B : Experimental & Theoretical Methane/Propane Ratio
2500 rpm, 6 hrs, 1500 psi, 50°C
Non-isothermal

Distance from Center of Spin, cm
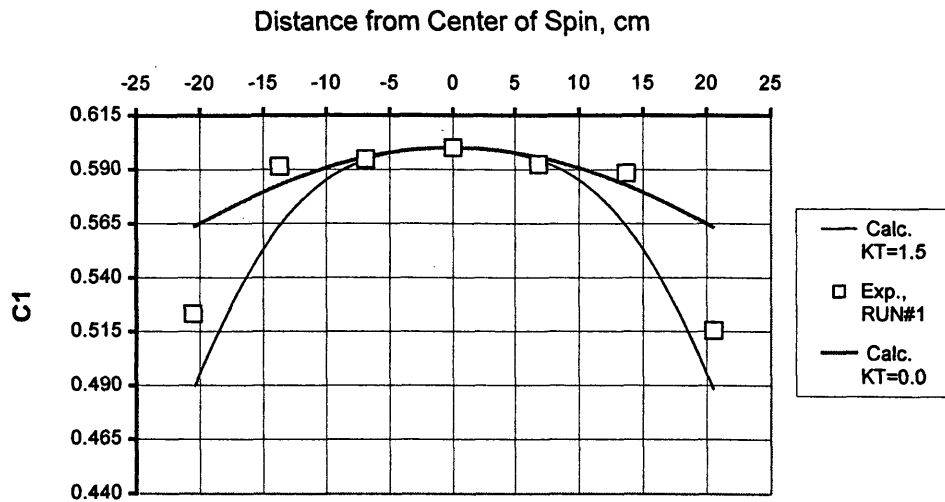
Figure 4.33A : Experimental & Theoretical Methane Mole Fraction
2500 rpm, 6 hrs, 1500 psi, 50°C
Non-isothermal

Distance from Center of Spin, cm
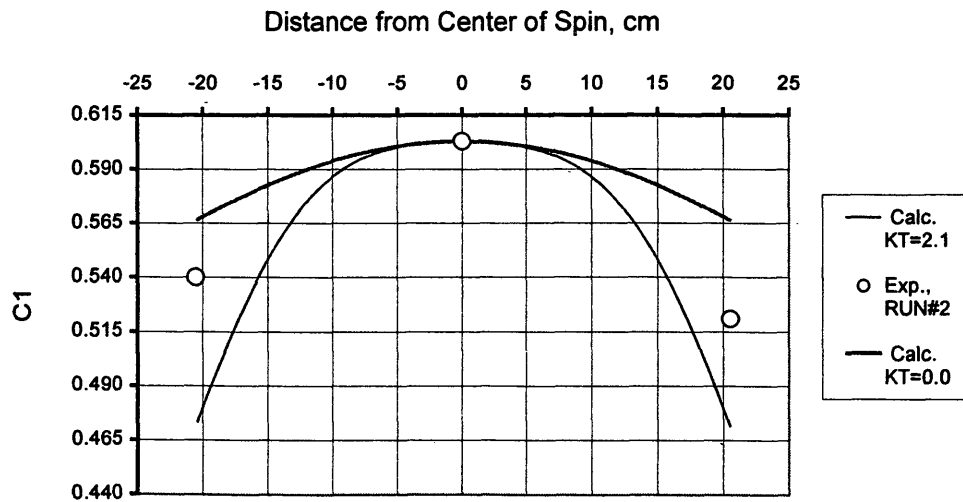
Figure 4.33B : Experimental & Theoretical Methane Mole Fraction
2500 rpm, 6 hrs, 1500 psi, 50°C
Non-isothermal

As mentioned earlier that there was no big difference between isothermal and non-isothermal data. This not the case if one would compare the isothermal and non-isothermal prediction of composition grading. As it is clear from Figure 4.33B above, there is a big difference between the isothermal curve (k_T=0.0) and non-isothermal case (k_T= 2.1). The predicted composition grading is plotted at different values of k_T that covers the range of k_T predicted for 1500 psig by the numerical program and Firoozabadi model as shown in Figure 4.34.

Distance from Center of Spin, cm
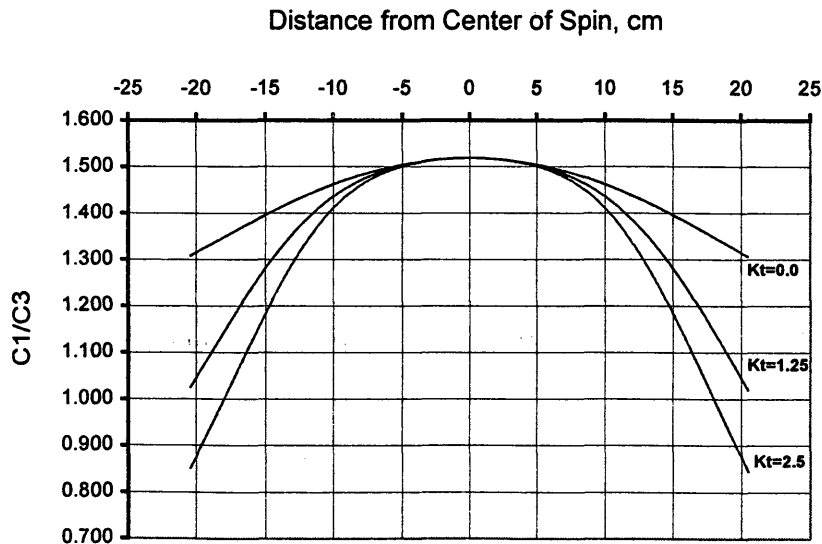
Figure 4.34A: Theoretical Methane/Propane Ratio at Different k_T
2500 rpm, 6 hrs, 1500 psi,50°C

Distance from Center of Spin, cm
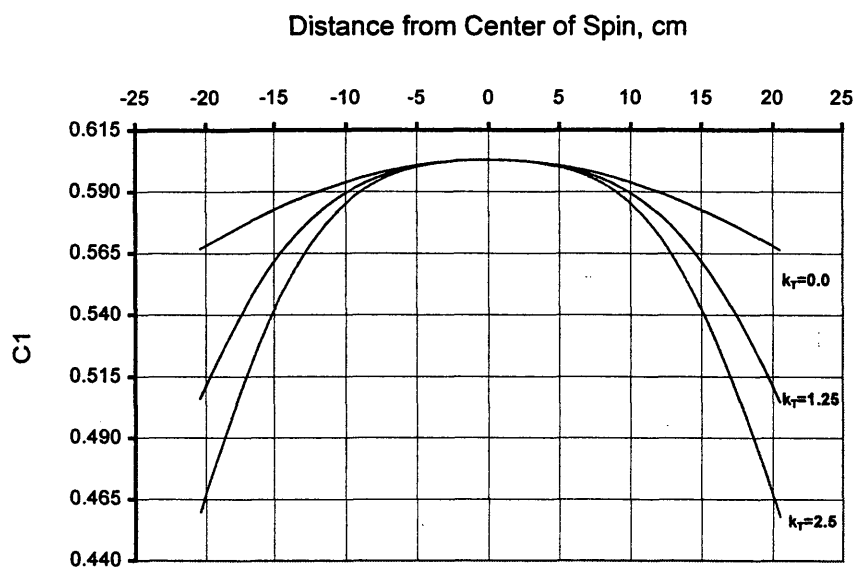
Figure 4.34B: Theoretical Methane Mole Fraction at Different k_T
2500 rpm, 6 hrs, 1500 psi,50°C

4.5 Discussion of Observations and Calculations

In this section, I discuss the observations of laboratory experiments, including the measured temperature gradient, the composition evolution with time, compositional gradient under the effect of gravity alone (isothermal tests) and compositional gradient under the combined effect of gravity and temperature (non-isothermal tests) for the binary gas mixture of 58.32 mole percent methane and 41.68 mole percent propane. Also the predicted time to reach steady-state,

the equivalent height in the reservoir, and the predicted compositional gradients using the numerical model that was developed in this study are discussed. Finally a comparison of the observed and the predicted compositional gradients for isothermal and non-isothermal conditions will be given.

The temperature gradient along the profile capture apparatus (PCA) was measured using different techniques as described in Chapter 3. The measured temperature difference between the center of spin and the edge of the PCA is 11 °F. Using the equivalent reservoir height of 500 feet, which was calculated in Chapter 3, the temperature gradient in the centrifuge tests corresponds to 0.022 °F/ft in a hydrocarbon reservoir. This temperature gradient is close to the average geothermal gradient of 0.015 °F/ft for reservoirs around the world. For isothermal experiments, observations indicate that temperature was fairly uniform across the PCA, varying less than 1 °F. The temperature data were fit with equations 3.3A and 3.3B using a regression routine. Equation 3.3A with r^2 radial dependence was found to fit the temperature data better than equation 3.3B, which has r^4 radial dependence. However, equation 3.3B was found to fit the composition gradient data much better than equation 3.3A.

The time needed to develop a steady-state composition gradient was observed in the lab through conducting experiments for a sequence of time periods for a pressure of 300 psig, a spin rate of 2500 rpm, and a temperature of 50 °C. It was found that a time period of 6 hours is sufficient to reach a time-independent composition gradient. This time period is comparable to the estimated time using transport theory as expressed in equation 4.1. According to that equation, the time for 90% completion of the process should be approximately 6 hours. The time to reach steady-state is useful as an estimate of time needed for the

composition gradient to collapse after the centrifuge is turned off. Since the time elapsed from the moment I turned the centrifuge off to when the valves are completely closed is approximately one minute, the composition gradient that is established during the experiment does not have time to collapse before the samples are captured.

To confirm the thermodynamic theory and experimental techniques, several centrifuge experiments were conducted at isothermal conditions for pressures starting at 150 psig and going up to 1500 psig. I conducted experiments at low pressure to test the equipment, to confirm the theory for ideal gases, and to develop a feel for how much change in composition can be achieved at low pressures. Compared to the gradients at lower pressures, the gradients at 900 psig and 1500 psig are much larger. The change in mole percent of methane from the center to the outside of the PCA at 900 psig is about 5% whereas the change at 1500 psig is about 13%. These gradients are compared to 0.3% and 0.5% at 150 psig and 300 psig, respectively, as shown in Table 4.11. Therefore, compared to the gradients at lower pressures, the gradients at 900 psig and 1500 psig are much more significant.

In an effort to reproduce more closely the real conditions of pressure and temperature in petroleum reservoirs, non-isothermal centrifuge experiments were conducted to investigate the combined effect of gravity and temperature on fluid composition. Using the same binary gas mixture used for isothermal tests, tests were performed starting at a pressure of 300 psig and higher at a spin rate of 2500 rpm and a spin time of 6 hours. In this case, the change in composition is larger as shown in Table 4.11B.

The composition gradients for isothermal and non-isothermal tests are compared graphically in Figures 4.21, 4.26, and 4.31. From these figures as well as from Table 4.11B, the gradients obtained for non-isothermal conditions are significantly higher than gradients for isothermal conditions. Even at low pressures, the non-isothermal composition gradients are larger than those for isothermal conditions.

able 4.11A Comparison of Measured and Calculated Methane Gradients
at Different Pressures, 2500 rpm, 6 hrs
(Isothermal)

Pressrue, psig	Data	Model
	Change in C1 Mole%	Change in C1 Mole%
150	0.3	0.5
300	0.5	0.8
600	0.7	1.4
900	5	3
1500	13	7

able 4.11B Comparison of Measured and Calculated Methane Gradients
at Different Pressures, 2500 rpm, 6 hrs
(Non-isothermal)

	Data	Model
Pressrue, psig	Change in C1 Mole%	Change in C1 Mole% ·
300	0.7	0.9
600	2.5	2.5
900	13	11
1500	23	19

Table 4.12 compares the measured and calculated methane gradient for isothermal and non-isothermal conditions. From Table 4.12 it can be concluded that the effect of gravity field (isothermal condition) on composition grading is of the same magnitude as the temperature effect (non-isothermal condition), which agrees with the conclusions of Schulte[2] and Hamoodi et al.[4] as discussed in Chapter 2.

Table 4.12 Comparison of Measured Methane Gradient
at Different Pressures, 2500 rpm, 6 hrs
(Isothermal and Non-isothermal)

Pressure, psig	Isothermal	Non-isothermal
	Change in C1 Mole%	Change in C1 Mole%
300	0.5	0.7
600	0.7	2.5
900	5	13
1500	13	23

A numerical program was developed that calculates the composition gradients for isothermal and non-isothermal conditions.   In this model I used both thermodynamic and transport approaches for calculating composition gradients. Redlich-Kwong and Peng-Robinson equations of state were incorporated in this model for calculating densities, fugacities and partial molar quantities of the binary gas mixture.

To check the validity of the model, its predictions of composition gradients for isothermal conditions with ideal gas behavior were compared with the predictions of the Sage and Lacey[1] model. The results of the two approaches are nearly

identical as shown in Table 4.1. As another check on the model, especially the phase-behavior portion of the model, predictions of partial molar volume for the methane-propane system at 1500 psia and 460 °F were compared with measured values reported by Sage and Lacey.[65,66] The comparison is shown in Figure 4.1.

Composition gradients under isothermal and non-isothermal conditions were predicted using the numerical model for all ranges of pressure. Predicted composition gradients at every pressure were compared with the measured gradients as shown earlier in this chapter. Table 4.11 shows a comparison of the measured and calculated methane gradients at different pressures for isothermal conditions. It is clear from this table that at higher pressures, the model underestimates the composition gradient. A likely reason for this is that Redlich-Kwong and Peng-Robinson equations of state fail in the vicinity of critical conditions. So proper selection of an equation of state is recommended for near-critical conditions. The Benedict-Webb-Rubin[71] equation of state is a good candidate.

In calculations for the non-isothermal experiments, the effect of the temperature field on composition gradient is controlled by the thermal diffusion ratio, k_T. The thermal diffusion ratio is known to depend on temperature, pressure, and composition. Here, however, the thermal diffusion coefficient is assumed to be constant. This may be a reasonable assumption for the temperature and composition gradients in this research, but much further testing is required to fully assess this assumption.

The measured composition gradients were fit with the numerical model by adjusting the thermal diffusion ratio as explained previously in this chapter. The measured and predicted composition gradients are compared in Table 4.11B. Better agreement between the measured and predicted gradients was obtained in this case as compared to isothermal case. The likely reason for the improved performance is that the k_T was adjusted to obtain a good fit. The good fit does not prove that the model is correct.

The best-fit values of thermal diffusion ratio obtained in this research using the numerical model were compared with those predicted by Firoozabadi et al.[20] model as shown in Table 4.13. Thermal diffusion ratios obtained in this research are 2 to 3 times larger than those predicted by the model of Firoozabadi et al. This suggests the need for measuring thermal diffusion ratios in the lab because it is important in modeling the compositional gradient.

Table 4.13 Comparison of Thermal Diffusion Ratios Predicted by
Numerical Model and by Firoozabadi et al.[20] Model
at Different Pressures, 2500 rpm, 6 hrs

Pressure, psig	This work	Firoozabadi *et al.*[20]
300	-0.012 to 0.0015	0.05
600	0.26-0.3	0.147
900	1.1-1.8	0.342
1500	1.5-2.1	0.661

CHAPTER 5

CONCLUSIONS AND RECOMMENDATIONS

Extensive efforts were spent on designing an experimental setup and procedures to produce an observable compositional gradient in the lab. To investigate the effect of gravity on compositional gradient in petroleum reservoirs and to confirm the thermodynamic theory and experimental techniques, several centrifuge experiments were conducted at isothermal conditions. In the following section, the conclusions from observations and calculations are discussed, along with some implications of the findings. Next, the important conclusions of this research are briefly listed. And, finally, recommendations for future studies are given.

5.1 Discussion of Conclusions from Observations and Calculations

The variation in gravitational potential across an equivalent hydrocarbon fluid column of 500 ft was simulated by centrifuging the profile capture apparatus (PCA) at 2500 rpm for pressures starting at 150 psig and going up to 1500 psig. A time period of 6 hours is considered enough time to centrifuge the PCA in order to observe a steady-state composition gradient for isothermal and non-isothermal conditions and for all pressure of interest.

The established composition gradients at low pressures were much smaller than those at higher pressure (approaching the vicinity of critical condition). The

change in mole percent of methane at 900 psig is about 5%, whereas the change at 1500 psig is about 13%. These gradients are compared to 0.3 % and 0.5 % at 150 psig and 300 psig. Therefore, compared to the gradients at lower pressures, the gradients at 900 psig and 1500 psig are much larger.

The combined effect of gravity and temperature on fluid composition was studied in several experiments with a temperature gradient of 11 °F along the profile capture apparatus (PCA). In these tests, having included the temperature gradient as another factor with the gravity force, the change in composition is more significant. The magnitude of the gradients obtained for non-isothermal conditions is significantly higher than the magnitude obtained for isothermal conditions. The influence of critical conditions on composition gradient is larger for non-isothermal tests than for isothermal tests. This is reflected in the magnitude of thermal diffusion ratio. The composition grading increases with increasing thermal diffusion ratio.

The measured methane gradients for isothermal and non-isothermal conditions are compared in Table 5.1. From Table 5.1, it is clear that composition variations are larger in the case of non-isothermal conditions where both gravity and temperature gradients are acting than in the case of isothermal condition where gravity force is acting alone. Also, it can be concluded that the effect of the gravity field (isothermal tests) on composition grading is of the same magnitude as the temperature effect (non-isothermal tests), which agrees with the conclusions of Schulte[2] and Hamoodi et al.[4] as discussed in Chapter 2. Therefore, it appears that gravitational grading alone can cause significant compositional variation and including temperature with gravity enhances the gradation. These observed composition gradients support those observed in

various oil and gas fields around the world that exhibit significant compositional variations with depth.

Table 5.1 Comparison of Measured Methane Gradients
at Different Pressures, 2500 rpm, 6 hrs
(Isothermal and Non-isothermal)

Pressure, psig	Isothermal Change in C1 Mole%	Non-isothermal Change in C1 Mole%
300	0.5	0.7
600	0.7	2.5
900	5	13
1500	13	23

The binary gas mixture of methane and propane used in this study is considered a simple system representing a hydrocarbon fluid system in the reservoir in which methane represents the light end components and propane represents the heavy end components. As observed in this study, methane mole fraction decreases and propane mole fraction increases with increasing depth. These changes affect other fluid properties such as bubble-point and dew-point pressures, gas oil ratio (GOR), gas formation volume factor, viscosity, and density.

The fluid properties mentioned above are most important to design processes for reservoir development, such as estimating reserves, recovery processes, field development, and the design of production facilities. Therefore an adequate knowledge of the fluid composition is necessary for activities relating to field delineation and development planning.

In estimating the original gas in place, for instance, the accuracy of the estimate is sensitive to gas formation volume factor that will vary with depth. So neglecting this variation will result in substantial errors in reserve estimates that might reach as high as 20% as reported by Wheaton[12].

Miscibility conditions for miscible injection processes are strongly dependent on the fluid composition. Minimum miscibility pressure (MMP) varies with depth in compositionally grading reservoirs especially for near-critical oil reservoirs and gas condensate reservoirs as reported by Hoier and Whitson.[70] According to these authors' examples, the MMP can vary as much as 30% from the top to the bottom of oil zones. They also reported variations with depth of MMPs for displacements of gas condensates.

The oil displacement efficiency of a water flood depends on the water-oil relative permeability characteristics and the oil and water viscosities. For compositionally grading reservoirs, the relative permeability curves at the top of the reservoir could differ from those at the bottom because of variations with depth in the amount of asphaltenes in the oil. Changes in the asphaltene content should alter wettability, which in turn will alter relative permeability. I have found no documentation in the literature of a link between composition gradients and measured relative permeability variations with depth.

5.2 Summary of Conclusions

The main conclusions of this research work can be summarized in the following:

1. Experiments were successfully designed and tested for isothermal and non-isothermal conditions at low and high pressure to reproduce the effect of gravity and temperature gradients on a thick hydrocarbon zone by applying large accelerations on a short fluid loop in a centrifuge.

2. Using the binary gas mixture of 58 mole percent methane and 42 mole percent propane, significant compositional gradients were established in the lab under isothermal and non-isothermal conditions. The mole fraction of methane that represents the lighter ends in the reservoir decreases with increasing depth and vise versa for mole fraction of propane that represents the heavier ends components in the reservoir.

3. The large magnitude of compositional gradients measured in this research supports those observed in various oil and gas fields around the world that exhibit significant compositional variations with depth.

4. The effect of temperature gradients is of the same order of magnitude as the gravity effect. In some experiments, the effect of temperature gradient was higher than the gravity effect. The combination of gravity and temperature-gradient effects may explain those large gradients observed in various oil and gas fields around the world that exhibit significant compositional variations with depth.

5. The magnitude of compositional gradient increases with increasing pressure and becomes very significant as the system approaching the vicinity of the critical condition.

6. Larger values of thermal diffusion ratios k_T were obtained as the system approached the critical condition. This was reflected in the increasing magnitude of composition grading; that is, increases in composition gradient correspond to increasing thermal diffusion ratio.

7. The development of the steady-state condition was observed in the lab by conducting several centrifugal experiments at different time periods (2, 3, 4, 5, and 6 hours) at a pressure of 300 psig, temperature of 50 °C and a speed of 2500 rpm.

8. The time needed to achieve steady-state condition in a centrifuge experiment was estimated to be about 6 hours for the binary gas mixture. This time was verified experimentally by performing several centrifugal experiments at different time periods as mentioned above.

9. Temperature gradient was observed and measured for non-isothermal experiments.

10. Thermodynamic and transport theories were confirmed through conducting several experiments under isothermal and non-isothermal conditions at low and high pressure.

11. A numerical program was written to calculate the composition gradient in the binary gas mixture of methane and propane. The program use both thermodynamic and transport approaches for calculating the composition gradient with the option of using either Peng-Robinson or Redlich-Kwong equations of state to calculate partial molar volumes, densities, and fugacities for the binary system.

12. This numerical model can be used for multi-component systems if a suitable-pseudo-components were determined to represent the multi-component system fluid phase behavior.

13. The composition gradients that were measured at low pressure agreed qualitatively with the prediction of the Sage-Lacey model and the numerical program that was developed for this research.

14. The predictions of the Sage-Lacey[1] model for ideal gases and the predictions for ideal gases using the numerical model developed in this research are identical.

15. The performance of the model was checked against measured data for partial molar volume for the methane-propane system reported by Sage and Lacey.

16. The variation of density from the spin axis to the outside radius of the PCA was examined for a wide variety of operating conditions. This examination showed that density increased with radius for the present binary system at

50 °C and all pressures considered. So, density driven convection was not expected in the experiments.

5.3 Recommendations for Future Research

For future work on compositional gradient problem, the following recommendations should be considered.

1. It is very important to have a means of closing the valves of the profile capture apparatus (PCA) automatically during the course of the run while centrifuge is spinning. This would eliminate the potential for mixing of gases between sample chambers.

2. Also it is very important to have a means of measuring the temperature while centrifuge is spinning to have an accurate temperature profile which will help in modeling the compositional gradients under non-isothermal conditions.

3. Build a profile capture apparatus (PCA) with more sample chambers than the current one to capture more samples and hence to have more points representing the composition along the PCA.

4. If a larger centrifuge becomes available, larger temperature gradients could be obtained with a longer profile capture apparatus. Larger temperature gradients should also be possible at higher spin rates in the current centrifuge. But, for higher spin rates, some improvements in the mechanical mounting of the PCA are recommended.

5. Measure thermal diffusion coefficients with conventional thermal diffusion cells. The results would be important for modeling the centrifuge data. This is also important in setting up the right conditions for establishing larger compositional gradients.

6. Conduct centrifuge experiments using different compositions of binary gas mixtures at different temperatures and pressures to see the effect of composition on compositional gradients.

7. Conduct centrifuge experiments using two-phase binary and ternary gas mixtures to simulate more closely the real conditions encountered in petroleum reservoirs.

8. Experimentally study the problem of compositional gradient in two dimensions; that is, consider the effect of convection.

NOMENCLATURE

c: number of components

D: molecular diffusivity

f: fugacity

g: constant of gravity

G: Gibbs free energy

j: molar flux

k_T: thermal diffusion coefficient

M: molecular weight

m: total mass

n: number of moles

P: pressure

Q: total heat

R: universal gas constant

r: radius

S: total entropy

T: Temperature

U: total internal energy

$\overline{U}$:   partial molar internal energy

V: total volume

$\overline{V}$:   partial molar volume

W: total work

x: mole fraction

z: depth

Greek Symbols

α_T: thermal diffusion coefficient

∇:   differential operator

μ: chemical potential

ρ: density

τ: ratio of the energy of vaporization and viscous flow

ω: spin rate, radian/sec.

Subscripts:

A,B,1,2, i,j:	indices of the species
ij:	binary components ij
L:	Liquid
P:	at constant pressure
T	at constant temperature
V:	vapor

REFERENCES

1. Sage, B. H. and Lacey, W. N. "Gravitational Concentration Gradients in Static Columns of Hydrocarbon Fluids," *Trans. AIME*, 1936, **28**, 249.

2. Schulte, A. M. "Compositional Variations Within a Hydrocarbon Column Due to Gravity," SPE 9235 presented at the 1980 SPE Annual Technical Conference and Exhibition, Dallas, September 21-24.

3. Holt, T., Linderberg, E., and Ratkje, S. K. " The Effect of Gravity and Temperature Gradients on Methane Distribution in Oil Reservoirs," SPE 11761, 1983.

4. Hamoodi, A. N. and Abed, A. F. "Modeling of a Large Gas-Capped Reservoir with Area and Vertical Variations in Composition," paper SPE 28937 presented at the 1994 69th SPE Annual Technical Conference and Exhibition, New Orleans, (Sept. 25-28, 1994).

5. Montel, F. and Gouel, P. L. " Prediction of Compositional Grading in a Reservoir Fluid Column," SPE 14410 presented at the 1985 SPE Annual Technical Conference and Exhibition, Las Vegas, September 22-25.

6. Creek, J. L. and Schrader, M. L. "East Painter Reservoir: An Example of a Compositional Graient from a Gravitational Field," paper SPE 14411 presented at the 1984 59th SPE Annual Technical Conference and Exhibition, Las Vegas, (Sept. 22-25, 1984).

7. Hirschberg, A. "Role of Asphaltenes in Compositional Grading of a Reservoir's Fluid Column," *JPT*, Jan. 1988, pp. 89-94.

8. Muskat, M. "Distribution of Non-Reacting Fluids in the Gravitational Field," *Physical Review*, June 1930, 35, pp. 1384-1393.

9. Lee, S. T. "Capillary-Gravity Equilibria for Hydrocarbon Fluids in Porous Media," paper SPE 19650 presented at the 1989 SPE Annual Technical Conference and Exhibition, San Antonio, (Oct. 8-11, 1989).

10. Jacqmin, D. "The interaction of Natural Convection and Gravity Segregation in Oil/Gas Reservoir," paper SPE 16703 presented at the 1987 62nd SPE Annual Technical Conference and Exhibition, Dallas, (Sept. 1987).

11. Belery, P. and da Silva, F. V. "Gravity and Thermal Diffusion in Hydrocarbon Reservoirs," paper presented at the Third Chalk Research Program, Copenhagen, June 11-12, 1990.

12. Wheaton, R. J. "Treatment of Variations of Composition with Depth in Gas-Condensate Reservoirs," *SPERE*, May 1991, pp. 239-244.

13. Chaback, J. J. "Discussion of Treatment of Variations of Composition with Depth in Gas-Condensate Reservoirs," *SPERE*, Feb. 1992, pp.157.

14. Faissat, B., Knudsen, K., Stemby, E. H., and Montel, F. "Fundamental Statements about Thermal Diffusion for a Multicomponent Mixture in a Porous Medium," *Fluid Phase Equilibria*, (submitted in 1993).

15. Whitson, C. H., and Belery, P.," Compositional Gradients in Petroleum Reservoirs," SPE 28000 presented at the 1994 University of Tulsa Continental Petroleum Engineering Symposium, Tulsa, Aug. 29-31.

16. Firoozabadi, A. *Thermodynamics of Hydrocarbon Reservoirs*, First Edition, McGraw Hill, New York city, (1999).

17. Firoozabadi, A., Dindoruk, B., and Chang, E. "Areal and Vertical Compositional Variation in Hydrocarbon Reservoirs- Part I: Formulation and Results, RIT-2, 2nd International Conference on Thermo-diffusion, Pau, France, (1996).

18. Arbabi, S. and Firoozabadi, A. "Near-critical Phase Behavior of Reservoir Fluids using Equation of State," *SPE Advanced Technology Series*, (1995), Vol. **3**, No. 1, 139.

19. Riley, M. F. and Firoozabadi, A. "Compositional Variation in Hydrocarbon Reservoirs with Natural Convection and Diffusion," *AICHEJ*, Vol. 44, No. 2, (Feb. 1998), pp. 452-464.

20. Shukla, K., and Firoozabadi, A. "A new Model of Thermal Diffusion Coefficient in Binary Hydrocarbon Mixtures," *Ind. Eng. Chem. Res.* (1998), Vol. 37, 3331.

21. Lira-Galeana, C., Firoozabadi, A., and Prausnitz, J. M. "Computation of Compositional Grading in Hydrocarbon Reservoirs: Application of Continuos Thermodynamics," *Fluid Phase Equilibria*, (1994) 102, 143-158.

22. Ghorayeb, K., Firoozabadi, A., and Anraku, T. "Interpretation of the Fluid Distribution and GOR Behavior in the Yufutsu Fractured Gas-Condensate Field," paper SPE 59437 presented at the 2000 Asia Pacific Conference on Integrated Modeling for Assest Management, Yokohama, Japan (April 2000).

23. Temeng, K. O., Al-Sadeg, M. J., and Al-Mulhim, W. A. "Compositional Grading in Ghawar Khuff Reservoirs," SPE 49270, prepared for presentation at the 1998 SPE Annual Technical Conference and Exhibition, New Orleans,Louisiana, Sept.27-30.

24. Machel, H. G., Krouse, H. R., and Sassen, R. "Products and Distinguishing Criteria of Bacterial and Thermo-chemical Sulfate Reduction," *Applied Geochemistry*, vol. 10, (1995) pp. 373-389.

25. Worden, R. H., Smalley, P. C, and Oxtoby, N. H. "Reactions Controlling H_2S Concentrations in Deep Carbonate Reservoirs," *AAPG, Bull.* Vol. **79**, (1995) 1257.

26. Worden, R. H., Smalley, P. C, and Oxtoby, N. H. "The Thermal Impact of Sulfate Reduction in The Khuff Formation," *Petroleum Abstract* No. 701806, (1997).

27. Worden, R. H., Smalley, P. C, and Oxtoby, N. H. "H_2S-Producing Reactions in Deep Carbonate Gas Reservoirs: Khuff Formation, Abu Dhabi," *Petroleum Abstract* No. 646604, (1996).

28. Riemens, W. G., Schulte, A. M., and de Jong, L. N. J. "Birba Field PVT Variation along the Hydrocarbon Column and Confirmatory Field Tests." *JPT* (Jan. 1988) **40**, No. 1, 83-88.

29. Grant, H. K. "Material-Balance Calculations," *The Oil and Gas Journal*, (Aug. 1959), 57 (35), 93-99.

30. Metcalfe, R. S., Vogel, J. L, and Morris, R. W. "Compositional Gradient in the Anschutz Ranch East Field," paper SPE 14412 presented at the 1985 SPE Annual Technical Conference and Exhibition, Las Vegas, September 22-25.

31. Hearn, C. L., Whitson, C. H. "Evaluating Miscible and Immiscible Gas Injection in Safah Field, Oman," paper SPE 29115 presented at the 1995 13th SPE Symposium on Reservoir Simulation, San Antonio, (Feb. 12-15, 1995).

32. Espach, R. H. and Fry, J. "Variable Characteristics of the Oil in the Tensleep Sandstone Reservoir, Elk Basin Field, Wyoming and Montana," *Trans. AIME* (1951), 192, 75-82.

33. Welge, H. J. Discussion Espach, R. H. and Fry, J. "Variable Characteristics of the Oil in the Tensleep Sandstone Reservoir, Elk Basin Field, Wyoming and Montana," *Trans. AIME* (1951), 192, 75-82.

34. Rzasa J. M. Discussion Espach, R. H. and Fry, J. "Variable Characteristics of the Oil in the Tensleep Sandstone Reservoir, Elk Basin Field, Wyoming and Montana," *Trans. AIME* (1951), 192, 75-82.

35. McCord, D. R. "Performance Predictions Incorporating Gravity Drainage and Gas Cap Pressure Maintenance LL-370 Area, Bolivar Coastal Field," *Trans. AIME* (1953), 198, 93-99.

36. Cupps, C. Q., Lipstate, P. H. Jr., and Fry, J. "Variance in Characteristics of the Oil in the Weber Sandstone Reservoir, Rangely Field, Colorado," Rep. Invest., USMB (1951).

37. El-Mandouh, M. S., Bette, S., Heinemann, R. F., Ogiamien, E. B., and Bathia, S. K. "Full Field Compositional Simulation of Reservoir with Complex Phase Behavior," paper SPE 25249 presented at the 1993 12th SPE Symposium on Reservoir Simulation, New Orleans, (Feb. 28-March 3, 1993).

38. Alonso, M. E. and Nectoux, A. C. "Experimental and Numerical Investigation of the Primary Depletion of a Critical Fluid," paper SPE 13266 presented at the 1984 59th SPE Annual Technical Conference and Exhibition, Houston, (Sept. 16-19, 1984).

39. Bachman, R. C., Papst, W., and Legers, R. G. "Investigation of Gas Cycling Schemes for the Westerose D-3 Pool," paper 87-38-53 presented at the 38th Annual Technical Meeting of the Petroleum Society of CIM held in Calgary, (June 7-10, 1987).

40. Kingston, P. E., and Niko, H. "Development Planning of the Brent Field," *J. of Pet. Tech.* (Oct.1975), p.1190.

41. Creek, J. L. and Schrader, M. L. "East Painter Reservoir: An Example of a Compositional Graient from a Gravitational Field," paper SPE 14411

presented at the 1984 59th SPE Annual Technical Conference and Exhibition, Las Vegas, (Sept. 22-25, 1984).

42. Broekers, M. P. and van Drop, W. G. "Miscible Gas Drive in Unit 1 of the Statford Reservoir," paper SPE 15876 presented at the 1986 SPE European Petroleum Conference, London, Oct. 20-22.

43. Neveux, A. R., Sakthikumar, S., and Nolray, J. M. "Delineation and Evaluation of a North Sea Reservoir Containing Near-Critical Fluids," *SPERE* (Aug. 1988) 842-848.

44. Maan, N., Rosales, E., and Medina, H. "Development and Exploitation Strategies in a High Pressure-Temperature Reservoir with a Complex Hydrocarbon Fluid Column," paper SPE 30759 presented at the 1995 60th SPE Annual Technical Conference and Exhibition, Dallas, (Oct. 22-25, 1995).

45. Ortega, L., Brito, L., and Ben-Naceur, K. "Hydraulic Fracturing for Control of Sand Production and Asphaltene Deposition in Deep Hot Wells," paper SPE 36461 presented at the 1996 61st SPE Annual Technical Conference and Exhibition, Denver, (Oct. 6-9, 1996).

46. Rosales, E., Ashford, F., Parra, E., and Parra, D. "Unexpected Near-Critical Reservoir Fluid Behavior in the North Monagas Oil Province, Venezuela," paper SPE 23689 presented at the 1992 Second Latin American Engineering Conference SPE, Caracas, Venezuela (March 8-11, 1992).

47. Sage, B. H. and Lacey, W. N. *Trans. AIME*, 1938, **132**, pp. 120-131.

48. Maan, N.,"*Development of Experimental Methods for Investigating Compositional Gradients in Gravitational Fields* ," MS Thesis presented at Colorado School of Mines, Golden, CO. Aug. 1997.

49. Ratulowski, J., Fuex, A. N., Westrich, J. T. and Sieler, J. J. "Theoretical and Experimental Investigation of Isothermal Compositional Grading,"

paper SPE 63084 presented at the 2000 75th SPE Annual Technical Conference and Exhibition, Dallas, (1-4, 2000).

50. Smith, J. m. and Van Ness, H. C. "*Introduction to Chemical Engineering Thermodynamics,*" *McGraw-Hill Company*, 3de Ed. , 1975.

51. Guggenheim, E. A. *Thermodynamics*, Wiley International Edition (1960), North Holland Publishing Company, Amsterdam (1965).

52. Cengel, Y. A. and Boles, M. A. *Thermodynamics*, McGraw-Hill Company, 3de Ed. , 1989.

53. Bird, R. B., Stewart, W. E. and Lightfoot, E. N. *Transport Phenomena*, Wiley International Edition (1960).

54. Modell, M. and Reid, R. C. *Thermodynamics and its Applications*, Third Edition, Prentice-Hall Inc., Englewood Cliffs, New Jersey, (1974), 489-495.

55. Hirschfelder, J. O., Curtiss, C. F., and Bird, R. B. *Molecular Theory of Gases and Liquids*, J. Wiley & Sons, Inc., (1954).

56. McCain, W. D. *The Properties of Petroleum Fluids*, Second Edition, PennWell Tulsa, (1990).

57. Ahmed, T. H. *Hydrocarbon Phase Behavior*, Vol. **7**, Gulf Publishing CO., Houston, (1989).

58. Reid, R.C., Prausnitz, J. M., and Sherwood, T. K. *The Properties of Gases and Liquids*, Third Edition, McGraw Hill, New York (1977).

59. Prausnitz, J. M., Lichtenthaler, R. N. and de Azevedo, E. G. *Molecular Thermodynamics of Fluid-Phase Equilibria*, Second Edition, Prentice-Hall Inc., Englewood Cliffs, N.J. (1986).

60. Hoffman, J. D. *Numerical Methods for Engineers and Scientists*, McGraw Hill, New York (1992).

61. Rutherford, W. M. *AIChE J.* (1963), **9**, 841.

62. Haase, R. Z. *J. Phys. Chem.* (1950), **196** , 219.

63. Kempers, L. J. T. *J. Chem. Phys.* (1989), **90**, 6541.

64. Dougherty, E. L., Jr. and Drickamer, H. G. *J. Phys. Chem.* (1955), **59** , 443.

65. Sage, B. H., Lacey, W. N., and Schaafsma, J. G. "Phase Equilibria in Hydrocarbon Systems: Volumetric and Phase Behavior of the Methane-Propane System," *Ind. and Eng. Chemistry*, Vol. 26, No. 2, (Feb., 1934) 214-217.

66. Reamer, H. H., Sage, B. H., Lacey, W. N. "Phase Equilibria in Hydrocarbon Systems: II. Methane-Propane System," *Ind. and Eng. Chemistry*, Vol. 42, No. 3, (1950) 534-539.

67. Al-Omair, O. A. "Video Imaging Method for Determining the Capillary Pressure Relationship with a Centrifuge," MS Thesis presented at Colorado School of Mines, Golden, (May, 1997).

68. Peng, D. Y., and Robinson, D. B. "A New Two-constant Equation of State," *Ind. Eng. Chem. Fund.* (1976), Vol. **15**, 59.

69. Redlich, O. and Kwong. J. "On the Thermodynamics of Solutions. An Equation of State. Fugacities of Gaseous Solutions," *Chemical Reviews*, Vol. 44, 1949, pp. 233-247.

70. Hoier, L. and Whitson, C. H." Miscibility Variations in Compositionally Grading Reservoirs," SPE 49269 presented at the 1998 SPE Annual Technical Conference and Exhibition, Louisiana, 27-30 Sept. 1998.

71. Benedict, M., Webb, G. B., and Rubin, L. C. *J. Chem. Phys.* (1942), **10**, 747.

APPENDIX-A
Numerical Programs Listing

```
*****************************************************************
*                    *                          *              *
*                    *                          *              *
*                    * COMPOSITION GRADIENT CALCULATION *       *
*                    *      BINARY GAS SYSTEM        *          *
*                    *      METHANE-PROPANE          *          *
*                    *                               *          *
*                    *      USING PR & RK EOS        *          *
*                    *                               *          *
*                    *                               *          *
*                    *                               *          *
*****************************************************************
*                                                              *
*    THIS PROGRAM SOLVES AN INITIAL-VLUE PROBLEM FOR DIFFERENTIAL *
*       EQUATIONS USING RUNGE-KUTTA PAIRS OF VARIOUS ORDERS.    *
*                                                              *
*       Y1'(r =F1(x1,P,r)                                      *
*       Y2'(X)=F2(x1,P,r)                                      *
*****************************************************************
C                        LIBRARY OF VARIABLES
*****************************************************************
C                                                              =
C   PC1 = CRITICAL PRESSURE FOR METHANE, bar                   =
C   PC2 = CRITICAL PRESSURE FOR PROPANE, bar                   =
C   TC1 = CRITICAL TEMPERATURE FOR METHANE, K                  =
C   TC2 = CRITICAL TEMPERATURE FOR PROPANE, K                  =
C   RM1 = MOLECULAR WEIGHT FOR METHANE, g/gmol                 =
C   RM2 = MOLECULAR WEIGHT FOR PROPANE, g/gmol                 =
C   R   = GAS CONSTANT, cm3 bar/gmol/k                         =
C   TF  = FINAL TEMPERATURE AT THE EDGE OF THE PCA, K          =
C   T0  = TEMPERATURE AT THE CENTER OF THE PCA, AT r=0, K      =
C   T   = TEMPERATURE AT DIFFERENT LOCATION ALONG THE PCA, K   =
C   RPM = SPINNING RATE IN REVOLUTION PER MINUTE               =
C   W   = SPINNING RATE IN RADIAN PER SECOND                   =
C   XKTISO = THERMAL DIFFUSION RATIO AT ISOTHERMAL CONDITION   =
C   A,B    = COEFFICIENTS IN THE TEMPERATURE PROFILE EQUATION  =
C   Y(2)   = PRESSURE AT THE CENTER OF THE PCA AFTER CENTRIFUGE, bar  =
C   Y(1)   = METHANE MOLE FRACTION AT THE CENTER OF THE PCA    =
C   RATIO  = RATIO OF METHANE TO PROPANE                       =
C   RTSNL  = RATIO OF METHANE TO PROPANE GIVEN BY SAGE AND LACEY MODEL  =
C   RI     = RATIO OF METHANE TO PROPANE AT THE CENTER OF SPIN =
C   RAD,RADEND =  DISTANCE FROM CENTER OF SPIN                 =
C                                                              =
*****************************************************************
      USE MSIMSL

        IMPLICIT DOUBLEPRECISION (A-H,O-Z)

      PARAMETER (NDE=2)
      REAL*8 Y(NDE),YPRIME(NDE)
      EXTERNAL FDIFF

      COMMON/PAR2/TC1,TC2,PC1,PC2,R,TF
      COMMON/PAR3/RM1,RM2,W,IFLAG
*****************************************************************
      OPEN(5,FILE='MODEL.INP1',STATUS='UNKNOWN')
        OPEN(6,FILE='MODEL.OUT1',STATUS='UNKNOWN')
        OPEN(7,FILE='MODEL.OUT2',STATUS='UNKNOWN')
*****************************************************************
      PC1 = 4.6000D+01
```

```
      PC2 = 4.2460D+01
      TC1 = 1.9060D+02
      TC2 = 3.6980D+02
      RM1 = 1.6043D+01
      RM2 = 4.4097D+01
      R   = 8.3140D+01
      TF  = 3.2172D+02
*****************************************************************************
C       CENTRIFUGE SPEED IN RPM AND RADIAN/SEC
*****************************************************************************
      RPM = 2.5000D+03
      W   = 2.5000D+03/9.549297D00
*****************************************************************************
C                       THERMAL DIFFUSION RATIO FOR ISOTHERMAL CONDITION
*****************************************************************************
      XKTISO = 0.0000D+00
*****************************************************************************
C                       TEMPRATURE PROFILE EQUATION
*****************************************************************************
      A= 2.8642D-05
      B= 3.1662D+02
      T0=A*RAD**4+B
*****************************************************************************
C               SYSTEMS TO BE SOLVED
*****************************************************************************
*     IFLAG=0 (IDEAL ISOTHERMAL)
*     IFLAG=1 (IDEAL NON-ISOTHERMAL)
*     IFLAG=2 (NON-IDEAL ISOTHERMAL)
*     IFLAG=3 (NON-IDEAL NON-ISOTHERMAL),KARIM FORM
*****************************************************************************
C
      IFLAG =3
C
*****************************************************************************
C   SYSTEM INITIAL CONDITIONS, COMPOSITION AND PRESSURE AT CENTER OF SPIN
*****************************************************************************
*****************************************************************************
      READ (5,*) Y(1),Y(2),RAD
      RADEND =  0.0D0

      T0=A*RAD*RAD*RAD*RAD+B

      X2=1-Y(1)
      RI=Y(1)/X2
*****************************************************************************
      WRITE(6,*)'===================== FINAL RESULTS  ============
     +========='
      WRITE(6,*)'              COMPOSITIONAL VARIATION ALONG TEST LOOP'
      WRITE(6,*)'                      BINARY SYSTEM              '
      WRITE(6,*)'                NON-IDEAL AND NON-ISOTHERMAL       '
      WRITE(6,*)'                USING REDLICH KWONG EOS          '
      WRITE(6,*)
      WRITE(6,*)'    COMPONENTS:        METHANE(1)  PROPANE(2)  '
      WRITE(6,*)
      WRITE(6,*)' PRESSURE =  300.00 PSIA'
      WRITE(6,*)
      WRITE(6,100)XKT
      WRITE(6,*)
      WRITE(6,*)'       r          T          P          C1          C3
```

```
      +     C1/C3        '
        WRITE(6,*)'       cm       oK       Bar        Y1         Y2

      +     Y1/Y2        '
        WRITE(6,*)
        WRITE(6,*)'      ======   ======   ======     ======     ======
      +     ======       '

100 FORMAT(2X,'THERMAL DIFFUSION RATIO, kT=',F7.4)
**********************************************************************************
C              SAGE AND LACEY PREDICTION
**********************************************************************************

      RTSNL=RI*EXP(0.5D0*W*W*(RM1-RM2)*(RADEND*RADEND)
      +/(R*1.0D6*TF))

      WRITE(6,10)RADEND,T0,Y(2),Y(1),X2,RATIO,RTSNL
**********************************************************************************
C              THIS WORK NUMERICAL MODEL
**********************************************************************************
      DO 1 IRAD=1,205

      RADEND =  RADEND+0.1 D0

      IDO=1
      CALL DIVMRK(IDO,NDE,FDIFF,RAD,RADEND,Y,YPRIME)
      IDO=3
      CALL DIVMRK(IDO,NDE,FDIFF,RAD,RADEND,Y,YPRIME)

      X2=1-Y(1)
      RATIO=Y(1)/X2

      T=A*RAD*RAD*RAD*RAD+B
C*******************************************************************************
      RTSNL=RI*EXP(0.5D0*W*W*(RM1-RM2)*(RAD*RAD)
      +/(R*1.0D6*TF))


1     WRITE(6,10)RADEND,T,Y(2),Y(1),X2,RATIO,RTSNL

10     FORMAT(1X,F6.3,2X,F7.2,2X,F6.2,2X,F10.8,2X,F10.8,2X,F7.5,2X,F7.5)

      STOP
      END
**********************************************************************************
      SUBROUTINE FDIFF(NDE,RAD,Y,YPRIME)
        IMPLICIT REAL*8 (A-H,O-Z)
      REAL*8 Y(*),YPRIME(*)

      COMMON/PAR1/T,P
      COMMON/PAR2/TC1,TC2,PC1,PC2,R,TF
      COMMON/PAR3/RM1,RM2,W,IFLAG

      X1=Y(1)
      P=Y(2)

      X2=1.0D0-Y(1)
      RM=Y(1)*RM1+X2*RM2
```

```
      A= 2.8642D-05
      B= 3.1662D+02
      T=A*RAD*RAD*RAD*RAD+B


**********************************************************************
C         CHANGING THE VALUE OF THERMAL DIFFUSION RATIO
**********************************************************************

      XKT=1.D+00

**********************************************************************
C                       IDEAL  &  ISOTHERMAL
**********************************************************************
      IF (IFLAG.EQ.0)THEN
      F1=W*W*RAD*Y(1)*X2*(RM1-RM2)/(R*1.0D6)

      YPRIME(1)=F1/TF
      YPRIME(2)=Y(2)*RM*W*W*RAD/(R*1.0D6*TF)
      ENDIF
**********************************************************************
C                       IDEAL  & NON-ISOTHERMAL
**********************************************************************
      IF (IFLAG.EQ.1)THEN
      F1=W*W*RAD*Y(1)*X2*(RM1-RM2)/(R*1.0D6)
      F2=XKT*(2.0D0*A*RAD+B)

      YPRIME(1)=(F1-F2)/T
      YPRIME(2)=Y(2)*RM*W*W*RAD/(R*1.0D6*T)
      ENDIF
**********************************************************************
C                       NON-IDEAL & ISOTHERMAL
**********************************************************************
      IF (IFLAG.EQ.2)THEN

      CALL FINDPV(X1,V1P,V2P)
      CALL FINDDLFDLX(X1,DLFDLX)
**********************************************************************
C         CALCULATING COMPOSITIONAL GRADIENT USING RIDLICH-KWONG EOS
**********************************************************************

C   CALL FINDZ(X1,Z)

**********************************************************************
C         CALCULATING COMPOSITIONAL GRADIENT USING PENG-ROBISNSON EOS
**********************************************************************

      CALL FINDZPR(X1,Z)

**********************************************************************

      F1=(RM1/V1P)-(RM2/V2P)
      F2=(1.0D0/(X1*V1P))+(1.0D0/(X2*V2P))

      YPRIME(1)=(1.D0/DLFDLX)*((F1/F2)*(W*W*RAD/(R*1.0D6*TF)))
      YPRIME(2)=Y(2)*RM*W*W*RAD/(Z*R*1.0D6*TF)
      ENDIF
```

```
*************************************************************************
C                        NON-IDEAL NON-ISOTHERMAL
*************************************************************************

      IF (IFLAG.EQ.3)THEN

      CALL FINDPV(X1,V1P,V2P)

      CALL FINDDLFDLX(X1,DLFDLX)

      CALL FINDZPR(X1,Z)

C     CALL FINDZ(X1,Z)

      F1=(X1*V1P*RM1)+(X2*V1P*RM2)
      F2=(X1*V1P)+(X2*V2P)
      F3=X1*(RM1-(F1/F2))*(W*W*RAD/(R*1.0D6*T))


      DTDR=4*A*RAD**3
      F4=XKT*DTDR/T

      YPRIME(1)=(1.D0/DLFDLX)*(F3-F4)
      YPRIME(2)=Y(2)*RM*W*W*RAD/(Z*R*1.0D6*T)

      ENDIF

*************************************************************************
      RETURN
      END
*************************************************************************
```

```
C===================================================================
C                    =                                    =
C                    =         KARIM AL-JAZIRI             =
C                    =         MASS DIFFUSIVITY            =
C                    =                 &                   =
C                    = THERMAL DIFFUSION COEFFICIENT       =
C                    =          CALCULATION                =
C                    =                                     =
C                    =          May 1, 2000               =
C                    =                                     =
C===================================================================
C LIBRARY OF VARIABLES:

C Y1,Y2 : MOLE FRACTION OF COMPONENTS 1 AND 2

C M1,M2,M : MOLECULAR WEIGHT OF COMPONENT 1 AND 2

C M : MOLECULAR WEIGHT OF THE MIXTURE

C T,P :  TEMPERATURE AND PRESSURE OF THE SYSTEM

C T1=T1*,T2=T2*,T12=T12* : REDUCED TEMPERATURE , T12*=kT/E12

C k,E12(epselon),EK1,EK2,EK12( ),SI1,SI2,SI12( ) :
C PARAMETERS IN THE POTENTIAL
C FUNCTION CHARACTERISTICOF 1-2 INTERACION

C R :GAS CONSTANT

C L1,L2:LAMDA:THERMAL CONDUCTIVITY IN cal/cm sec K
C CALCULATED FROM EQ. 8.2-31(REF#1)
C L12 :QUANTITY DEFINED IN EQUATION 8.2-34 (REF#1)

C GD12,G11,G12,G13,G22,G122,G222 : COLLISION INTEGRALS FUNCTIONS OF T*

C KTE,KTC :EXPERIMENTAL AND CALCULATED THERMAL DIFFUSION RATIOS CALCULATED

C USING EQUATION 8.2-50 (REF#1)

C D12 : MASS DIFFUSIVITY, cm/sec2 CALCULATED USING EQUATION 16.4-13 (REF#2)

C D1T : THERMAL DIFFUSION COEFFICEINT,g/cm.sec CALCULATED USING
C EQ.18.4-15 (REF#2)
C TC1,TC2 : CRITICAL TEMPERATURES

C PC1,PC2 : CRITICLA PRESSURES

C A12,B12,C12 : FUNCTIONS OF T12* DEFINED IN EQUATIONS 8.2-15-17 (REF#1)

C XL,YL,U1,UY,U2: FUNCTIONS DEFINED IN EQUATION 8.2-36 (REF#1)
```

```
C S1,S2 : QUANTITY DEFINED IN EQUATION 8.2-34 (REF#1)
C
C===================================================================
C REFERENCE#1: J.O.Hirschfelder, C.F.Curtiss, and R.B.Bird,"Molecular Theory
C of gases and Liquids"Wiley, New York (1954)chapter-8.
C
C REFERENCE#2:19.  Bird, R. B., Stewart, W. E. and Lightfoot, E. N.:"Transport
C Phenomena", Wiley International Edition (1960).
C
C===================================================================
      IMPLICIT REAL*8 (A-H,O-Z)
      REAL M1,M2,M,Y1,Y2,T,T1,T2,T12,P,R
      REAL S1,S2,XL,YL,U1,UY,U2,A12,B12,C12
      REAL L1,L2,L12,GD12,G11,G12,G13,G22,G122,G222
      REAL EK1,EK2,EK12,SI1,SI2,SI12
      REAL KTE,KTC,D12,D1T

      OPEN(5,FILE='TDIFCOF1.INP',STATUS='UNKNOWN')
      OPEN(6,FILE='TDIFCOF1.OUT',STATUS='UNKNOWN')

      READ(5,*)M1,M2
      READ(5,*)Y1,Y2
      READ(5,*)T,P

      READ(5,*)EK1,EK2,SI1,SI2
      READ(5,*)GD12,G11,G12,G13,G22,G122,G222,KTE

      WRITE(6,*)'=============== INPUT DATA ============'
      CALL INPUT(M1,M2,T,P,Y1,Y2,EK1,EK2,SI1,SI2,
     +GD12,G11,G12,G13,G22,G122,G222,KTE)

      R=82.05

      A12=G22/G11
      B12=(5*G12-4*G13)/G11
      C12=G12/G11

      EK12=SQRT(EK1*EK2)
      SI12=(SI1+SI2)/2
      M=Y1*M1+Y2*M2

      T1=T/EK1
      T2=T/EK2
      T12=T/EK12

      L1=0.00019891*SQRT(T/M1)/(SI1**2*G122*T1)
      L2=0.00019891*SQRT(T/M2)/(SI2**2*G222*T2)
      L12=0.00019891*SQRT(T*(M1+M2)/2*M1*M2)/(SI12**2*G22*T12)

      U1=4*A12/15-(12*B12/5+1)*M1/(M2*12)+(M1-M2)**2/(2*M1*M2)
```

```
        U2=4*A12/15-(12*B12/5+1)*M2/(M1*12)+(M2-M1)**2/(2*M1*M2)
        UY=4*A12*((M1+M2)**2/(15*4*M1*M2))-(12*B12/5+1)/12-
       +5*(12*B12/5-5)*(M1-M2)**2/(32*A12*M1*M2)

        XL=Y1**2/L1+2*Y1*Y2/L12+Y2**2/L2
        YL=Y1**2*U1/L1+2*Y1*Y2*UY/L12+Y2**2*U2/L2

        S1=(M1+M2)*L12/(2*M2*L1)-15*(M2-M1)/(4*A12*2*M1)-1
        S2=(M2+M1)*L12/(2*M1*L2)-15*(M1-M2)/(4*A12*2*M2)-1

C       CALCULATING THERMAL DIFFUSION RATIO

        KTC=Y1*Y2*(S1*Y1-S2*Y2)*(6*C12-5)/(6*L12*(XL+YL))

C       CALCULATING MASS DIFFUSIVITY

        D12=0.0018583*SQRT(T**3*(1/M1+1/M2))/(P*SI12**2*GD12)

C       CALCULATING THERMAL DIFFUSION COEFFICIENT

        D1T=KTC*D12*P*M1*M2/(R*T*M)

        CALL OUTPUT1(T,T1,T2,T12,P,Y1,Y2)

        WRITE(6,100)D12,KTE,KTC,D1T

        CALL OUTPUT2(P)
        WRITE(6,200)Y1,T,KTE,KTC

100     FORMAT(10X,F7.5,6X,F7.4,3X,F7.4,2X,F12.10)
200     FORMAT(10X,F7.3,7X,F5.1,3X,F7.4,6X,F7.4)

        STOP
        END
C=================================================================
C       REPORTING THE INPUT DATA
C=================================================================
        SUBROUTINE INPUT(M1,M2,T,P,Y1,Y2,EK1,EK2,SI1,SI2,
       +GD12,G11,G12,G13,G22,G122,G222,KTE)
        REAL M1,M2,T,P,Y1,Y2,KTE
        REAL EK1,EK2,SI1,SI2,GD12,G11,G12,G13,G22
        WRITE(6,*)
        WRITE(6,*)'      BINARY SYSTEM:  NITROGEN(1)- HYDROGEN(2) '
        WRITE(6,*)
        WRITE(6,50)Y1,Y2
50      FORMAT(6X,'MOLE FRACTIONS:  Y1=',F7.4,3X,'Y2=',F7.4)
        WRITE(6,*)
        WRITE(6,*)'PARAMETERS USED
        WRITE(6,*)
        WRITE(6,51)T
51      FORMAT(6X,'SYSTEM TEMPERATURE, K:',3X,F7.1)
        WRITE(6,*)
        WRITE(6,52)P
52      FORMAT(6X,'SYSTEM PRESSURE,  ATM:',3X,F7.3)
        WRITE(6,*)
        WRITE(6,53)M1,M2
53      FORMAT(6X,'MOLECULAR WEIGHT:   M1=',F7.3,3x,'M2=',F7.3)
        WRITE(6,*)
        WRITE(6,54)GD12
```

```
54      FORMAT(6X,'COLLISION INTEGRAL, : GD12=',F6.4)
        WRITE(6,*)
        WRITE(6,55)G11,G12
55      FORMAT(6X,'COLLISION INTEGRAL, : G11=',F6.4,4X,'G12=',F6.4)
        WRITE(6,*)
        WRITE(6,56)G13,G22
56      FORMAT(6X,'COLLISION INTEGRAL, : G13=',F6.4,4X,'G22=',F6.4)
        WRITE(6,*)
        WRITE(6,57)G122,G222
57      FORMAT(6X,'COLLISION INTEGRAL, : G122=',F6.4,4X,'G222=',F6.4)
        WRITE(6,*)
        WRITE(6,58)EK1,EK2
58      FORMAT(6X,'Lennard-Jones, K: EK1=',F5.1,4X,'EK2=',F5.1)
        WRITE(6,*)
        WRITE(6,59)SI1,SI2
59      FORMAT(6X,'Lennard-Jones, A: SI1=',F5.3,4X,'SI2=',F5.3)
        WRITE(6,*)
        WRITE(6,60)KTE
60      FORMAT(6X,'Experimental Thermal Diff. Ratio: kTexp=',F7.5)
        WRITE(6,*)
        RETURN
        END


C========================================================================
C       REPORTING THE OUTPUT DATA
C========================================================================
        SUBROUTINE OUTPUT1(T,T1,T2,T12,P,Y1,Y2)
        REAL T,P,Y1,Y2,T1,T2,T12
        WRITE(6,*)'=============== FINAL RESULTS  ===================='
        WRITE(6,*)'              MASS DIFFUSIVITY                    '
        WRITE(6,*)'              THERMAL DIFFUSION RATIO             '
        WRITE(6,*)'              THERMAL DIFFUSION COEFFICIENT       '

        WRITE(6,*)'              FOR LOW DENSITY GASES               '
        WRITE(6,*)
        WRITE(6,*)'       BINARY SYSTEM:      NITROGEN(1)- HYDROGEN(2)  '
        WRITE(6,50)Y1,Y2
50      FORMAT(6X,'MOLE FRACTIONS',6X,F7.4,6X,F7.4)
        WRITE(6,*)
        WRITE(6,*)'     T1*        T2*        T12*          '
        WRITE(6,*)' ========   ========   =======      '
        WRITE(6,100)T1,T2,T12
100     FORMAT(1X,3(F7.2,3X))
        WRITE(6,*)
        WRITE(6,200)T
200     FORMAT(2X,'SYSTEM TEMPERATURE, K:',4X,F7.2)
        WRITE(6,*)
        WRITE(6,300)P
300     FORMAT(2X,'SYSTEM PRESSURE, ATM:',4X,F7.3)
        WRITE(6,*)
        WRITE(6,*)' GAS      MASS                  THERMAL DIFFUSION      '

        WRITE(6,*)' PAIR  DIFFUSIVITY     RATIO    RATIO    COEFFICIENT '
        WRITE(6,*)' 1-2     cm2/sec       Exptl.   Calcd.   gmol/cm.sec '
        WRITE(6,*)'======  ===========   =======  =======  ============'
        WRITE(6,*)'N2-H2                                               '

        RETURN
```

```
      END
C=====================================================================
      SUBROUTINE OUTPUT2(P)
      REAL P
      WRITE(6,*)'=============== FINAL RESULTS  ====================='
      WRITE(6,*)
      WRITE(6,*)'            THERMAL DIFFUSION RATIO              '
      
      WRITE(6,*)'            FOR LOW DENSITY GASES               '
      WRITE(6,*)
      WRITE(6,300)P
300   FORMAT(2X,'SYSTEM PRESSURE, ATM:',4X,F7.3)
      WRITE(6,*)
      WRITE(6,*)' GAS        MOLE                 THERMAL DIFFUSION RATIO'

      WRITE(6,*)' PAIR      FRACTION    TEMP.   xperimental  Calculated'
      WRITE(6,*)' 1-2         Y1         K                            '
      WRITE(6,*)'=======  ============  =====   ===========  =========='
      WRITE(6,*)'N2-H2                                               '

      RETURN
      END
C=====================================================================
C                                     END OF PROGRAM
C=====================================================================
```